Elucidation of the cellular sensing mechanisms for the contact allergens nickel and cobalt

INAUGURAL DISSERTATION

submitted in partial fulfillment of the requirements for the

Dr. biol. hom. degree

to the faculty of Medicine, Justus Liebig University Giessen

By

Badrinarayanan Raghavan

from Chennai, Tamilnadu, India.

Giessen, 2016

From the Experimental Dermatology and Allergy research group, Department of Dermatology and Allergology, Faculty of Medicine, Justus Liebig University Giessen, Germany (Director: **Prof. Dr. Thilo Jakob**).

Gutachter: Prof. Dr. Thilo Jakob

Gutachter: Prof. Dr. Christos Samakovlis

Tag der Disputation: 16.11.2017

கேடில் விழுச் செல்வங் கல்வி யொருவற்கு
மாடல்ல மற்றை யவை

- **Thiruvalluvar's Thirukkural**, verse no. 400

Meaning: Learning is the true imperishable wealth; not all other things are riches.

Dedicated to the four pillars of my life -
Grandma, Parents, Wife and Daughter.

Table of Contents

1 Introduction

“Beauty lies in the eyes of the beholder” - Plato

Every human being has different inclinations on what is beautiful. However, for a majority of people, beauty may be skin deep. A radiant and rash-free skin contributes towards an individual's overall appearance largely. Fashion industry thrives on jewelry, cosmetics and fragrances. But on a dermatological perspective, jewelry metals and perfume ingredients top the list of substances most likely to cause contact dermatitis [1]. There is a steady rise in the incidence of contact allergy over the last few centuries due to industrialization [2]. Thus, in this modern era, the innate immune system in association with the skin, has to defy all odds to tackle the challenges posed by a variety of natural and synthetic chemicals.

1.1 Innate immunity and the skin

Immunity has evolved into an intriguing system comprising both innate and adaptive components, which must operate in tandem against a plethora of noxious substances to protect the host. The innate immune responses work via distinct modules in order to protect against pathogens. Pattern-recognition receptors (PRRs), the most critical component of this system, sense the pathogen and activate the antimicrobial defences [3].

PRRs distinguish the molecular signatures present in various microbes via pathogen-associated molecular patterns (PAMPs) and so far identified PRRs include Toll-like receptors (TLRs), Nod-like receptors (NLRs) and RIG-I-like helicase receptors (RLRs) [4]. Indeed, the discovery of TLRs shattered several misconceptions and rightly pointed out that the innate immune responses show a high degree of target specificity. Moreover, PRRs are completely germline encoded and have been selected by evolution to recognize pathogen-derived compounds that are essential for pathogen survival or endogenous molecules that are released by the host in response to infection [5]. They are widely expressed in immune as well as non-immune cells, unlike the T cell and B cell antigen receptors. These innate immune receptors have been identified in the serum, on the cell surface, in endosomes, and in the cytoplasm [5].

Once a specific PAMP is detected, PRRs unleash a stringent array of innate immune responses subsequently followed by priming antigen-specific adaptive responses [6].

Apart from their primary function in innate immunity, PRRs are also involved in the pathogenesis of numerous diseases including auto-immune disorders, chronic inflammatory conditions like asthma and allergy, renal dysfunction and in some types of cancers [7-11].

Skin is a dynamic organ, though in the past it was just regarded as a passive wall guarding the internal organs and tissues [12]. Being the largest organ of the human body, it is the most accessible cover to the environment [13]. It offers the first line of protection against a wide range of physical and biological assaults [11]. As in other organs, toxic substances that encounter the skin are recognized by PRRs. Recent findings reveal that the skin is associated with complex functionalities in order to maintain homeostasis. The distinct feature of the skin to perform multifaceted tasks is definitely due to its structural organisation.

Skin is composed of two distinct layers namely the outer epidermis and an inner dermis, isolated by a basement membrane. The epidermis is arranged outwardly by layers of the stratum basale, the stratum spinosum, the stratum granulosum, and the stratum corneum with the latter consisting of keratinized squamous epithelial cells referred to as corneocytes [14].

Keratinocytes, Langerhans cells, melanocytes and Merkel cells are the resident cell types found in the epidermis [11]. Primary function of the keratinocytes is to proliferate and maintain the outer layer of epidermis with a stratified epithelial zone and a water-resistant layer of lipids. The melanocytes are crucial for the biosynthesis of melanin thereby rendering uniform skin pigmentation as well as protection against UV radiation [11]. The intraepithelial T lymphocytes and Langerhans cells that serve as cutaneous antigen presenting cells (APCs) are interspersed between the keratinocytes and melanocytes. Merkel cells are oval sensory cells often known as nerve-ending cells, essential for light-touch and discrimination of shapes and texture [14]. They may have a neuroendocrine function as well. The connective tissues anchor the epidermis beneath to dermis. The dermis is highly vascularised and has a rich amount of nerve fibres, macrophages, fibroblasts and lymphocytes. The epidermal cell types express a varied range of TLRs, which respond to their ligands by activating the proinflammatory nuclear factor kappa-light-chain-enhancer of activated B cells (NF-κB) pathway leading to the release of

cytokines [15]. Several studies report that keratinocytes express TLRs 1, 2, 3, 5, 9 and 10 [16-19], while there is conflicting data regarding TLR4 expression [16, 19].

1.2 Allergic contact dermatitis

Contact dermatitis is one of the most prevalent skin diseases, with significant socio-economic impact [20]. In Europe, about 20% of the general population suffers from contact allergy to at least one contact allergen [21]. Based on the molecular mechanism involved, two main types of contact dermatitis may be distinguished. Irritant contact dermatitis develops due to the proinflammatory and toxic effects of xenobiotics able to activate the innate immunity of the skin whereas allergic contact dermatitis (ACD) requires the activation of hapten-specific acquired immunity leading to the development of effector T-cells, which mediate the skin inflammation. ACD accounts for about 10% of all the dermatological disorders and about 50% of all occupational skin diseases [22]. ACD is defined as an inflammatory reaction of the skin caused by repeated exposure with harmful exogenous substances [23]. Contact allergens are widespread in the environment and it may be of natural or synthetic origin. Presently, more than 4000 contact allergens are known [24].

Hypersensitivity reactions are classified into four categories namely type I, II, III and IV [25]. Being a type IV delayed hypersensitivity reaction, ACD is the most common immunotoxicity seen among humans [26]. Contact allergy evolves through a cascade of intriguing immune-mediated processes made up of two distinct phases, namely the afferent/sensitization phase and the elicitation phase [27]. Primary prevention of ACD is aimed at minimizing the risk of induction, whereas secondary and tertiary prevention are targeted to reducing elicitation. In the afferent or sensitization phase, the skin is primed by the topical exposure to a concentration of the allergen, which may be sufficient to trigger the immune response. However, in some cases the hapten itself may not be able to generate innate immune activation but with the help of a coincident infection. Upon re-exposure to the same allergen, there is an onset of a rapid and aggressive secondary immune response. In the elicitation phase, T cells play a crucial role in the innate immune response. Amplification of the immune response is brought about by the release of an array of proinflammatory and chemotactic factors resulting in the stimulation of local blood vessels through the recruitment of mast cells, macrophages and neutrophils [28, 29].

Clinical manifestation of ACD requires a minimum period of 48 h [30, 31]. The acute inflammatory skin response is also known as eczematous dermatitis and its morphology ranges from a milder erythema to a severe edema. Upon removal of the contact allergen, these symptoms disappear [32].

Studies on genetic and immunological factors in contact allergy are hampered by the fact that mechanisms may vary for sensitization and elicitation and different allergens may induce different pathways [33]. For a majority of contact allergens, the basic principles of ACD have been understood while the sensitization and elicitation processes are still unclear at the molecular level.

1.2.1 Etiology and clinical significance

Common causes of ACD include metal allergens, fragrances, rubber, dyes, preservatives and poison ivy [13]. Among the metals allergens, allergies to nickel (Ni^{2+}), cobalt (Co^{2+}) and chromium (Cr^{6+}) are the most prevalent form [34]. Palladium and gold, are also known to cause ACD [35-37]. The occurrence of ACD for metal allergens Ni^{2+}, Co^{2+} and Cr^{6+} was about 15%, 5% and 3%, respectively [38]. The rate of Ni^{2+}/Co^{2+} induced ACD is higher at younger age, while the prevalence of Cr^{6+} ACD remained high for the whole life [39]. The prevalence of ACD in the German population is reported to be 8% in men and 21% in women [21]. Metal ions differ from the classical haptens in its binding with partner molecules by forming reversible, well defined coordination complexes [40].

The most common cause of ACD in women is Ni^{2+} in many countries around the world [41]. Being a potent environmental pollutant and as such several Ni^{2+}-compounds are carcinogenic, exposure to this heavy metal may lead to severe health hazards [42]. In industrialized countries, up to 40% of young females and increasingly males are sensitized to Ni^{2+} and develop allergic dermatitis upon contact with Ni^{2+}-releasing metal alloys such as costume jewelry, body piercings and coins [43-45]. Women are more predisposed due to usage of high Ni^{2+}-content jewelry [46]. Ear piercing is considered as the primary reason for the high prevalence.

Cobalt is ubiquitous in the environment because of its broad usage in metallurgical and electronic industries, magnetic alloys production and the building construction sector. Most common sources of Co^{2+} include ceramics, paints, jewelry, hair dyes and fertilizers

[47]. Co^{2+} has also been detected at significant levels as air pollutant and exerts numerous biological effects apart from ACD, including mimicking of hypoxia systemically [48].

Moreover, the usage of these allergens is alarming in the context of biocompatibility of cardiovascular stents, orthopaedic and dental biomedical alloys [49-51]. The understanding of how these metal allergens exert their toxic and allergic effects at a molecular level may be important in risk assessment, as well as in the treatment and prevention of occupational diseases.

1.2.2 Occupational contact dermatitis and economics

Occupational contact dermatitis (OCD) ranks first among occupation-related diseases in many countries [52]. The annual incidence rate reported for OCD is 0.5-1.9% [53]. Epidemiological studies play an important role in observing disease trends, analysing risk factors, and monitoring the effect of preventive measures. The most affected professions include construction workers, cashiers, hair-dressers, healthcare workers, employees in the food industry, cleaners and metallurgy workers [54]. Importance of ACD is not only related to the high incidences worldwide, but also to the high costs for health care systems and the economy as well as in an impairment of the quality of life for the patients. In this context, people with ACD of the face or those who are obliged to change job reported the worst quality of life [55].

1.3 Molecular mechanisms of metal-induced ACD

The key mechanism by which metal allergens induce ACD is a T cell-mediated reaction with production and release of various cytokines [56]. Ni^{2+} possesses irritant capacity and triggers a direct innate immune signal associated with activation of proinflammatory signaling pathways. A previous study from our laboratory has shown that Ni^{2+} is able to cause a rapid induction of endothelial activation markers as early as 8 h after ACD elicitation in sensitized individuals, a time point well before Ni^{2+}-reactive T cells and other leukocytes infiltrate the skin [57].

1.3.1 Endothelium and inflammation

Endothelium, strategically located between the blood and the tissue compartments, is an important component of the innate immune system. It has long been considered as only a physical barrier between the extra- and intravascular space. Recent studies reveal that the endothelium is an independent and metabolically active organ. It is involved in the regulation of blood pressure, the mass transfer between blood and tissue, coagulation, angiogenesis and in several immunological processes [58]. The role of endothelial cells (ECs) in inflammatory processes is of particular interest in the present work. Activation of ECs by endogenous or environmental factors is a crucial step in the initiation of inflammatory responses [59, 60].

Inflammation is an immune reaction caused by injury or tissue damage and characterized by redness, heat, swelling, and pain. The primary objective of inflammation is to localize and eradicate the irritant and repair the surrounding tissue. Ligand interactions between endothelium and leukocytes play a vital role in the regulation of cellular trafficking at the site of immunologic challenge [61]. Clinically, inflammation is characterized by dilation of connected arterioles, venules and capillaries with an increased blood flow, increased permeability of the blood vessels to cells and soluble components from the blood and the trans-endothelial migration of leukocytes into the surrounding tissue. Cause of this chain of reactions is the expression of soluble and cell surface-bound proteins, such as chemokines, cytokines, and adhesion molecules by the endothelial cells [62-65].

In primary human ECs, metal allergens have been shown to activate proinflammatory signaling cascades such as the NF-κB pathway [66]. NF-κB, which was first described in 1986 [67], has become a collective term for structurally related homo-and heterodimeric transcription factors of the Rel family. These are highly conserved among different species, and play a central role in the transcriptional control of rapidly inducible proteins [68, 69]. NF-κB is located in the cytosol as an inactive complex of the NF-κB dimer coupled with an inhibitory protein I-κB kinase (IKK). This classic "NF-κB" dimer consists of p65 and p50 subunits. The IKK complex entails two kinases IKKα and IKKß and a regulatory subunit NEMO (NF-κB essential modulator), also called as IKKγ [70]. Phosphorylation of the IKK complex at two serine residues (Ser32 and Ser36) leads to the ubiquitination and degradation of IKKα. The release of NF-κB from its inhibitory protein

leads to the translocation of the transcription factor into the nucleus where it binds to the promoter region of its target genes [71, 72] (**Fig. A**).

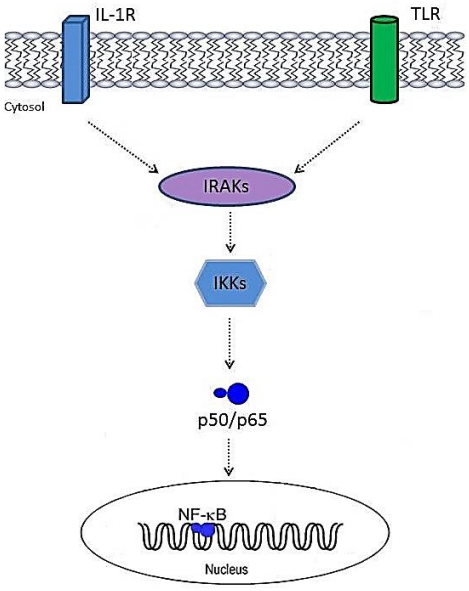

Fig. A: A schematic representation of NF-κB activation. In response to an extracellular signal, IL-1R or TLRs induces the IKK complex mediated NF-κB activation. Modified adaptation from Janssens and Beyaert (2003) [73].

Normally, the activation of NF-κB leads to the expression of a variety of gene products, especially inflammatory cytokines, chemokines, cell adhesion molecules and immunoregulatory surface molecules [74]. This triggers a rapid immune response finally leading to a systemic activation of the immune system. Thus, the transcription factor NF-κB functions as a gene switch and central coordinator of the immune response.

In the case of metal allergens, NF-κB activation finally leads to the synthesis and secretion of proinflammatory adhesion molecules such as ICAM-1, VCAM-1, and E-selectin. These adhesion molecules are required for leukocyte recruitment to the site of exposure [66]. Preliminary observations ascertained that co-stimulation with irritants or unlinked haptens during the sensitization or elicitation phase allows induction of contact hypersensitivity (CHS) [75-77]. The degree of the induced innate immune signal critically determines the responsiveness to a given contact allergen [78]. For instance, adequate induction of an innate immune signal during the sensitization phase of CHS is required for appropriate activation and deployment of dendritic cells (DCs). In turn clonal expansion of hapten-specific T-effector cells are mediated by DCs in the dermal lymph node [79]. Failure to induce hapten-specific T cells results in tolerance due to improper activation of DCs [80].

Therefore, better knowledge of the molecular mechanisms by which haptens activate the innate immune system is crucial to establish novel therapeutic strategies.

The clinically asymptomatic sensitization phase of ACD is well documented while the mechanisms involved in the elicitation phase are poorly understood [81, 82]. It is currently believed that cutaneous application of an allergen (hapten) induces two equally important signals for the elicitation of contact eczema. The initial signal is a hapten-specific signal that involves the action of hapten-specific T lymphocytes whereas the second one is a non-specific proinflammatory signal resulting in the induction of cytokines, chemokines and adhesion molecules that contribute to the recruitment of hapten-specific T lymphocytes to the skin (**Fig. B**).

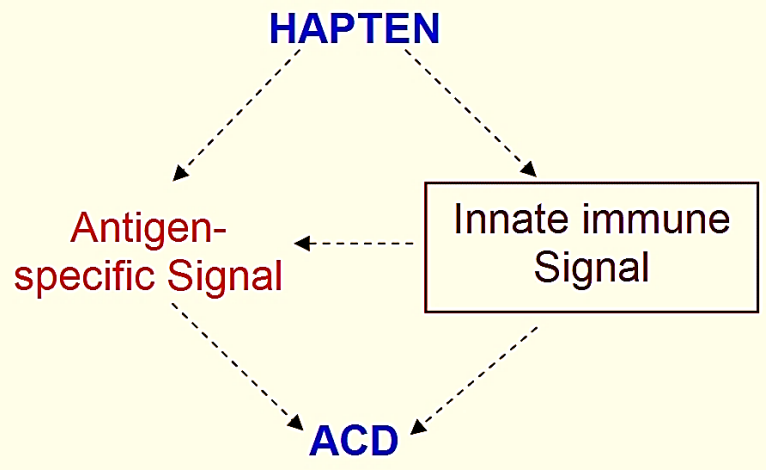

Fig. B: Diagrammatic representation of efficient development of ACD requiring both a T-lymphocyte-specific signal and a proinflammatory immune signal.

From the current understanding, it is uncertain how cells identify the proinflammatory signal provided by the hapten. Some haptens can deliver this innate immune signal independently, while weak allergens may depend on unrelated stimuli such as a microlesion or a coincidental infection to exert their full allergic potential [20]. A recent study showed that innate immune receptors in the form of TLRs have a crucial role in the development of contact hypersensitivity, the mouse model of ACD [83]. Moreover, one of our preliminary studies revealed that the Ni^{2+} induced CCL2 (or MCP-1) expression was blocked when using a dominant negative IL-1 receptor-associated kinase 1 (IRAK-1) (**Fig. C**). It is very well known that IRAKs play a vital role in both IL1R and TLR signaling [84]. However, IRAK1 mediated IL-1 signaling could be excluded as IL-1 neutralizing

antibodies did not block the response of this metal allergen [66]. Therefore, it is very clear that a TLR might be involved in the elicitation of metal induced eczema.

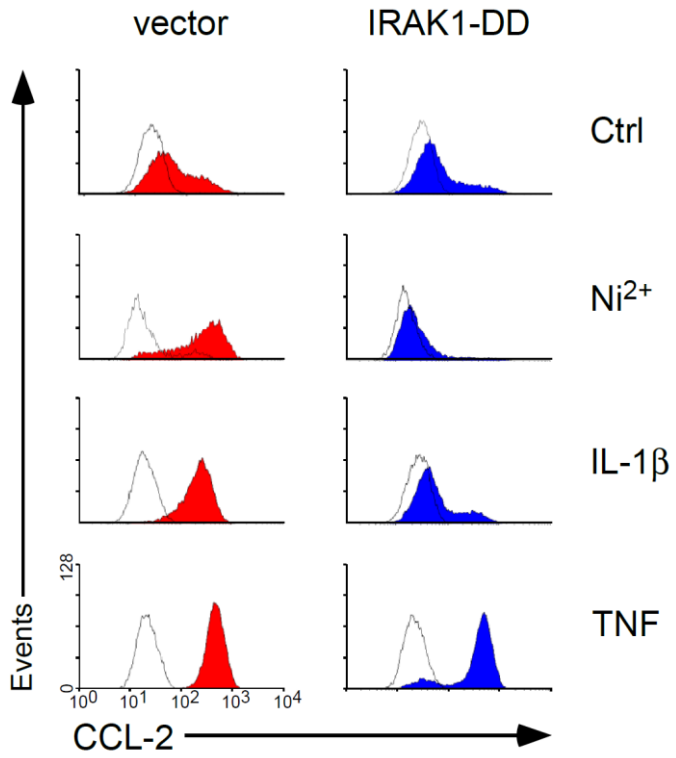

Fig. C: Abrogation of Ni^{2+}-induced expression of NF-κB target gene CCL2 by a dominant negative mutant of IRAK1 (IRAK1-DD). Intracellular expression of CCL2 was analysed by flow cytometry after stimulating ECs with Ni^{2+} (1.5 mM) or IL-1ß (100 U ml^{-1}) or TNF (2 ng ml^{-1}). The colored (red or blue) profiles indicate the CCL2 expression while white outline profile represents the isotype controls. Cells were gated on GFP^{+}, which was co-transfected to determine the transfection efficiency. Data represents two independent experiments. Data courtesy: Prof. Dr. M. Goebeler and S. Schmid.

1.3.2 The TLR system

Until now the existence of 10 and 12 TLRs are reported in human and mice, respectively [85]. TLRs are highly conserved from Drosophila to humans and share structural and functional similarities. Immune cells like monocytes or DCs express various TLRs but somatic cells like keratinocytes also express some TLRs [11]. These receptors belong to the class of type-I transmembrane glycoproteins [86] and are localised on the plasma membrane, the endocytic vesicle membrane, or intracellular organelles [87]. Structurally, TLR paralogs are composed of extracellular, transmembrane and intracellular signaling domains. The ligand recognition is attributed to the repeated leucine-rich repeats (LRRs) found on the ectodomain [88]. Additionally, accessory molecules may also be involved in

ligand binding in addition to a cytoplasmic toll/interleukin-1 (IL-1) receptor (TIR) domain, which interacts with TIR-domain-containing adaptor molecules [87].

TLR4, the founding member of TLR family, was identified as the receptor for lipopolysaccharide (LPS), a structural component of the outer membrane of Gram-negative bacteria [89]. The receptor binds to its co-receptor MD2 (also known as lymphocyte antigen 96), on the cell surface, and serves as the main LPS-binding component [90]. Recent biophysical studies on the LPS-bound TLR4 complex has shown that five of the six lipid chains of the ligand binds to the hydrophobic pocket of MD2, and the remaining lipid chain that is exposed to the surface on MD2 associates with TLR4 [91, 92].

The resulting formation of a receptor multimer composed of two copies of the TLR4-MD2-LPS complex (**Fig. D**) initiates signal transduction by recruiting intracellular adaptor molecules. Additional proteins such as LPS-binding protein (LBP) and CD14 are also involved in LPS binding [90]. Stimulation of TLR4 by LPS, activates myeloid differential factor 88 (MyD88) and TIR domain-containing adapter inducing IFN-beta (TRIF)-dependent signaling pathways leading to activation of NF-κB and IFN-regulatory factor 3 (IRF3) [93].

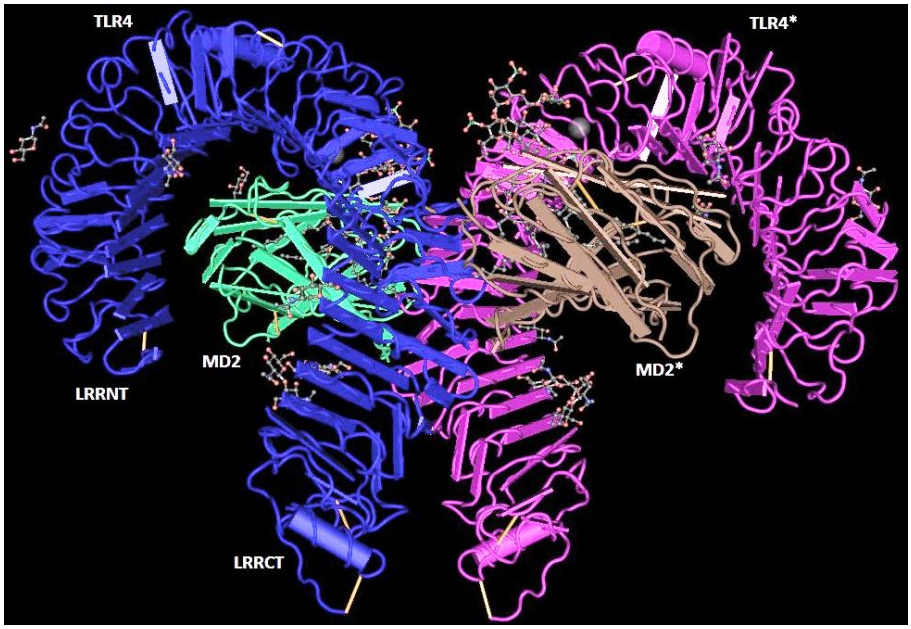

Fig. D: Depiction of a symmetrical dimer structure of the TLR4–MD2–LPS complex. The primary interface between TLR4 and MD2 is formed before binding LPS, and the binding of LPS induces the dimerisation interface. TLR4 is divided into N-, central and C-terminal domains [91]. The LRRNT and LRRCT modules cover the amino and carboxy termini of the LRR modules. Modified adaptation from Park and colleagues [92].

1.4 Objectives

Cobalt and nickel share similar chemical properties as they are adjacent to each other in the periodic table of elements [94]. Similar to Ni^{2+}, Co^{2+} has also been shown to have irritant capacity and elicits a direct innate immune signal resulting in the activation of proinflammatory cascades such as the IKK2/NF-κB pathway in primary ECs [66]. The effects of the metal allergens Ni^{2+} and Co^{2+} thus resemble those induced by proinflammatory cytokines such as TNF or IL-1ß that activate NF-κB pathways in ECs. However, it is presently unclear how exactly these metal allergens trigger the upstream molecules of the NF-κB pathway. Likewise, there is not enough data for the proinflammatory responses to Ni^{2+}/Co^{2+} in other relevant cell types and species.

Therefore, the main goal of this study is to elucidate the sensory mechanisms by which metal allergens Ni^{2+} and Co^{2+} induce its proinflammatory responses that foster the development of allergic reactions. Based on our preliminary data, it is evident that a TLR complex might be involved in the sensory process to these metal allergens, we particularly would like to address the following questions

a) Which TLR is involved in the elicitation of the metal allergies?

b) Can these metals directly interact/bind with the TLR or its co-receptor?

c) Is the mechanism of activation common for both the metal allergens?

We are also interested in the elucidation of novel targets for therapeutic intervention with contact allergy responses of the skin.

2 Material

2.1 Chemicals

All standard chemicals and reagents were purchased from AppliChem (Darmstadt), Fluka (Neu-Ulm), Merck Millipore (Darmstadt) and Roth (Karlsruhe), unless stated otherwise.

2.2 Buffers and solutions

Common laboratory solutions and buffers were prepared according to protocols described by Sambrook et al. [95]. The buffer solutions required for performing the experiments are listed below:

2.2.1 Buffers and solutions for western blot and gel electrophoresis

- 4 x Laemmli-sample buffer
  250 mM Tris-HCl (pH 6.8), 8% sodium dodecyl sulphate (SDS), 40% glycerol, 10% β-mercaptoethanol, 0.01% bromophenol blue in double distilled (dd) H_2O
- Running gel buffer
  0.75 M Tris-HCl (pH 8.8), 0.2% SDS in dd H_2O
- Stacking gel buffer
  0.25 M Tris-HCl (pH 6.8), 0.2% SDS in dd H_2O
- 1 x SDS-polyacrylamide gel electrophoresis (PAGE) buffer
  25 mM Tris-HCl, 192 mM glycine, 0.1% SDS in dd H_2O
- 1 x blotting buffer
  25 mM Tris-HCl, 192 mM glycine, 20% methanol in dd H_2O
- 1 x Tris-buffered saline (TBS)
  20 mM Tris-HCl, 137 mM sodium chloride in dd H_2O, pH adjusted to 7.6 with concentrated HCl
- 1 x TBS-tween 20 (TBS-T)
  0.05% tween 20 in 1 x TBS
- Milk powder – blocking buffer
  5% non-fat dry milk powder in 1 x TBS
- Stripping buffer
  100 mM β-mercapto-ethanol, 2% SDS, 62.5 mM Tris-HCl (pH 6.7) in dd H_2O

- 6 x sample buffer for agarose-gel electrophoresis

  0.25% bromophenol blue, 40% sucrose in dd H_2O
- 1 x Tris acetate EDTA (TAE) - buffer

  Commercially available 50 x TAE buffer (Thermo Fisher, Darmstadt) was diluted in dd H_2O.
- E1A lysis buffer (ELB)

  150 mM sodium chloride, 50 mM HEPES (pH 7.5), 5 mM EDTA, 0.1% NP-40 in dd H_2O; Before use, add freshly 20 mM β-glycerophosphate, 0.5 mM sodium orthovanadate and 1 x complete protease inhibitor (Roche, Mannheim).
- Enhanced chemiluminescence (ECL) detection buffer

  Solution A: 0.1 M Tris-solution (pH 8.5) freshly supplemented with 2.5 mM luminol, 0.4 mM p-coumaric acid

  Solution B: 0.1 M Tris-solution (pH 8.5) freshly supplemented with 0.18% H_2O_2.

  Prior to detection, solution A and B were mixed and blots were incubated immersed for 1 min.

2.2.2 Buffers and solutions for transfections

- 2 x HBS-buffer

  280 mM sodium chloride, 10 mM potassium chloride, 1.5 mM disodium-hydrogen phosphate, 12 mM glucose, 50 mM HEPES in dd H_2O; adjust pH to 7.05 with NaOH; sterile filtered.
- 2.5 M calcium chloride solution; sterile filtered
- 1 mM HEPES in PBS; sterile filtered
- 10 mg ml^{-1} DEAE-Dextran in dd H_2O; sterile filtered
- 100 mM Chloroquine in dd H_2O; sterile filtered

2.3 Stimulants and inhibitors

Stimulant	Concentration	Company
Recombinant TNFα	2 - 5 ng ml^{-1}	R&D (Minneapolis, USA)
Recombinant IL-1β	10 - 100 U ml^{-1}	R&D (Minneapolis, USA)
LPS 055:B5 from *E. coli*	1 µg ml^{-1}	Sigma-Aldrich (Deisenhofen)
LPS R595 from *S. minnesota*	1 µg ml^{-1}	Enzo (Lörrach)
LPS 026:B6 from *E. coli*	1 µg ml^{-1}	Sigma-Aldrich (Deisenhofen)
Nickel chloride ($NiCl_2 \cdot 6H_2O$)	1.5 mM	Merck (Darmstadt)
Cobalt chloride ($CoCl_2 \cdot 6H_2O$)	1.5 mM	Sigma-Aldrich (Deisenhofen)
Brefeldin A	0.2 µg ml^{-1}	Calbiochem (Darmstadt)

Inhibitor	Concentration	Company
Polymyxin B-sulphate (PMB)	50 µg ml^{-1}	Sigma-Aldrich (Deisenhofen)

2.4 Antibodies

2.4.1 Antibodies used for western blot / immunoprecipitation

Primary antibody	Dilution	Company
Mouse anti-IL-8	1 µg ml^{-1}	BD Pharmingen (Franklin Lakes, USA)
Mouse anti-alpha-Tubulin	1:10000	Sigma (St. Louis, USA)
Mouse anti-FLAG M2	1:2000	Sigma (St. Louis, USA)
Rabbit anti-FLAG	1:2000	Rockland (Gilbertsville, USA)
Rat anti-HA (high affinity)	50 ng ml^{-1}	Roche (Mannheim)
Mouse anti-HA (12CA5)	1 µg ml^{-1}	Abgent (San Diego, USA)
Rabbit anti-ERK2	1:2000	Santa Cruz Biotechnology (Santa Cruz, USA)

Secondary antibody	Dilution	Company
Sheep anti-mouse HRP	1:2000	GE Healthcare (Munich)
Donkey anti-rabbit HRP	1:2000	GE Healthcare (Munich)
Goat anti-rat HRP	1:2000	Santa Cruz Biotechnology (Santa Cruz, USA)

2.4.2 Antibodies used for flow cytometry

Primary antibody	Dilution	Company
Mouse anti-IL-8	1:100	BD Pharmingen (Franklin Lakes, USA)
Rat anti-HA	1:100	Roche (Mannheim)
Mouse anti-TLR4	1:100	BioLegend (San Diego, USA)
Mouse IgG isotype control	1:100	Dako (Hamburg)

Secondary antibody	Dilution	Company
Donkey anti-mouse Cy5	1:200	Dianova (Hamburg)
Anti-rat FITC	1:250	BD Pharmingen (Franklin Lakes, USA)

2.5 Kits

Kit name	Company
Qiagen plasmid kits (mini, midi, maxi)	Qiagen (Hilden)
QIAquick gel extraction kit	Qiagen (Hilden)
DyeEx 2.0 spin kit	Qiagen (Hilden)
BigDye terminator cycle sequencing kit	Thermo Fisher (Darmstadt)
BD OptEIA human IL-8 ELISA set	BD Pharmingen (Franklin Lakes, USA)

BD OptEIA mouse TNF ELISA set	BD Pharmingen (Franklin Lakes, USA)
Dual-Glo luciferase assay system	Promega (Madison, USA)
Quick start Bradford dye reagent	BioRad (Munich)
RNeasy mini kit	Qiagen (Hilden)
High Fidelity cDNA synthesis kit	Roche (Mannheim)
Quick-change II site directed mutagenesis kit	Stratagene-Agilent (Böblingen)
RT^2 First Strand Kit (qRTPCR array)	Qiagen (Hilden)

2.6 Transfection reagents

Reagent	Company
DEAE-dextran	Sigma (Taufkirchen)
Lipofectamine 2000	Thermo Fisher (Darmstadt)
FuGENE HD	Roche (Mannheim)
Oligofectamine	Thermo Fisher (Darmstadt)
Calcium chloride	Sigma (Taufkirchen)

2.7 Cell culture materials

2.7.1 Media and media additives

Media/Additives	Company
Endothelial cell basal medium (EBM)	Lonza (Wiesbaden)
EGM-SingleQuot supplements and growth factors	Lonza (Wiesbaden)
Dulbecco's Modified Eagle's Medium (DMEM) + glutaMAX I	Gibco (Karlsruhe)
Medium M199 with Earle's salt	GE Healthcare (Munich)
RPMI 1640 medium + glutaMAX I	Gibco (Karlsruhe)
OptiMEM I reduced serum medium	Thermo Fisher (Darmstadt)
Foetal bovine serum (FBS)	PAA (Pasching)
100 x penicillin/streptomycin (10.000 E / 10 mg ml^{-1})	Linaris (Wertheim)
L-glutamine	Linaris (Wertheim)
Gentamycin	Sigma (Taufkirchen)
Liquemine N5000 (heparin-sodium)	Roche (Mannheim)
100 x non-essential amino acids	Biochrom (Berlin)
Sodium pyruvate	Sigma (Taufkirchen)
Puromycin	AppliChem (Darmstadt)
Amphotericin B	Sigma (Taufkirchen)

2.7.2 Miscellaneous cell culture materials

Reagent	Company
1 x Phosphate buffered saline (PBS) without Ca^{2+}/Mg^{2+}	Gibco (Karlsruhe)
Dimethyl sulfoxide (DMSO)	Serva (Heidelberg)
10 x Trypsin/EDTA (0.5% / 0.2% in PBS)	Pan (Aidenbach)
Trypan blue	Sigma (Taufkirchen)

Cell culture dishes	Greiner (Frickenhausen)
Cell culture flasks	BD Falcon (Heidelberg)
0.45 and 0.8 μm syringe filter	Sartorius (Göttingen)
Microtiter plate (ELISA plates)	Nunc (Wiesbaden)
Microbank cryo tubes	Nunc (Wiesbaden)

2.8 Plasmids

For Promoter-reporter assays (Luciferase assay) a 6x κB-dependent firefly luciferase construct and an ubiquitin-dependent Renilla luciferase construct was used (kindly provided by B. Baumann, University of Ulm). Expression vectors for hMD2 and mMD2 were kindly provided by Dr. M. Muroi, National Institute of Health Sciences, Tokyo, Japan [96]. Hemagglutinin (HA)-tagged TLR4 receptor plasmids of mouse and human origin were generously provided by A. M. Hajjar, Department of Immunology, University of Washington Medical School, Seattle, USA [97]. FLAG-tagged CMV1-TLR4 plasmid was purchased from Tularik Inc. (San Francisco, USA).

2.9 siRNAs (double stranded - oligo nucleotides)

The following commercially available siRNAs (Qiagen, Hilden) were used to knock down the expression of individual proteins in HUVEC:

siRNA Scr	Negative control siRNA Alexa fluor 488 (# 1022563)
	Target sequence AATTCTCCGAACGTGTCACGT
siRNA MyD88	Hs_MYD88_5_HP Validated siRNA (# SI00300909)
	Target sequence AACTGGAACAGACAAACTATC
siRNA MD2	Hs_LY96_8_HP Validated siRNA (#SI03246446)
	Target sequence AACAATATCATTCTCCTTCAA
siRNA TLR4	Hs_TLR4_1 (# SI00151004)
	Target sequence CTCGATGATATTATTGACTTA

2.10 Primary cells, cell lines and bacteria

HUVEC	Primary human umbilical vein endothelial cell; Promocell (Heidelberg)
NHEK	Juvenile primary normal human foreskin epidermal keratinocytes; Promocell (Heidelberg)
HEK293	Human embryonic kidney epithelial cell line; InvivoGen (Toulouse, France)

HEK293-hMD2/CD14	HEK293-cell line, stably expressing human MD2 and CD14; InvivoGen (Toulouse, France)
HEK293-hTLR4	HEK293-cell line, stably expressing human TLR4; InvivoGen (Toulouse, France)
HEK293-hTLR4/MD2/CD14	HEK293-cell line, stably expressing human TLR4, human MD2 and CD14; InvivoGen (Toulouse, France)
THP-1	Human monocytic cell line; DSMZ (Braunschweig)
RAW 264.7	Mouse macrophage cell line; ATCC TIB#71 (Manassas, USA)
DH5α	Heat competent *E. coli* strain for the amplification from recombinant plasmids; Bethesda Research Laboratories (Bethesda, USA)

2.11 General equipments

Incubator: HERAcell 150	Thermo Fisher (Dreieich)
Laminar flow hood: HERAsafe	Thermo Fisher (Dreieich)
Mega centrifuge: megafuge 1.0R	Thermo Fisher (Dreieich)
Mini centrifuges: MiniSpin plus and 5417R	Eppendorf (Hamburg)
Microscopes: Leica DM IL and Leica DM IRB	Leica (Solms)
Balances: Sartorius TE1502S and Sartorius BP301S	Sartorius (Göttingen)
PCR-cycler: Flex cycler	Biozym (Oldendorf)
Electrophoresis chambers (DNA-gels)	Biometra (Göttingen)
Gel-iX imager	Intas (Göttingen)
Western blotting chambers (protein gels)	BioRad (Munich)
Nano drop 2000c	Peqlab (Erlangen)
Multiplate reader	Tecan (Crailsheim)
X-ray film developing machine	Kodak (Stuttgart)
FACS Canto	Becton Dickinson (Heidelberg)
RT-PCR: Stratagene MX3005p	Agilent (Böblingen)
Magnetic stirrers	Heidolph (Schwabach)
pH meter	Knick (Berlin)
Bacteria shaker	Edmund Bühler (Hechingen)
Thermomixer	Eppendorf (Hamburg)

3 Methods

3.1 Cell culture

All cell culture work was carried out under sterile conditions (under laminar air flow, using sterile solutions and media, sterile consumables). All primary cells and cell lines were grown at 37°C, 5% CO_2 and high humidity.

3.1.1 Storage, freezing and re-cultivation of cells

Long-term storage of all the cells was carried out in liquid nitrogen. For freezing, the cells in the culture dish/flask were washed two times with PBS and incubated with 1 x trypsin/EDTA for 5 min. The effect of trypsin was neutralized with an equal volume of PBS containing 10% FBS. The cells were centrifuged, pelleted and reconstituted in 1 ml of freezing medium composed of 10% DMSO, 10% Fetal Bovine Serum (FBS) and 80% of the respective culture medium. The cells were aliquoted in cryotubes and frozen overnight at -80°C in a Styrofoam rack. The aliquots were transferred into liquid nitrogen after two days. For experimental culture, cell aliquots were thawed from liquid nitrogen in a water bath at 37°C, suspended in pre-warmed medium and distributed to culture vessels.

3.1.2 Cell culture methodology

3.1.2.1 Primary human umbilical vein endothelial cells (HUVECs)

HUVECs were purchased from PromoCell (Heidelberg). The stock aliquots were propagated till passage 3, frozen and stored in liquid nitrogen as described above. For experiments, HUVECs were seeded as adherent monolayer cells at a density of at least 4300 cells/cm^2 of the cell culture vessels. The medium was changed every 2 days, until they reached the desired confluency.

Culture medium: It constituted of a mixture of 1 part of endothelial basal medium (EBM) supplemented with EGM SingleQuot Supplements and Growth Factors (500 ml of basal medium are supplemented with 10 ml FBS, 0.5 ml of human endothelial growth factor (hEGF), 0.5 ml hydrocortisone, 0.5 ml of gentamycin/amphotericin B and 2 ml of bovine

brain extract with heparin) and 2 parts of M199 medium with 10% FBS, 30 mg ml^{-1} gentamycin, 15 pg ml^{-1} amphotericin B and 0.8 IU ml^{-1} heparin.

3.1.2.2 HEK293, HEK293 hMD2, HEK293 hTLR4 and HEK293 hTLR4/MD2

HEK293 is an experimentally transformed cell line obtained from cultures of human embryonic kidney cells sheared with adenovirus 5 DNA. Additionally, HEK cells stably expressing transfectants hMD2 (HEK293 MD2) or hTLR4 (HEK293 hTLR4) alone or both in combination (HEK293 hTLR4/MD2/CD14) were also obtained from InvivoGen (Toulouse, France). All HEK cell lines were held in continuous adherent monolayer culture. Parental (WT) HEK293 cells were split 1:8-1:10 and derived cell lines at 1:4 twice a week at 70-80% confluence. For this, the cells were gently washed once with PBS and then incubated briefly (about 1 min) with 1 x trypsin/EDTA. The trypsin was inactivated by the detachment of the cells with an equivalent volume of medium containing 10% FBS. The cells were centrifuged for 5 min at 1200 rpm, pelleted and resolved in fresh medium, and then seeded in cell culture vessels at a density of at least 4300 cells/cm^2.
Culture medium: DMEM supplemented with 10% FBS, and 30 mg ml^{-1} gentamycin.

3.1.2.3 THP-1

The human monocytic suspension cell line THP-1 was cultured according to the protocol of DSMZ (Braunschweig, Germany) at a density between 2 x 10^5 and 1 x 10^6 cells/ml. Therefore, after every 2-3 days the number of cells was determined by Neubauer chamber and the cells were split accordingly. For the change of medium or passaging, the cell suspension was centrifuged for 5 min at 1200 rpm and then the pellet was resuspended in fresh medium. This suspension was seeded at a density of 3.5 x 10^5 cells/ml for further passaging or the day before an experiment at densities of 2 x 10^5 cells/ml in 24-well plate.
Culture medium: RPMI1640 supplemented with 10% FBS, 1 x non-essential amino acids, 1 x penicillin/streptomycin, 1 mM sodium pyruvate and 2 mM glutamine.

3.1.2.4 NHEK

Primary normal human epidermal keratinocytes (NHEK) isolated from neonatal foreskin were purchased from PromoCell (Heidelberg). The stock aliquots were expanded until passage 4 and then cells were incubated with EDTA prior trypsinization and frozen in liquid nitrogen with chelex treated 10% FCS. Chelex was used here to remove calcium from the FCS thereby preventing calcium-induced differentiation of NHEKs upon

subculture. For experiments, frozen NHEKs from liquid nitrogen were pre-passaged and were seeded as adherent monolayer cells at a density of at least 4300 cells/cm^2 of the cell culture vessels. The medium was changed every 2 days, until they reached the desired confluency.

Culture medium: 1:1 mixture of serum-free keratinocyte growth medium (Thermo Fisher, Darmstadt) containing 50 µg ml^{-1} bovine pituitary extract (BPE) and 5 ng ml^{-1} epidermal growth factor (EGF) and calcium-free EMEM (without further supplements). The final calcium concentration of the mixture medium was 0.05 mM.

3.1.2.5 RAW 264.7

RAW 264.7 is a mouse macrophage cell line obtained from ATCC (Manassas, USA). The cells were in continuous adherent monolayer culture, split 1:5 twice a week at 70-80% confluence. Subcultures were prepared by scraping. For this, the cells were washed twice with PBS and then scraped gently with a sterile cell scraper. The detached cells were resolved with the culture medium and collected in a falcon tube. Further the cells were centrifuged for 5 min at 1200 rpm, pelleted and resolved in fresh medium, and then seeded in cell culture vessels at a density of at least 2200 cells/cm^2.

Culture medium: DMEM supplemented with 10% FBS, and 30 mg ml^{-1} gentamycin.

3.1.2.6 Primary human dendritic cells

Primary human immature dendritic cells (iDCs) were generated from $CD14^+$ monocytes isolated from patient blood samples by our collaborators in Freiburg according to an earlier published method [98]. The protocol was approved by the Ethics Committee of the University Freiburg Medical Center, Freiburg, Germany. Seeding of iDCs were done a day before the stimulation experiment. After the respective incubation times, supernatant medium was harvested, frozen and transported to Department of Dermatology, Venerology and Allergology, Giessen for further analysis.

3.2 Gene transfer methods in eukaryotic cells

Depending on the cell type and purpose of the experiment, different protocols of transfection were used. For transient transfection in HUVECs, the DEAE-dextran method was employed. For RNAi in HUVECs, oligofectamine transfection method was used. HEK293 lines were transfected with the calcium phosphate precipitation or Lipofectamine 2000. For NHEKs the commercially available transfection reagent FuGENE HD suited as

the best method. For all the methods, cells on the day of transfection were in the logarithmic growth phase (about 40-60% confluence).

3.2.1 DEAE-dextran transfection

This method was employed for HUVECs in 10 cm dishes. Cells were washed once with HEPES / PBS (1 mM). Then the transfection mix containing 4 ml of HEPES/PBS (1 mM, pH 7.4), 100 µl of DEAE-dextran solution (10 mg ml^{-1}) and 4 µg DNA, was added to the cells followed by a 30 min incubation step at 37°C and 5% CO_2. Further, 6 ml of chloroquine solution containing M199 medium supplemented with 10% FBS and 0.15 mM chloroquine, was added to the cells and incubated for 3 h at 37°C and 5% CO_2. After the incubation, the medium was aspirated and a fresh 3 ml of serum-free M199 medium containing 10% DMSO was added and the cells were kept in a tumbling shaker for 150 seconds at room temperature. Finally, the medium was completely aspirated and the cells were cultured in normal culture medium for further use.

3.2.2 Calcium phosphate transfection

Calcium phosphate transfection of cells in a 10 cm culture dish was performed according to a modified protocol of Graham and van der Eb [99]. Cells were seeded in an antibiotic-free culture medium one day prior to transfection. On the day of transfection, the DNA precipitate was prepared in a microcentrifuge tube, containing 12 µg DNA and sterile dd H_2O (volume adjusted to 450 µl). Then, 50 µl of $CaCl_2$ solution (2.5 M) was added slowly with gentle stirring. After vortexing, 500 µl of 2 x HBS was pipetted gently in a circular motion from the bottom of the tube to the top without touching the walls of the tube. After fully adding the buffer, the mixed solution was taken up and down to mix with bubbles through the pipette. Finally, the transfection mix was added drop-wise to the cells in the petri dish. The dish was then gently mixed and incubated at 37°C and 5% CO_2. On the next day, the medium was aspirated and fresh medium was added.

3.2.3 Oligofectamine transfection

HUVECs were transfected with small interfering RNA (siRNA), using oligofectamine reagent. HUVECs were seeded in 6-well plates (1.2 x 10^5 cells/well) a day prior to the transfection. On day 2, the transfection mix was prepared as two separate parts namely solution A and solution B. Solution A was composed of 10 µl siRNA (20 µM) and 90 µl OptiMEM medium and solution B consisting of 6 µl oligofectamine and 94 µl OptiMEM.

Both the solutions were first separately incubated for 10 min at room temperature, mixed together and allowed to stand for 30 min. Cells were washed twice with OptiMEM during the incubation time. Finally, 800 µl of OptiMEM and the entire 200 µl of the mixed solutions of A + B were added to the cells followed by an incubation of 4 h at 37°C and 5% CO_2. The final concentration of siRNA in this mix was 200 nM. Normal culture medium was freshly added after aspirating the siRNA transfection mix.

3.2.4 Lipofectamine transfection

For co-immunoprecipitation experiments, HEK293 and HEK293 hMD2 cells were seeded with antibiotic-free culture medium at a density of 5 x 10^6 cells per 10 cm culture dish, one day prior to transfection. The cells were transiently transfected with 24 µg DNA and 60 µl of Lipofectamine 2000 according to manufacturer's suggestions. Medium was changed 6 h post transfection and cells were grown in complete culture medium for at least 40 h for further analysis.

3.2.5 Fugene HD transfection

NHEK cells were seeded in 6-well culture dishes with antibiotic-free culture medium at a density of 1 x 10^5 cells per well, two days prior to transfection. The cells were transiently transfected with 1 µg DNA and 3 µl of FuGENE HD reagent according to manufacturer's description. Medium was changed 6 h post transfection and cells were grown in complete culture medium for at least 40 h after which they were utilized for stimulation experiments.

3.3 qRT PCR

Total RNA was isolated by a spin column-based technique using an RNeasy mini kit (Qiagen, Hilden). RNA concentration was photometrically determined, and cDNA was synthesized from 1 µg of total RNA using the high fidelity cDNA synthesis kit (Roche, Mannheim). Primers and probes were purchased from Thermo Fisher (Darmstadt) for human TLR4 (Hs00152939_m1), human MD2 (Hs00209770_m1), GAPDH (Hs99999905_m1) and Loricrin (Hs01894962_s1). qRT-PCR was performed using the primer probe method (TaqMan gene expression master mix; catalogue number 4369016, Thermo Fisher, Darmstadt) and raw data acquired with Stratagene's Mx3005P (Agilent, Böblingen). Pipetting errors were corrected by passive 5-carboxy-X-rhodamine (ROX) fluorescence. Gene expression was normalized to the housekeeping control gene GAPDH,

and the relative expression of genes of interest compared to the respective experimental control was calculated using the comparative PCR method and MxPro-Mx3005 software (version 4.01) from Stratagene (Agilent, Böblingen) as described elsewhere [100].

3.4 Cell lysis for protein analysis

For lysis, cells were washed twice with ice-cold PBS in the culture dish and incubated for at least 60 min at 4°C with E1A lysis buffer (ELB). After the incubation period the cell lysates were scraped from the culture dish by a cell scraper and transferred onto microcentrifuge tube. The insoluble cell components were removed by centrifugation at 14,000 rpm for 10 min at 4°C. The protein content was determined using the standard quick start Bradford dye reagent (BioRad, Munich) according to manufacturer's instructions. The lysates for western blot were mixed in a ratio of 3:1 with 4 x SDS sample buffer, denatured for 5 min at 95°C and stored until use at -20°C.

3.5 Western blot

3.5.1 SDS-polyacrylamide gel electrophoresis (SDS-PAGE)

SDS-PAGE separates the proteins on the basis of their molecular weight, with smaller polypeptides migrating more rapidly. The SDS-polyacrylamide gels were casted with two sequential layers, namely the upper stacking gel and the lower resolving gel. The stacking gel is slightly acidic (pH 6.8) and has a low acrylamide concentration to make a porous gel. Under these conditions, proteins separate poorly but form thin, sharply defined bands. The resolving gel, is more basic (pH 8.8), and has a higher polyacrylamide content, which causes the gel to have narrower pores. The acrylamide content of the resolving gel (8% to 12%) was calculated according to the size of the proteins under investigation. The following table contains the pipetting scheme, after which the individual gels were cast. The composition of the pre-mixes for resolving gel and stacking gel are described in section 2.2.1.

Concentration of the stacking / resolving gels	**8%**	**10%**	**12%**
30% Acrylamide	2.66 ml	3.33 ml	4 ml
Resolving gel pre-mix	5 ml	5 ml	5 ml
Stacking gel pre-mix	-	-	-

deionised H_2O	2.33 ml	1.66 ml	1 ml
Ammonium per sulphate (APS)	100 µl	100 µl	100 µl
Tetra methyl ethylene diamine (TEMED)	4 µl	4 µl	4 µl
Optimum Separation for	> 90 kDa	40-90 kDa	< 40 kDa

The polymerized gel was fixed in a vertical apparatus and the reservoir was filled with running gel buffer (Section 2.2.1). Then the samples were mixed with SDS sample buffer and loaded on separate wells of the stacking gel. At least 30 µg of protein was loaded in each well. Electrophoresis was for 50-60 min at a constant current of 40-50 mA using the mini-gel system.

3.5.2 Protein transfer

The wet blot method was used for the immunological detection of the separated proteins from SDS-PAGE. Based on the advice of the antibody manufacturer, a nitrocellulose membrane (Schleicher and Schüll, Dassel) or a methanol-activated polyvinylidene fluoride (PVDF) membrane (Immobilon®, Millipore, Schwalbach) was employed for the transfer. Proteins having a higher molecular weight (>50 kDa) were blotted for 90 min and those less than 50 kDa were blotted for 60 min at a constant current of 400 mA.

3.5.3 Immuno detection

To saturate non-specific binding, the membrane after the blot was blocked for 1 h at room temperature (RT) in powdered fresh milk blocking buffer (Section 2.2.1). For the detection of individual proteins, the membrane was then treated with the appropriate primary antibody diluted in fresh milk blocking buffer, incubated at 4°C overnight. After washing three times with TBS-T (each 7 min), the incubation was carried out with the respective horseradish peroxidase (HRP) coupled secondary antibody for 1 h at RT. The membrane was washed again four times with TBS-T for the removal of non-specifically bound secondary antibody. The bound HRP-coupled secondary antibodies were detected according to the principle of enhanced chemiluminescence (ECL) with ECL western blotting detection reagents and X-ray films from GE Healthcare (Munich) according to the manufacturer's protocol. Alternatively, self-produced ECL reagent was used sometimes (0.1 M Tris-HCl (pH 8.5), 2.5 mM luminol, 0.4 mM para hydroxycoumaric acid and 0.02% H_2O_2 in dd H_2O).

3.5.4 Stripping

For a second time use of a blot for antibody incubation, previously bound antibody complexes were removed by 30 min incubation at 50°C in stripping buffer (Section 2.2.1). Subsequently, the membrane was again incubated with blocking buffer and antibody dilutions as described in Section 3.5.3.

3.6 Enzyme-linked immunosorbent assay (ELISA)

For the detection of IL-8 or TNF in cell culture supernatant, ELISAs were performed. At the end of the stimulation period, cell culture supernatant was transferred into a microcentrifuge tube, centrifuged at 5000 rpm to remove the cell debris, and stored at -20°C until further use. The concentration of IL-8/TNF in these samples was measured using the commercially available BD OptEIA human IL-8/TNF ELISA kits (BD Pharmingen, Franklin Lakes, USA) according to the manufacturer's protocol. For this, the ELISA microtiter plates were coated overnight with IL-8/TNF detection antibody. IL-8/TNF binds to its specific antibodies on the surface of the microtiter plate and detected by a detection complex of HRP avidin and IL-8/TNF detection antibody. This detection complex was colorimetrically analysed using the ELISA reader and the results were quantitatively evaluated by comparing with the internal standard curve series. All the samples were analyzed at least in duplicate and the values obtained are shown relative to unstimulated controls.

3.7 Promoter-reporter assay (luciferase assay)

For determining the activation of the transcription factor NF-κB, HUVEC or HEK293 cells were transfected in culture dishes using the DEAE-dextran method or calcium phosphate method, respectively (sections 3.2.2 and 3.2.3). The DNA of interest along with a 6 x κB promoter-dependent *Firefly* luciferase and a ubiquitin promoter-dependent *Renilla* luciferase were transfected in the ratio of 30:1. One day later, cells were washed with sterile PBS and detached from the culture dishes with 1 x trypsin-EDTA, and seeded in a 96-well flat-bottom microtiter plate at a density of 20,000 cells per well for HUVECs and 30,000 cells per well for HEK293 lines. After 24 h, the cells were stimulated for 8 h, luciferase activity was measured according to the manufacturer's suggestions using the DualGlo luciferase assay system from (Promega, USA). 6 x κB-dependent luciferase activities were normalized to the luminescence generated by the *Renilla* luciferase control

reporter and expressed as fold stimulation. All experimental samples were at least measured in triplicates.

3.8 Flow cytometry

For the surface expression analysis of HA-tagged hTLR4 and intracellular detection of IL-8, flow cytometry was performed as follows. At 48 h after transfection, cells were exposed to Ni^{2+}, Co^{2+}, LPS or medium as control for 8 h. We added 0.2 μg ml^{-1} brefeldin A in order to avoid secretion of the chemokine via the Golgi pathway. Cells were subsequently harvested, washed, fixed with 4% paraformaldehyde in PBS at 4°C for 20 min, and then co-incubated with different combinations of monoclonal antibodies against HA/IL-8 or the corresponding isotype control monoclonal antibodies that had been diluted in permeabilization buffer containing 1% fetal calf serum, 0.1% saponin, and PBS. Thereafter, cells were successively stained with FITC-coupled anti-rat secondary antibody or Cy5-coupled anti-mouse detection antibody. Fluorescence was determined with a FACSCanto II (Becton Dickinson, Heidelberg), which is a four-color, dual-laser, benchtop system capable of both cell analysis and sorting. Readout molecules were then analyzed after gating on the HA-positive population. Non-viable cells were excluded by means of forward scatter and side scatter parameters.

3.9 Immunoprecipitation

HEK293 WT cells and HEK293 hMD2 cells transiently expressing the different FLAG- or HA-tagged hTLR4 proteins were lysed in E1A lysis buffer as detailed earlier. Total protein (1.5 μg) was then subjected to immunoprecipitation with mouse anti-FLAG monoclonal antibody for overnight and protein-G-agarose (Roche, Mannheim) for 1 h. After the incubation, samples were washed with high salt E1A lysis buffer containing 500 mM sodium chloride for three times. The immunoprecipitates were then boiled in SDS loading buffer, resolved on SDS-PAGE and transferred to polyvinylidene difluoride or nitrocellulose membranes. The membrane then was subjected to western blots using α-HA or α-FLAG antibodies as detailed in section 3.5.

3.10 Site directed mutagenesis

For replacement of the codons (single and double point mutations) in hTLR4 and mTLR4, site-directed mutagenesis was performed using Quick-change II site directed mutagenesis

kit® (Stratagene-Agilent, Böblingen) according to the manufacturer's suggestions using TLR4 complementary primers containing single nucleotide mismatches at the target codon sequence. Following primers were used for the single mutants:

Mutant	Primers
hTLR4 H431A	Forward 5'CAACTAGAACATCTGGATTTCCAGGCTTCCAATTTGAAACAAATGAGTGA3' Reverse 5'TCACTCATTTGTTTCAAATTGGAAGCCTGGAAATCCAGATGTTCTAGTTG3'
hTLR4 N433A	Forward 5'GAACATCTGGATTTCCAGCATTCCGCTTTGAAACAAATGAGTGAGTTTTC3' Reverse 5'GAAAACTCACTCATTTGTTTCAAAGCGGAATGCTGGAAATCCAGATGTTC3'
hTLR4 H456A	Forward 5'CCTCATTTACCTTGACATTTCTGCTACTCACACCAGAGTTGCTTTC3' Reverse 5'GAAAGCAACTCTGGTGTGAGTAGCAGAAATGTCAAGGTAAATGAGG3'
hTLR4 H458A	Forward 5'CATTTACCTTGACATTTCTCATACTGCCACCAGAGTTGCTTTCAATG3' Reverse 5'CATTGAAAGCAACTCTGGTGGCAGTATGAGAAATGTCAAGGTAAATG3'
mTLR4 Y454H	Forward 5'AGCTACTTTACCTTGACATCTCTCATACTAACACCAAAATTGACTTC3' Reverse 5'GAAGTCAATTTTGGTGTTAGTATGAGAGATGTCAAGGTAAAGTAGCT3'
mTLR4 N456H	Forward 5'AAAGCTACTTTACCTTGACATCTCTTATACTCACACCAAAATTGACTT3' Reverse 5'AAGTCAATTTTGGTGTGAGTATAAGAGATGTCAAGGTAAAGTAGCTTT3'

The hTLR4 double mutant was produced by introducing a H456A replacement in the HA-hTLR4-H458A construct using the following primer set:

Mutant	Primers
hTLR4-H456A/H458A	Forward 5'CCTCATTTACCTTGACATTTCTGCTACTGCCACCAGAGTTGCTT3' Reverse 5'AAGCAACTCTGGTGGCAGTAGCAGAAATGTCAAGGTAAATGAGG3'

The mTLR4 double mutant was produced by introducing an Y454H replacement in the HA-mTLR4-N456H construct using the following primers:

Mutant	Primers
mTLR4-Y454H/N456H	Forward 5'AGCTACTTTACCTTGACATCTCTCATACTCACACCAAAATTGACT3' Reverse 5'AGTCAATTTTGGTGTGAGTATGAGAGATGTCAAGGTAAAGTAGCT3'

The soluble form of the hTLR4 (sTLR4) comprises the extracellular domain of native TLR4 (aa 27-628) lacking the N-terminus that encodes its signal sequence. Instead, the respective N-terminal region was replaced by N-terminal in-frame fusion to the signal peptide of the Igκ chain leader sequence to allow secretion in the absence of MD2. sTLR4 cDNA was constructed from pDisplay-HA-hTLR4 [97] by stop codon insertion at position Q628 using site-directed mutagenesis using the primers listed below:

Mutant	Primers
hTLR4-Q628* (sTLR4)	Forward 5'GTGCTGAGTTTGAATATCACCTGTTAGATGAATAAGACCATCATTG3' Reverse 5'CAATGATGGTCTTATTCATCTAACAGGTGATATTCAAACTCAGCAC3'

All the mutant cDNAs were sequenced to confirm the mutations.

3.11 qRT PCR array

Isolated total RNA (0.1 - 1 μg) was reverse transcribed using RT^2 First Strand Kit (Qiagen, Hilden) to obtain cDNA and internal controls. cDNA was then used to simultaneously monitor mRNA expression of 84 different human cytokine and cytokine receptor genes per sample by SYBR-green based qRT-PCR using the RT^2 Profiler™ PCR Array System (Array PAHS-022, Qiagen, Hilden). Experiments were performed according to the manufacturer's protocol using the suggested reagents. To allow statistical evaluation, average fold-induction and p-values from four independent experiments were calculated using an analysis template provided by the manufacturer. Data were each normalized to the expression of 4 different housekeeping genes run on the same 96-well plate. Only genes showing a mean regulation of at least 2.5-fold and a p-value <0.05 were considered to be significantly regulated. Genomic DNA contamination potentially masking reliable gene regulation was controlled for using a specific probe run in parallel. Gene-specific primers consistently delivering multiple PCR products or low T_m values as determined by melting curve analysis were excluded from the analysis to avoid false positives due to unspecific amplification or primer dimers, respectively.

3.12 Molecular biology techniques

Standard molecular biology methods were carried out as described by Sambrook et al. [95].

3.12.1 Transformation of plasmid DNA in bacteria

Transformation was performed by integrating the plasmid DNA into competent DH5α-bacteria using heat shock method, according to Sambrook et al. [95]. The transformed bacteria were plated for selection of plasmid-colonies with ampicillin resistance on Lysogeny Broth (LB) agar plates containing 50 µg ml^{-1} ampicillin. Single colonies were picked from overnight cultures and were expanded in LB medium with 50 µg ml^{-1} ampicillin.

3.12.2 Mini, midi and maxi preparation of plasmid DNA

Plasmid DNA preparations from the overnight cultures were purified using anion exchange columns from the Qiagen plasmid purification kits according to the manufacturer's protocol. At the end of the purification steps, the precipitated DNA was pelleted and adequate volume of dd H_2O was added depending on the size of the pellet (200 to 500 µl). The DNA concentration was measured photometrically determining absorbance at 260 nm using a Nanodrop 2000c system (Peqlab, Erlangen). The plasmid DNA was stored at -20°C for further usage.

3.12.3 Sequencing

Sequencing was performed using the BigDye terminator cycle sequencing kit from Thermo Fisher (Darmstadt) and carried out according to the method of Sanger [101]. Instead of radio-labeled Didesoxynucleosidetriphosphate (ddNTPs) distinct fluorescent ddNTPs were used. Mini preparation DNA was used as templates for the sequencing. The amount of DNA used was 50-100 ng and the primer concentration was 2 pmol $µl^{-1}$. All other reagents were used as recommended in the manufacturer's instructions. Alternatively, a commercial sequencing service from MWG-Eurofins (Munich) was used and samples processed according to the guidelines of the service company.

3.12.4 Restriction digestion, separation of DNA fragments by agarose gel electrophoresis

This method makes use of the property of restriction endonucleases to recognize and cut a specific and short sequence of DNA. For control of the successful preparation of plasmid DNA, 5 µl of the DNA solution was digested with 0.5 µl (corresponding to 5 Units) of two different appropriate restriction enzymes in 2 µl of 10 x buffer solution and 14 µl dd H_2O. Digestion reaction was performed for 1 to 2 h at 37°C. Preferentially, enzymes were

chosen that they cut out the insert from the plasmid DNA, so that a characteristic identification of the DNA fragment is created. Depending on the length of the expected fragments, gels were casted with an agarose concentration ranging from 0.8% to 1.5%. The agarose was dissolved completely by boiling briefly in an appropriate volume of 1 × TAE buffer. After cooling the solution to 50-60°C, the solution was mixed with 1 mg ml^{-1} ethidium bromide (about 1 µl/100 ml) and poured onto a gel compartment with comb for proper wells. The solidified gel was completely covered with TAE buffer in the electrophoresis chamber. The samples and a DNA molecular weight marker were dissolved in 6 x bromophenol blue sample buffer (see Section 2.2.1) and the mixture was transferred into the respective wells. After electrophoretic separation in an agarose gel, the DNA fragments were detected by UV light (λ = 312 nm) using the fluorescent intercalated ethidium bromide.

4 Results

4.1 Ni^{2+} activates NF-κB pathway

Previous studies from our laboratory have shown that the contact allergen Ni^{2+} is capable of directly targeting proinflammatory intracellular signal transduction cascades resulting in the activation of transcription factor NF-κB (**Fig. 1**) and the mitogen-activated protein (MAP) kinase p38 [57, 66, 102]. However, the molecular mechanisms underlying generation of the proinflammatory signal at that time were unknown. Subsequent gene profiling studies revealed that Ni^{2+} elicits an expression pattern reminiscent of innate immune signals, which is dominated by proinflammatory genes [59].

The initiation of such signals relies on membrane-bound and intracellular receptors known as PRRs. The best known classes are the TLR family, which primarily senses microbial pathogens, and the NOD-like receptors that not only detect microbes but also inorganic agents such as crystalline urates, asbestos, silica and aluminium [3] [103] [104].

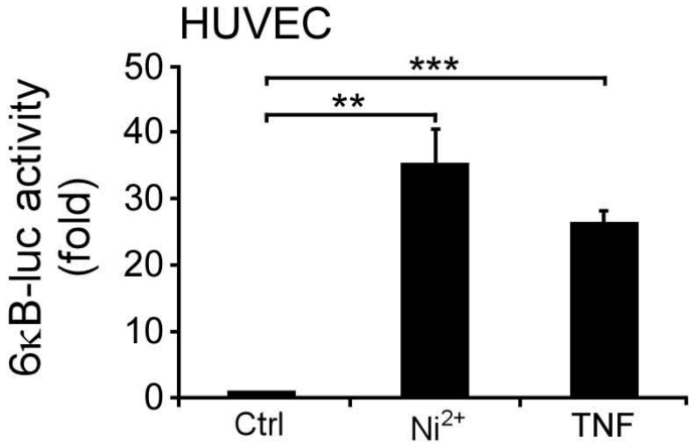

Fig. 1: Activation of NF-κB by the contact allergen Ni^{2+}. Fold average luciferase activation of a 6κB luciferase (luc) reporter transfected into HUVEC. Cells were stimulated for 16 h with Ni^{2+} (1.5 mM), TNF (2 ng ml^{-1}) or medium as control (Ctrl). Data represent mean ± S.D of three independent experiments. ** $p < 0.01$, *** $p < 0.001$ (unpaired *t*-test).

From the preliminary data, it was clear that one of the TLRs was likely to mediate the response to Ni^{2+}. It is well known that MyD88 is a general adaptor molecule for the Toll/IL-1R family of receptors and HUVECs display unique TLR4 surface expression, but lack functional expression of other surface TLRs [105].

Therefore, we evaluated the dependency of MyD88 by post transcriptional gene silencing. RNA interference (RNAi) of endogenous MyD88 abolished the Ni^{2+}-induced expression of IL-8 in ECs (**Fig. 2**). In agreement with published data [106], the response to IL-1β was blocked as well while TNFα-dependent IL-8 expression was unaltered. These data indicate that Ni^{2+} induces NF-κB-dependent gene expression via MyD88.

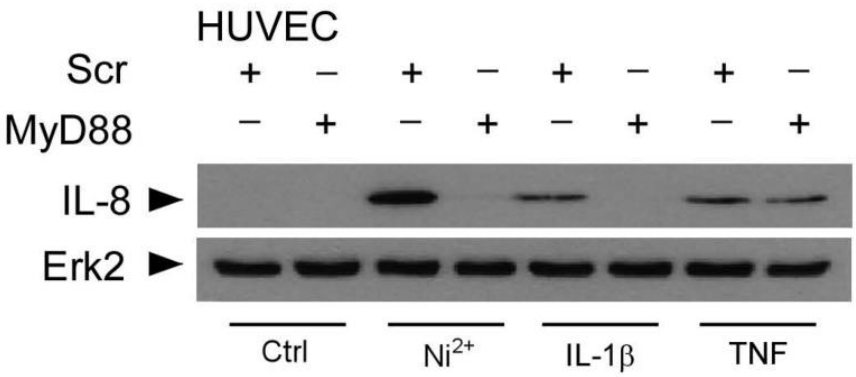

Fig. 2: Immunoblot of IL-8 expression upon stimulation with medium (Ctrl), Ni^{2+} (1.5 mM), IL-1β (10 U ml^{-1}) or TNF (2 ng ml^{-1}) in HUVEC transfected with siRNA for MyD88 or a scrambled siRNA control (Scr). Immunoblots are representative of three independent experiments.

We examined the involvement of TLR4 in the Ni^{2+}-induced response after excluding autocrine stimulation by IL-1 [66]. LPS, the natural ligand of TLR4 and potent proinflammatory activator, induced IL-8 to a similar extent as Ni^{2+} in ECs (**Fig. 3**).

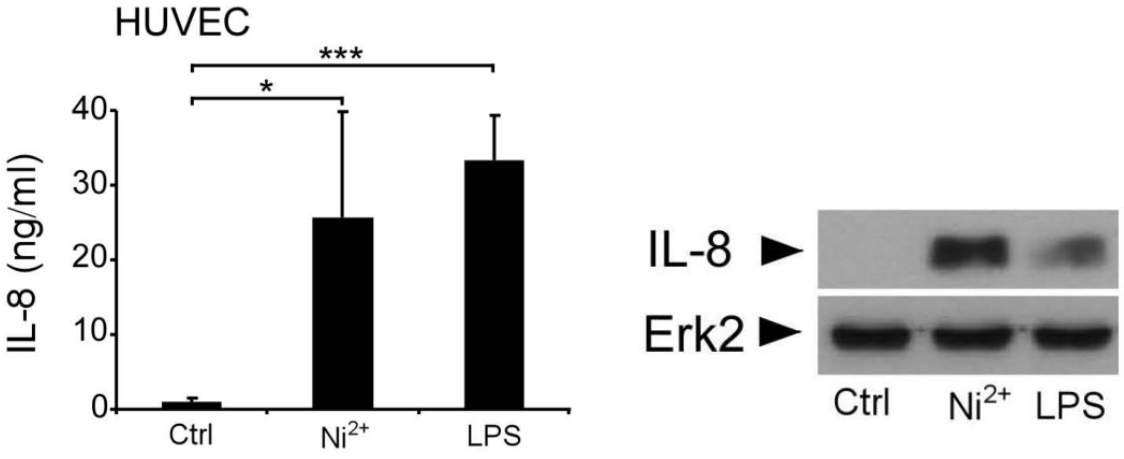

Fig. 3: IL-8 production determined by ELISA of supernatants (*left*) or immunoblot of cell lysates (*right*) in HUVEC stimulated with medium (ctrl), Ni^{2+} (1.5 mM) or the TLR4 agonist LPS (*E. coli* 026:B6; 1 µg ml^{-1}). Bar diagrams (*left*) represent average values of three independent experiments ± s.d. Immunoblots (*right*) are representative of three independent experiments. *$p < 0.05$, *** $p < 0.001$, unpaired *t*-test.

4.2 Ni^{2+}/Co^{2+}-induced TLR4 activation requires MD2

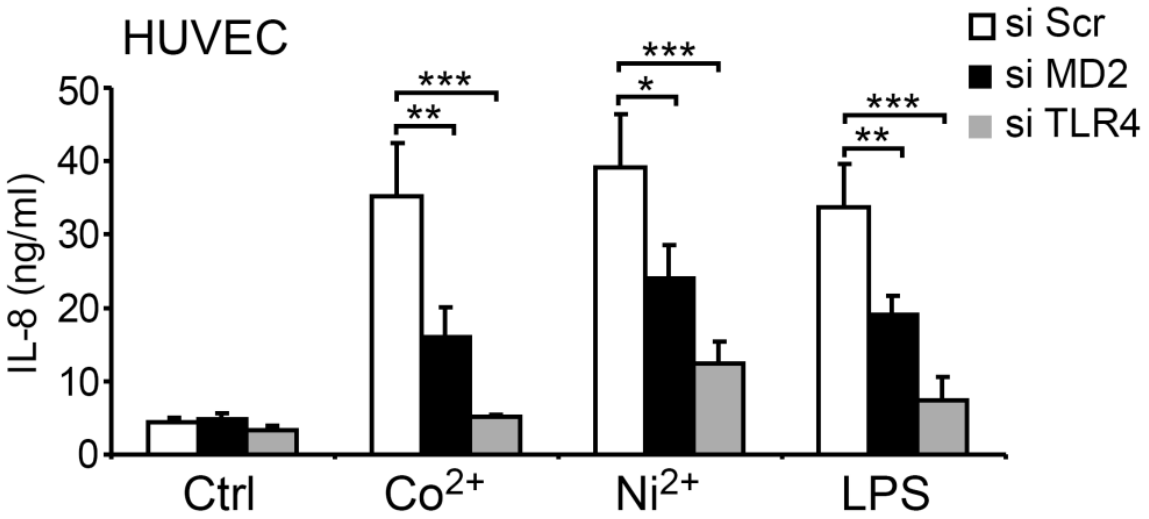

Fig. 4: Analysis of IL-8 production by ELISA from HUVEC transfected with siRNAs against MD2 or hTLR4 for 48 h prior to stimulation. Cells were then stimulated for 8 h with medium (ctrl), LPS (*S. minnesota* R595; 1 µg ml^{-1}), Ni^{2+} (1.5 mM) or Co^{2+} (1.5 mM), respectively. Bar diagrams represent average values of three independent experiments ± S.D. * $p < 0.05$, ** $p < 0.01$, *** $p < 0.001$ (unpaired *t*-test).

To unequivocally confirm that TLR4/MD2 expression was responsible for the observed innate immune activation by Ni^{2+}/Co^{2+}, we employed small interfering RNA (siRNA). Depletion of either TLR4 or MD2 significantly decreased LPS-, Ni^{2+}- and Co^{2+}-induced IL-8 production in ECs (**Fig. 4**).

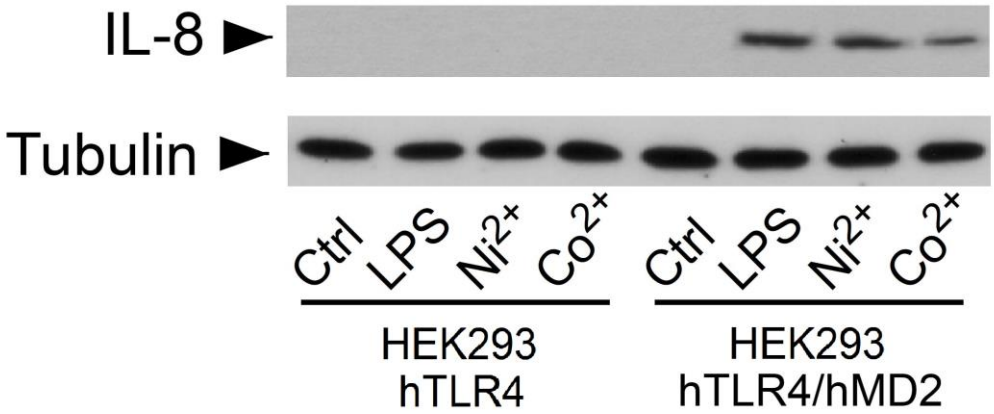

Fig. 5: Analysis of Ni^{2+}/Co^{2+}-induced IL-8 protein expression in the indicated cell lines as determined by western blot analysis of total lysates. Cells were stimulated for 8 h with medium (ctrl), Ni^{2+} (1.5 mM), Co^{2+} (1.5 mM) or LPS (*E. coli* 026:B6; 1 µg ml^{-1}) as positive control, respectively. The immunoblot is representative of three independent experiments.

Supplementation experiments in human HEK293 cells, which lack endogenous TLR4 and MD2 expression [107] confirmed a requirement of both receptor components for Ni^{2+}/Co^{2+}-induced NF-κB activation and proinflammatory gene expression (**Fig. 5-7**).

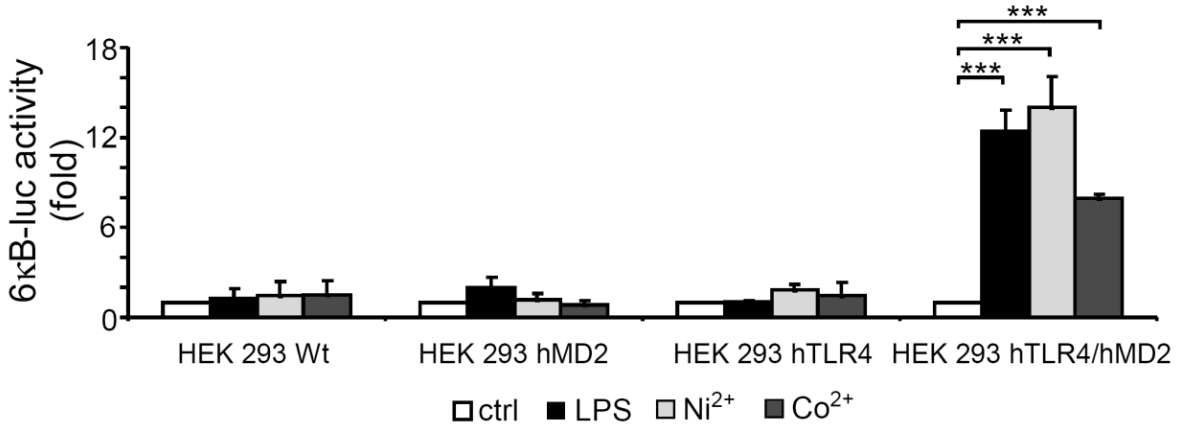

Fig. 6: Average fold luciferase activation of a 6κB luciferase (luc) reporter transfected into HEK293 WT, HEK293 cells stably expressing human MD2 (HEK293-hMD2), hTLR4 (HEK293-hTLR4) or hTLR4 and hMD2 (HEK293-hTLR4/hMD2), respectively. HEK cell lines were stimulated for 8 h with medium (ctrl), LPS (*S. minnesota* R595; 1 μg ml^{-1}), Ni^{2+} (1.5 mM) or Co^{2+} (1.5 mM) respectively. Data represent mean values of three independent experiments ± S.D. *** p <0.001 (unpaired t-test).

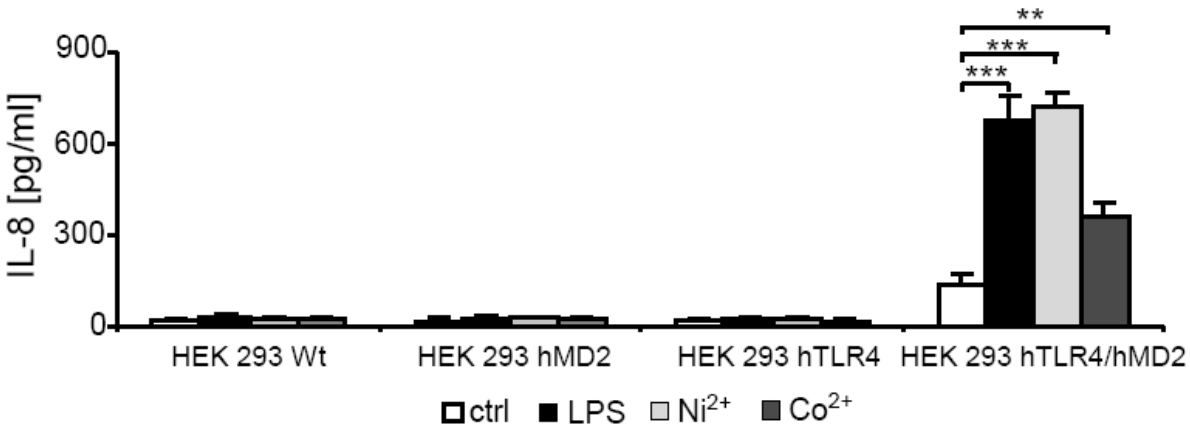

Fig. 7: Analysis of Ni^{2+}/Co^{2+}-induced IL-8 protein expression in the indicated cell lines as determined by ELISA of supernatants. Cells were stimulated for 8 h with medium (ctrl), LPS (*S. minnesota* R595; 1 μg ml^{-1}), Ni^{2+} (1.5 mM) or Co^{2+} (1.5 mM), respectively. Bar diagrams represent mean values of three independent experiments ± S.D. ** p <0.01, *** p <0.001 (unpaired t-test).

The response to Ni^{2+}/Co^{2+} was not due to LPS contamination since treatment with the LPS-inactivating drug polymyxin B sulphate failed to block activation by Ni^{2+}/Co^{2+} (**Fig. 8**). Together, these data show that Ni^{2+}/Co^{2+}-induced proinflammatory gene expression is independent of LPS but requires both hTLR4 and hMD2.

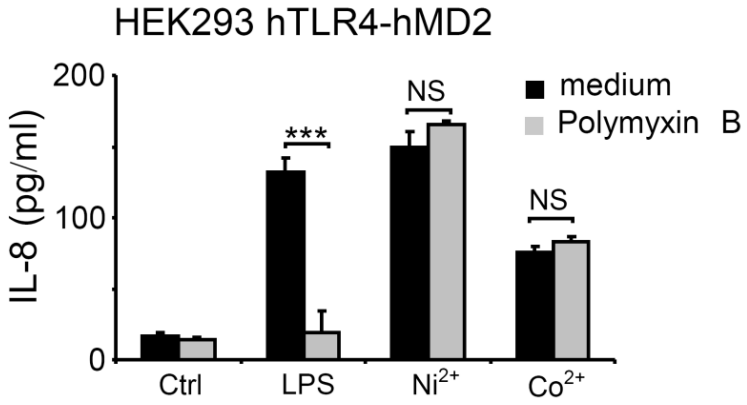

Fig. 8: Quantification of IL-8 in the supernatants of HEK293-hTLR4/hMD2 cells upon 8 h stimulation with medium (Ctrl), LPS (*E. coli* 055:B5; 1 µg ml^{-1}), Ni^{2+} (1.5 mM) or Co^{2+} (1.5 mM) in the absence or presence of polymyxin B sulphate (50 mg ml^{-1}). Data represent average values ± s.d. of three independent experiments. *** $p < 0.001$, NS, not significant (unpaired *t*-test).

4.3 Co^{2+} induces expression of multiple proinflammatory genes in primary ECs similar to that of Ni^{2+}

To understand more about the proinflammatory signaling cascades driven by Co^{2+}, we employed a quantitative real time PCR- (qRT-PCR-) based array system to study the RNA profiles of 84 human cytokine genes and receptors in primary human ECs. To evade the resultant consequences, we treated exponentially growing HUVECs for only a short time period (5 h) with 1.5 mM $CoCl_2$ and subjected RNA extractions from those samples to the qRT-PCR array. Material from four different experiments were analyzed in parallel to guarantee a high statistical significance.

Table 1 lists the proinflammatory genes that were significantly activated by Co^{2+}. These comprised of genes that were regulated by NF-κB such as CXCL3 (Gro-γ) or CCL20 (MIP3-α) [108] in addition to genes such as CXCL-10 (IP-10), which rather specify a type-I interferon response [109]. A comparison of the Co^{2+}-induced proinflammatory genes to those found in an earlier gene-chip microarray study of Ni^{2+}-regulated transcripts [59] showed a remarkable similarity of target genes by both stimuli, demonstrating a comparable style of action by both metal haptens.

A **Upregulated genes**

Gene Symbol	Description	Fold up by Co^{2+}	p-value	Regulation by Ni^{2+}
CXCL3 (Gro-γ)	Chemokine (C-X-C motif) ligand 3	36.28	0.042799	On
CCL20 (MIP3-α)	Chemokine (C-C motif) ligand 20	23.32	0.011699	On

CXCL2 (Gro-β)	Chemokine (C-X-C motif) ligand 2	14.84	0.048677	35.97
CXCL6 (GCP2)	Chemokine (C-X-C motif) ligand 6 (granulocyte chemotactic protein 2)	14.28	0.000209	21.68
CCL5 (RANTES)	Chemokine (C-C motif) ligand 5	13.40	0.033357	No
IL-8	Interleukin-8	11.72	4.47E-08	32.95
CXCL1 (Gro-a)	Chemokine (C-X-C motif) ligand 1 (melanoma growth stimulating activity, alpha)	8.01	0.002375	23.70
CXCL5 (ENA 78)	Chemokine (C-X-C motif) ligand 5	7.36	0.020081	12.75
LTB (TNFC)	Lymphotoxin beta (TNF C)	6.46	1.06E-07	On
IL1A	Interleukin 1, alpha	5.72	0.006050	On
TNF (TNF-α)	Tumor necrosis factor alpha	5.47	0.010384	No
CEBPB (NF-IL6)	CCAAT/enhancer binding protein, beta	5.18	0.010484	4.27
LTA (TNFB)	Lymphotoxin alpha (TNF ß)	3.63	0.000125	On
CXCL10 (IP-10)	Chemokine (C-X-C motif) ligand 10	3.40	0.009645	On

B Downregulated genes

Gene Symbol	Description	Fold down by Co^{2+}	p-value	Regulation by Ni^{2+}
CXCL12 (SDF1)	Chemokine (C-X-C motif) ligand 12 (stromal cell-derived factor 1)	-17.71	0.005603	No
AIMP1 (SCYE1)	Aminoacyl tRNA synthetase complex-interacting multifunctional protein 1/Small inducible cytokine subfamily E, member 1	-3.49	0.001465	-2.85
IL10RB	Interleukin 10 receptor, beta	-2.67	0.000044	No

Table 1: RNA isolated from HUVECs stimulated with Co^{2+} (1.5 mM) or medium as control for 5 h was used for qRT-PCR SYBR green array where the expression of 84 genes encoding cytokines and cytokine receptors was evaluated. Genes listed here correspond to the transcripts indicating at least a 2.5-fold mean up- or down-regulation by Co^{2+} in comparison to the unstimulated controls. Stringent evaluation of the genes with a unique amplification plot assessed by melt curve analysis and statistical significance (p-values < 0.05) from four individual experiments were deemed fit for the data analysis. A previously published Ni^{2+}-responsive genes identified in HUVEC [59] was utilized for co-regulation comparison.

4.4 Distinct skin cell types show divergent proinflammatory responsiveness to Ni^{2+}/Co^{2+}

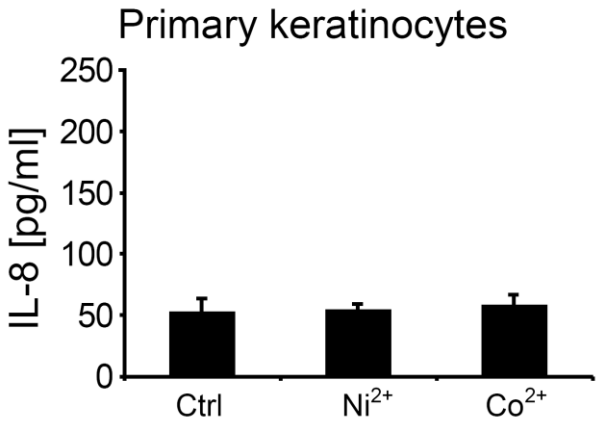

Fig. 9: Quantification of IL-8 levels in the culture supernatants of juvenile primary normal human epidermal keratinocytes (NHEK). Cells were stimulated for 8 h with Co^{2+} (1.5 mM), Ni^{2+} (1.5 mM) or medium as control (Ctrl). Bar diagrams represent average values of three independent experiments ± S.D.

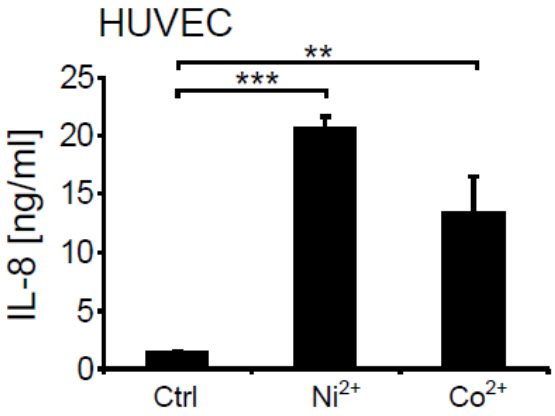

Fig. 10: Ni^{2+}/Co^{2+}-induced production of the NF-κB-dependent cytokine IL-8 as determined by ELISA of supernatants from HUVECs endogenously positive for hTLR4/MD2. Cells were stimulated for 8 h with Co^{2+} (1.5 mM), Ni^{2+} (1.5 mM) or medium as control (Ctrl). Bar diagrams represent average values of three independent experiments ± S.D. ** $p < 0.01$, *** $p < 0.001$ (unpaired *t*-test).

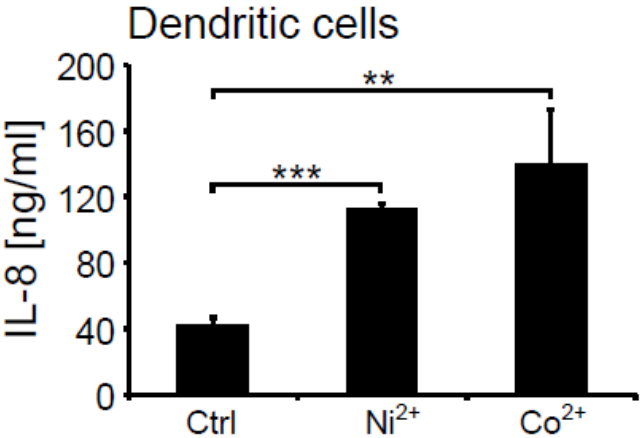

Fig. 11: Ni^{2+}/Co^{2+} induced IL-8 release from human immature DCs (iDCs). Cells were stimulated for 8 h with Co^{2+} (1.5 mM), Ni^{2+} (1.5 mM) or medium as control (Ctrl). Bar diagrams represent average ± S.D. values from three different donors. ** $p < 0.01$, *** $p < 0.001$ (unpaired *t*-test).

Innate immune activation of resident skin cells is the crucial step necessary for the clonal proliferation of hapten-specific T cells [110]. Therefore, it is essential to determine and compare the responsiveness of various primary human cell types of the skin towards Ni^{2+} and Co^{2+}. Other than DCs that are critically needed for the production of hapten-specific T cells, we also assessed keratinocytes which are not only the major cell type found in the epidermis but also the early responders of metal allergies *in vivo* [57, 78, 102]. Moreover, keratinocytes lend a big hand in the deployment of leukocytes into the endangered epidermal area upon re-exposure to the same allergen [111]. Surprisingly, we observed that both Ni^{2+} and Co^{2+} failed to trigger IL-8 synthesis in NHEKs only (**Fig. 9**) but not in primary human ECs and iDCs (**Fig. 10, 11**). From these results, it is clear that keratinocytes have an identifiable deficiency in perceiving signals from Ni^{2+} and Co^{2+} while, other skin cells do not share this trait.

4.5 Failure of keratinocytes to induce proinflammatory responses to Ni^{2+}/Co^{2+} is due to lack of TLR4

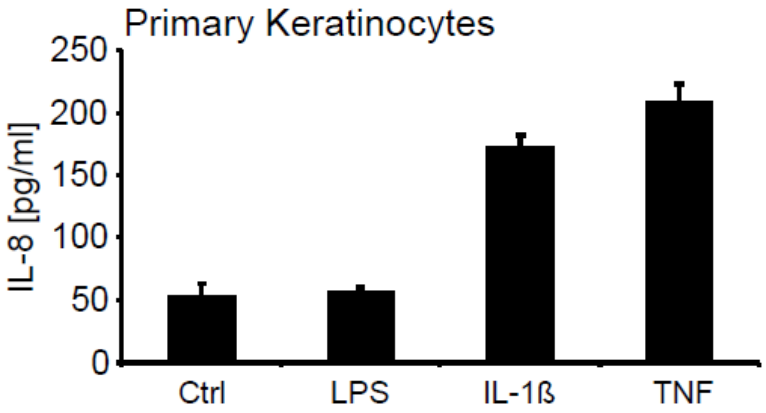

Fig. 12: IL-8 protein measurement in the supernatants of NHEK stimulated for 8 h with LPS (*S. minnesota* R595; 1 µg ml^{-1}), IL-1β (100 U ml^{-1}), TNF (10 ng ml^{-1}) or medium as control (Ctrl). Bar diagrams represent average values of three independent experiments ± S.D.

To evaluate if the failure of primary human keratinocytes may result from defective hTLR4 function, we stimulated NHEK with LPS, the native ligand for hTLR4 [112]. NHEK could not also upregulate the LPS driven IL-8 synthesis due to its failure in triggering hTLR4 activation (**Fig. 12**). However, they induced IL-8 upon stimulation with IL-1β or TNF, demonstrating that their insensitivity to hTLR4 stimulation was not due to a defect in the IKK2/NF-κB module or inability of those cells to produce IL-8 (**Fig. 12**).

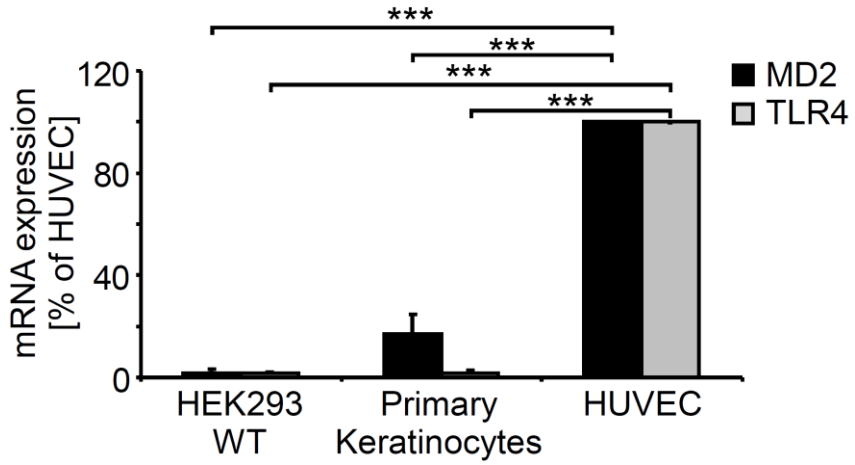

Fig. 13: qRT-PCR analysis of hMD2 (*black bars*) and hTLR4 (*grey bars*) mRNA expression in NHEK as compared to hTLR4/hMD2-negative HEK293 cells or hTLR4/hMD2-positive HUVEC. RNA was isolated from unstimulated cells and cDNA was subjected to qRT-PCR analysis using specific Taq-Man probes. Gene expression was each normalized to GAPDH expression. Data are presented as average-fold regulation ± S.D. as compared to the relative expression in HUVEC (arbitrarily set to 100%). Bar diagrams represent average values of three independent experiments ± S.D. *** p <0.001 (unpaired t-test).

Subsequent qRT-PCR experiments revealed that keratinocytes lacked detectable mRNA expression of hTLR4 but expressed low levels of the co-receptor MD2 (**Fig. 13**). Both $CaCl_2$ induced keratinocyte differentiation (**Fig. 14 a**) [113] verified by upregulation of differentiation marker loricrin (**Fig. 14 b**) as well as provoking with different proinflammatory stimuli including Co^{2+} or Ni^{2+} themselves was not able to upregulate hTLR4 mRNA expression above detectable limits (**Fig. 15**).

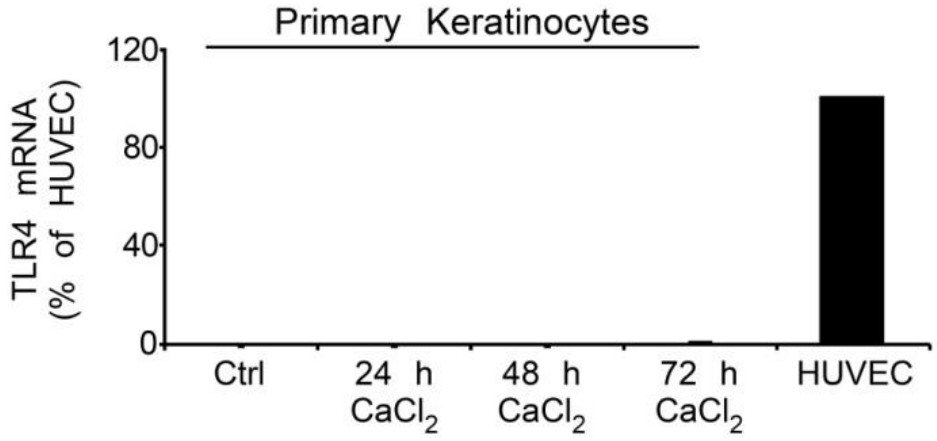

Fig. 14 a: Keratinocytes fail to induce TLR4 expression during differentiation. qRT-PCR analysis of TLR4 mRNA expression in NHEK as compared to TLR4/MD2-positive HUVEC. RNA was isolated from calcium differentiated NHEKs (1.0 mM $CaCl_2$ for the indicated times). After reverse transcription, cDNA was subjected to qRT-PCR analysis using specific Taq-Man probes. Gene expression was each normalized to GAPDH expression. Data are presented as average-fold regulation ± S.D. as compared to the relative expression in HUVEC (arbitrarily set to 100%). Bar diagrams represent average values of three independent experiments ± S.D.

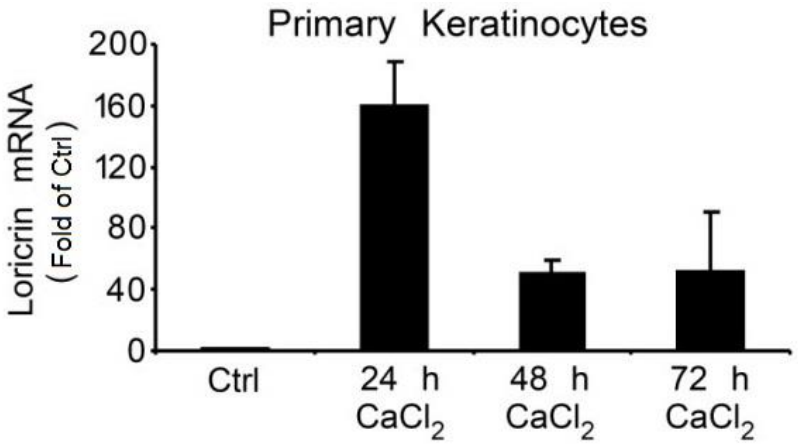

Fig 14 b: Differentiation was verified by increased mRNA expression of the differentiation marker loricrin. Data are presented as average-fold regulation ± S.D. as compared to the relative expression in HUVEC (arbitrarily set to 1). Data represents at least three independent experiments.

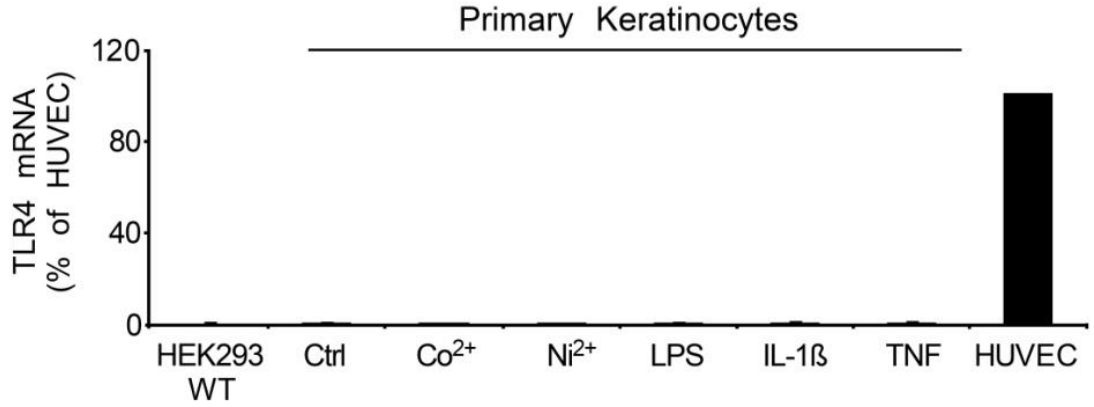

Fig. 15: Keratinocytes fail to induce TLR4 expression upon proinflammatory activation. qRT-PCR analysis of TLR4 mRNA expression in NHEK treated with the indicated proinflammatory stimuli for 16 h. After reverse transcription, cDNA was subjected to qRT-PCR analysis using specific Taq-Man probes. Gene expression was each normalized to GAPDH expression. Data are presented as average-fold regulation ± S.D. as compared to the relative expression in HUVEC (arbitrarily set to 100%). Data represent at least three independent experiments.

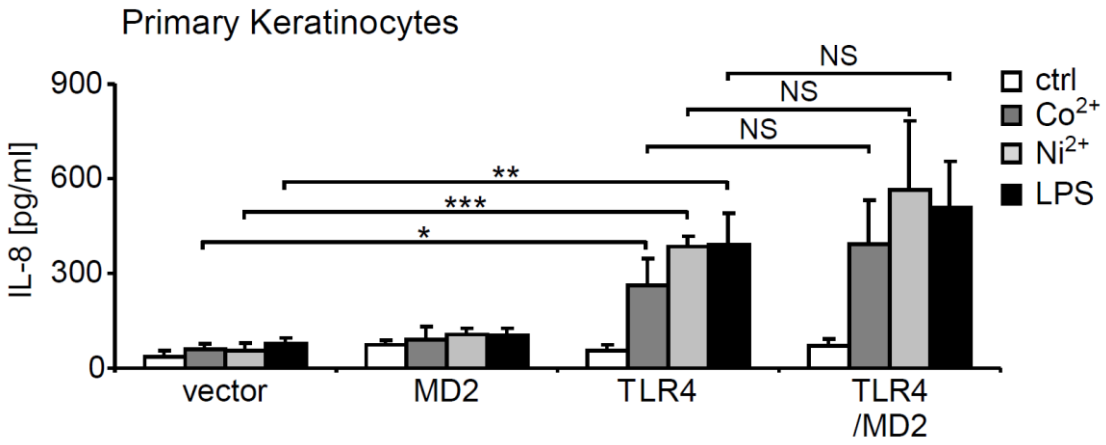

Fig. 16: ELISA data showing IL-8 production in supernatants of NHEK transfected with hMD2, hTLR4, or both in combination. Cells were stimulated for 8 h with medium (ctrl), LPS (*S. minnesota* R595; 1 μg ml^{-1}), Ni^{2+} (1.5 mM) or Co^{2+} (1.5 mM), respectively. Bar diagrams represent average values of three independent experiments ± S.D. * $p < 0.05$, ** $p < 0.01$, *** $p < 0.001$, NS - not significant (unpaired *t*-test).

This suggests that lack of hTLR4 expression is not a specific feature of undifferentiated or non-activated keratinocytes. Transfection of hTLR4 alone without MD2 was adequate to impart sensitivity to Ni^{2+} and Co^{2+} in these cells (**Fig. 16**) indicating that the absence of hTLR4 accounts for the non-reactivity of keratinocytes to these metal allergens.

4.6 Ni^{2+}/Co^{2+} activates hTLR4, but not mTLR4

Next, we evaluated whether Ni^{2+}/Co^{2+} could trigger proinflammatory gene expression in other cell types. Human monocytic cell line THP-1 (**Fig. 17**) significantly up-regulated IL-8, which is a direct target gene of NF-κB upon Ni^{2+}/Co^{2+} stimulation. Interestingly, mouse-derived cells like bEND2 and Raw 264.7 macrophages (**Fig. 18**) did not synthesise TNF upon Ni^{2+}/Co^{2+} stimulation. However, LPS stimulation resulted in a significant upregulation of TNF (**Fig. 18)** indicating that the failure of murine cells to Ni^{2+}/Co^{2+} was not due to the absence of TLR4 or MD2.

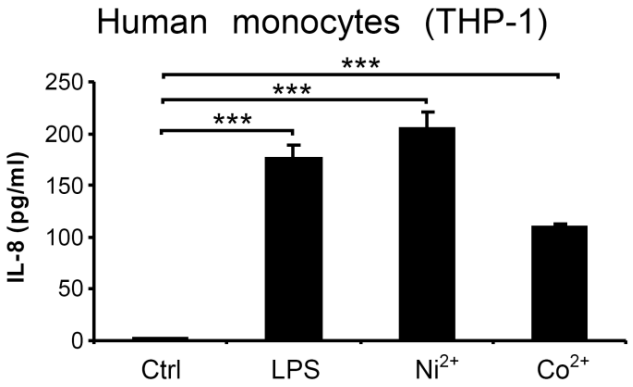

Fig. 17: Ni^{2+}/Co^{2+}-dependent production of IL-8 in the human monocytic cell line THP-1. Cells were stimulated for 8 h with medium (ctrl), LPS (*E. coli* 055:B5; 1 µg ml^{-1}), Ni^{2+} (1.5 mM) or Co^{2+} (1.5 mM), respectively. Bar diagrams represent average values of three independent experiments ± S.D. *** p <0.001, (unpaired *t*-test).

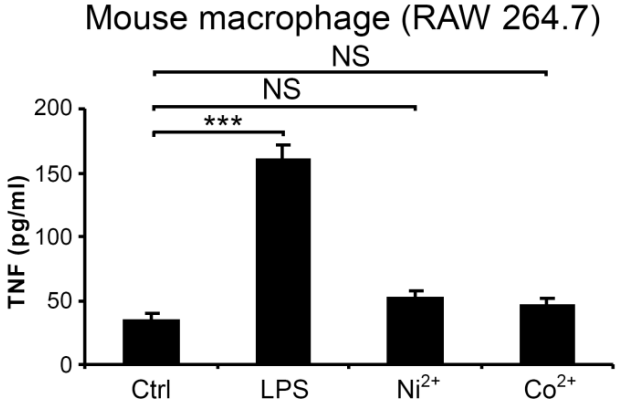

Fig. 18: Failure of Ni^{2+}/Co^{2+} to induce the NF-κB target TNF in the mouse macrophage cell line (RAW 264.7). Cells were each stimulated for 8 h with medium (ctrl), Co^{2+} (1.5 mM), Ni^{2+} (1.5 mM) or LPS

(*S. minnesota* R595; 1 µg ml^{-1}). Data represent averages of three independent experiments ± s.d. *** $p < 0.001$, NS, not significant (unpaired *t*-test).

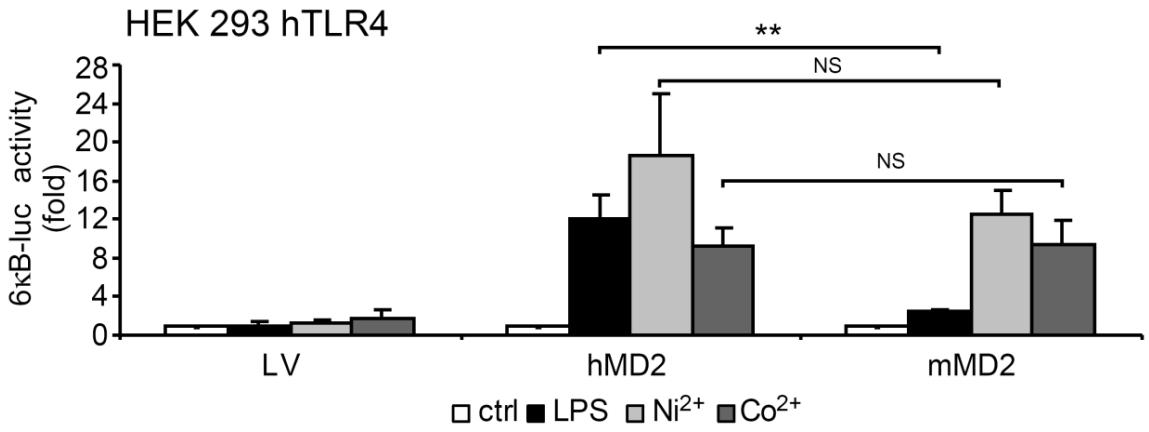

Fig. 19: Activation of a 6κB-luciferase reporter from hTLR4 expressing HEK293 cells transfected with hMD2, mMD2 or empty vector and stimulated with medium (ctrl), Co^{2+} (1.5 mM), Ni^{2+} (1.5 mM) or LPS (*S. minnesota* R595; 1 µg ml^{-1}). Data represent averages of three independent experiments ± s.d. ** $p < 0.01$, NS, not significant (unpaired *t*-test).

Further, HEK293 cells stably expressing hTLR4 were transfected with either hMD2 or mMD2 to test if the NF-κB activation by Ni^{2+}/Co^{2+} was due to species-specific differences in MD2. To our surprise the signals mediated by Ni^{2+}/Co^{2+} were perceived by hTLR4 (**Fig. 19, 20**) regardless of the source of the transfected MD2, indicating that the species specificity is conferred by TLR4.

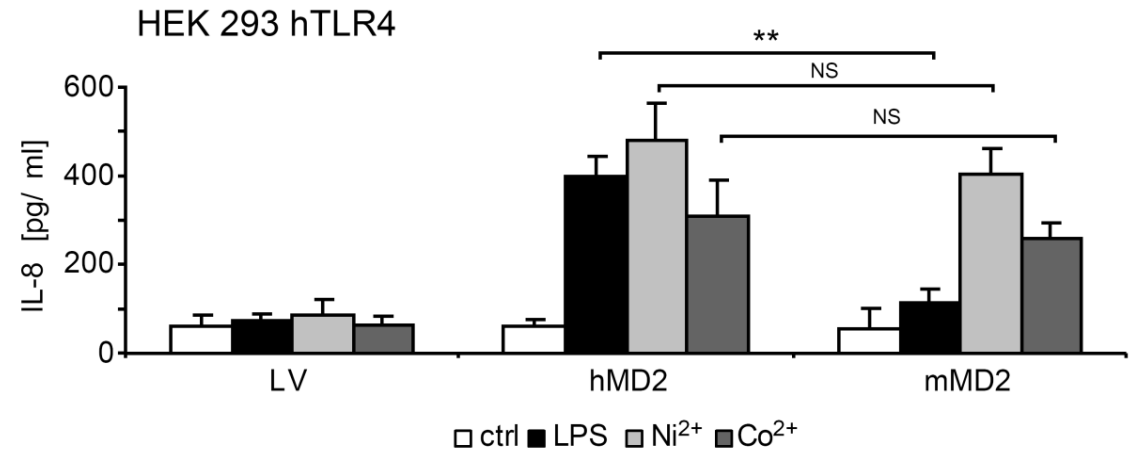

Fig. 20: IL-8 release determined by ELISA of supernatants from hTLR4 expressing HEK293 cells transfected with hMD2, mMD2 or empty vector and stimulated with medium (ctrl), Co^{2+} (1.5 mM), Ni^{2+} (1.5 mM) or LPS (*S. minnesota* R595; 1 µg ml^{-1}). Data represent averages of three independent experiments ± s.d. ** $p < 0.01$, NS, not significant (unpaired *t*-test).

4.7 Ni^{2+}-induced gene expression requires sequence motifs present in hTLR4 but not in mTLR4

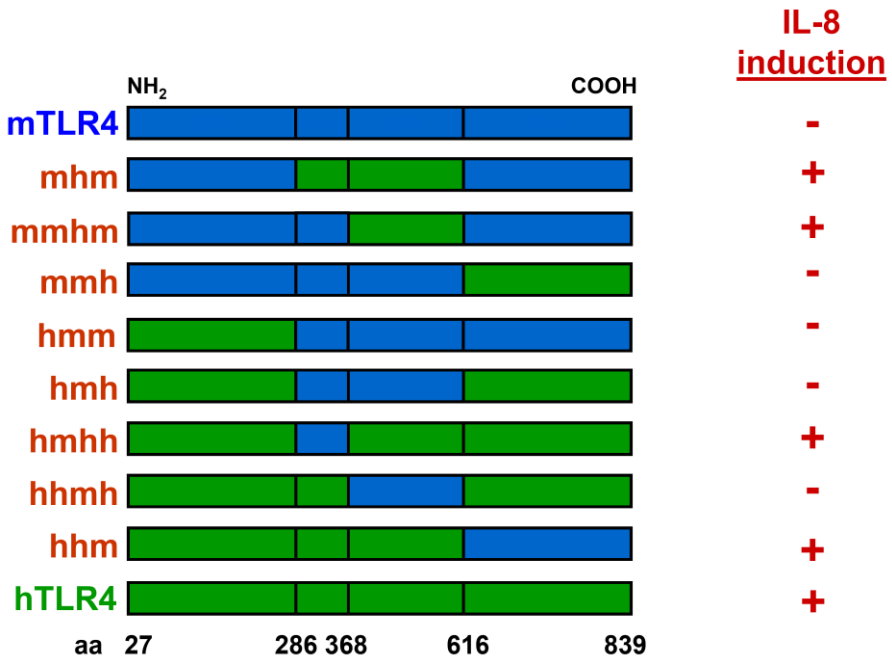

Fig. 21: ELISA of IL-8 release (− indicates < 2-fold increase; + indicates ≥ 2-fold increase) in HEK293 hMD2 cells and transfected with HA-hTLR4, HA-mTLR4 or the indicated chimeric HA-TLR4 constructs. Cells were exposed to medium (Ctrl), Ni^{2+} (1.5 mM) or LPS (*S. minnesota* R595; 1 µg ml^{-1}) for 8 h. Data are representative of four independent experiments. Human sequence parts are shown in green and mouse parts in blue colour.

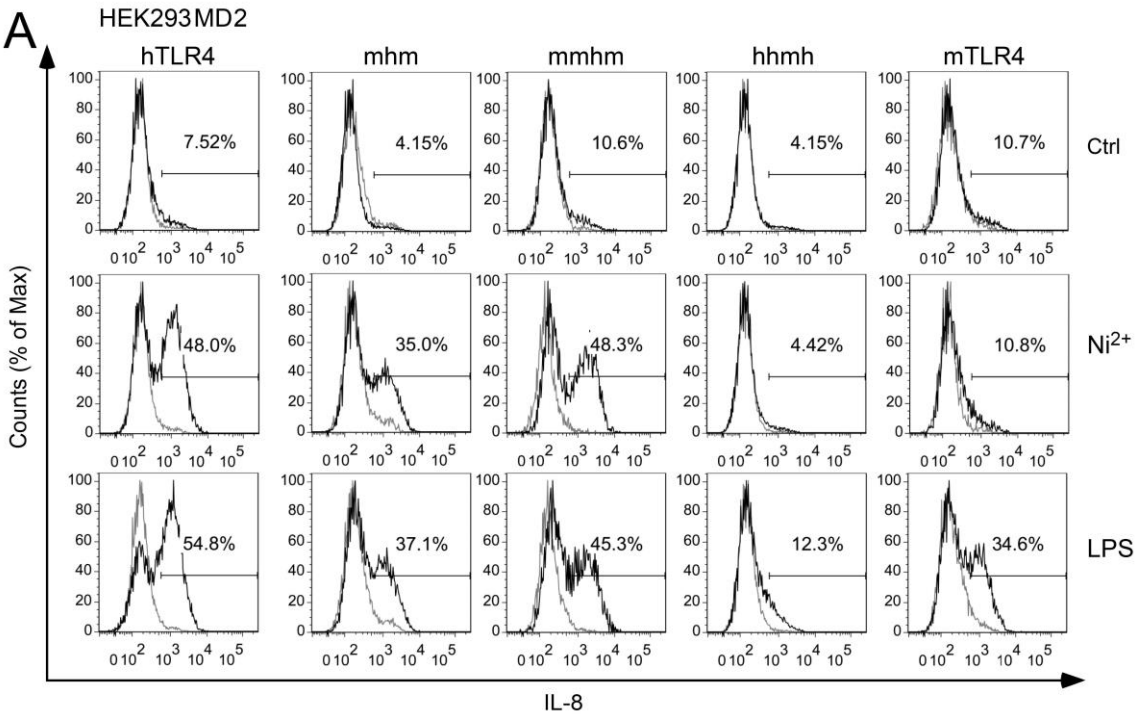

Fig. 22: Flow cytometry of intracellular IL-8 protein expressed by positively transfected cell population. Stable HEK293 hMD2 cells were transfected with HA-hTLR4, HA-mTLR4 or the indicated chimeric HA-TLR4 constructs and exposed to Ni^{2+} (1.5 mM) or LPS (*S. minnesota* R595; 1 µg ml^{-1}) for 8 h. Transfection efficiency was monitored by HA-immunostaining and gating on the HA-positive population. Histogram overlays of IL-8 staining (*black lines*) and isotype-staining (*grey lines*) representative of three independent

experiments are provided. Numbers denote the percentage of IL-8 expressing cells in the HA-gated population.

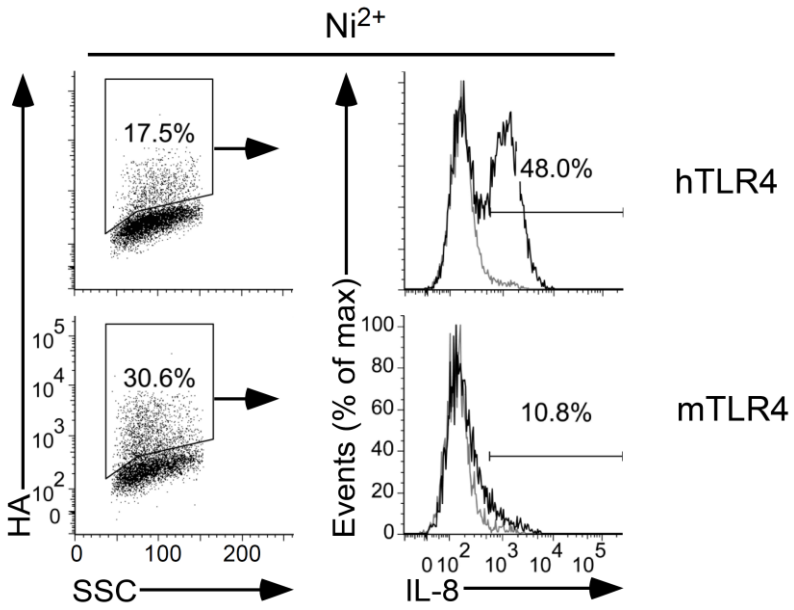

Fig. 23: The failure of mTLR4 to respond to Ni^{2+} is not due to inefficient expression. Flow cytometry analysis of intracellular IL-8 and HA staining in hMD2-expressing HEK293 cells transfected with HA-hTLR4 or HA-mTLR4 after treatment with Ni^{2+} (1.5 mM) for 8 h. The indicated cell population in the dot blots represents the successfully transfected HA-positive live cell population (HA^+), used as gate for the IL-8 quantifications (histograms). Histograms are identical to those presented in **Fig. 22**. Percentages of total HA positivity in the live population and of IL-8 positivity in the gated HA^+ population are indicated. Data are representative of three independent experiments.

The difference in responsiveness to Ni^{2+}/Co^{2+} between hTLR4 and mTLR4 triggered our curiosity. Therefore, either HA-tagged wild type constructs for hTLR4 or mTLR4 were transfected into HEK293 cells stably expressing hMD2, in addition to HA-tagged chimeric TLR4 with unique single or multiple residue alterations of hTLR4 and mTLR4 [97]. Initially we stimulated transfected cells with Ni^{2+} or LPS. These experiments showed that cells expressing hTLR4-hMD2 gave a very strong response to Ni^{2+}, whereas those with mTLR4-hMD2 could not prompt IL-8 synthesis upon Ni^{2+} exposure (**Fig. 21, 22**). Moreover, we got clear evidences that the amino acid sequence from 369 to 616 of the hTLR4 is critically necessary for the activation of NF-κB-dependent gene expression by Ni^{2+} (**Fig. 21, 22**). These differences did not arise due to non-responsive constructs or different levels of expression, which was controlled by co-staining with a specific HA-tagged antibody (**Fig. 23**).

4.8 Histidine residues mediate Ni^{2+} responsiveness

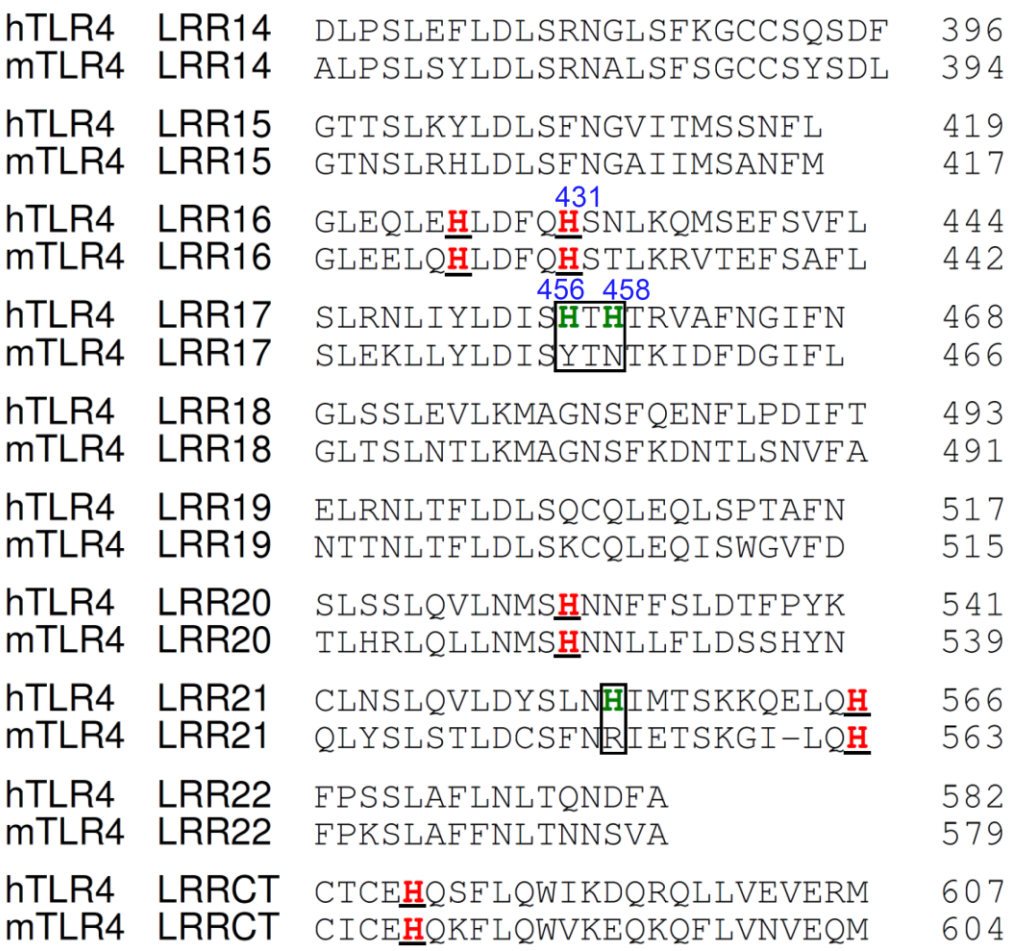

Fig. 24: Protein sequence alignment of hTLR4 and mTLR4 between aa 371-604 covering the leucine-rich repeats (LRR) 14-22 located in the C-terminal domain of the TLR4 β sheet [92]. Conserved histidine residues (H) are shown underlined and in red colour bold letters, non-conserved histidines are indicated by boxed green colour.

Using protein sequence alignment, amino acid variations of hTLR4 and mTLR4 in the N-terminal leucine-rich repeats (LRR) 14 to 22 were determined (**Fig. 24**). The non-conserved histidine (H) residues at 456, 458 and 555 in the hTLR4 sequence caught our attention due to the fact that histidine-tagged proteins can be purified by nickel/cobalt columns. We hypothesized that the non-conserved histidines may be vital for the responsiveness to Ni^{2+} signals. From the crystal structure of hTLR4-hMD2 [92], we could easily identify that the two non-conserved histidines at 456 and 458 are very close to the conserved histidine residue at 431. In a heterodimer confirmation, these residues are postulated to form a cluster of six histidine moieties at the base of the two-fold symmetry axis of the hTLR4 monomers (**Fig. 25**). This layout revealed various prospective cross-linking binding sites for Ni^{2+}. Additionally, biophysical analysis of the putative metal

binding interface showed that the imidazole groups of H456 and H458 are predominantly in optimal interval for Ni^{2+} interaction, but the ones from H431 are far-off (**Fig. 25**).

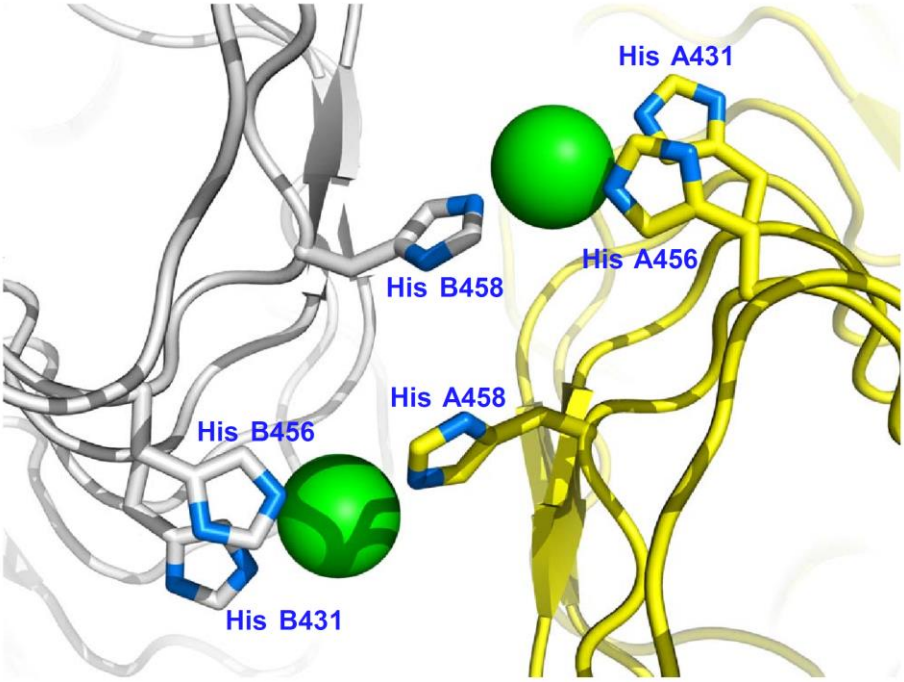

Fig. 25: Model of the potential double metal-binding site in hTLR4 showing a close-up view from the top along the two-fold symmetry axis. The model is based on the crystal structure of the hTLR4-hMD2 complex (PDB entry 3FXI) with LPS omitted. The side chains of the histidine residues H431, H456 and H458 (sticks with nitrogen colored blue) were repositioned with appropriate side chain rotamers, followed by addition of Ni^{2+} ions (green spheres) to yield a pair of metal-binding sites with a geometry similar to that seen in an engineered serine protease/inhibitor complex (PDB entry 1SLW) [114].

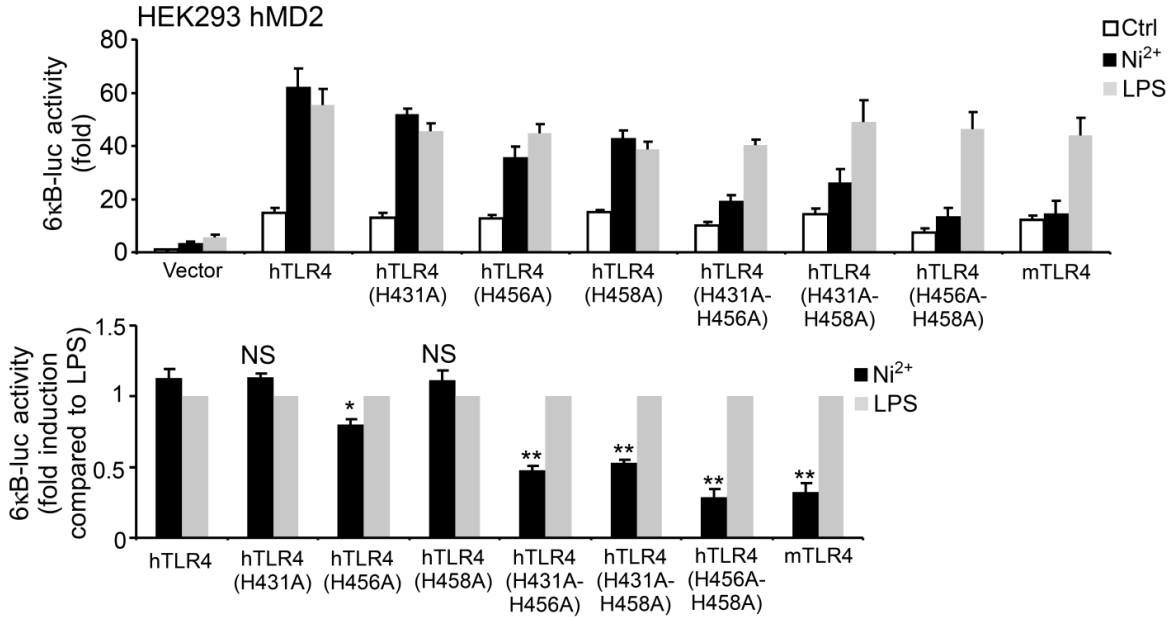

Fig. 26: Luciferase activity of a 6κb-luc reporter transfected into HEK293 cells stably expressing hMD2 and the indicated TLR4 constructs. Cells were stimulated for 8 h with medium (Ctrl), Ni^{2+} (1.5 mM) or LPS

(*S. minnesota* R595; 1 µg ml^{-1}). Luciferase activity is presented as fold stimulation (*top*) or as Ni^{2+} stimulation in relation to LPS (arbitrarily set to 1, *bottom*), respectively. Data represents mean ± s.d. of three independent experiments. *$p < 0.01$, ** $p < 0.001$, NS, non-significant, unpaired *t*-test.

To analyse the necessity of the histidines at 431, 456 and 458, numerous single or double alanine replacement mutants were synthesised and transfected into HEK293 cells stably expressing hMD2. In luciferase assays, single mutations at H431 and H458 had no impact on NF-κB activation induced by Ni^{2+} while mutation at H456 rendered a partial decrease in Ni^{2+} responsiveness (**Fig. 26**). Contrastingly, all double mutants effectively diminished NF-κB-dependent gene expression regulated by Ni^{2+} with the best inhibition ensuing upon mutation at the non-conserved human-specific H456 and H458 (**Fig. 26**).

4.9 Histidines H456 and H458 in hTLR4 are required for Ni^{2+}-induced proinflammatory gene expression

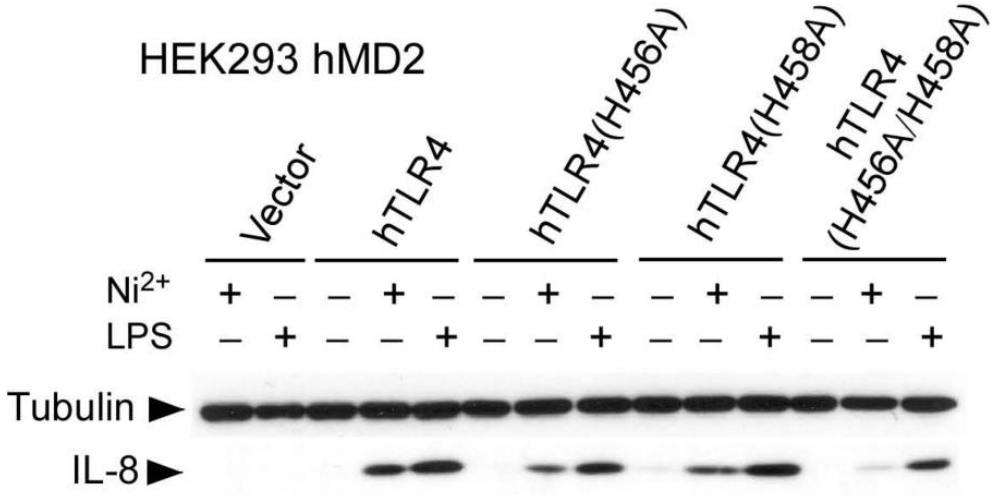

Fig. 27: Immunoblot analysis of IL-8 protein in lysates. HEK293 cells stably expressing hMD2 were transfected with HA-tagged wild type or mutated hTLR4 constructs (hTLR4-H456A, hTLR4-H458A or hTLR4-H456A-H458A) and stimulated with medium (ctrl), Ni^{2+} (1.5 mM) or LPS (*S. minnesota* R595; 1 µg ml^{-1}). Equal loading was controlled by immunolabeling for tubulin. The immunoblot is representative of three independent experiments.

Consistently, double replacement of histidines with alanine at 456 and 458 positions, diminished the Ni^{2+}-induced IL-8 production significantly in various outcomes including western blot (**Fig. 27**), flow cytometry (**Fig. 28**) and ELISA (**Fig. 29**), while the single mutants H456 or H458 had very little or no effects, respectively. Interestingly, LPS induced gene regulation was not altered by any of the mutants (**Fig. 26-29**), demonstrating that LPS and Ni^{2+} require distinctive binding sequences for TLR4 activation.

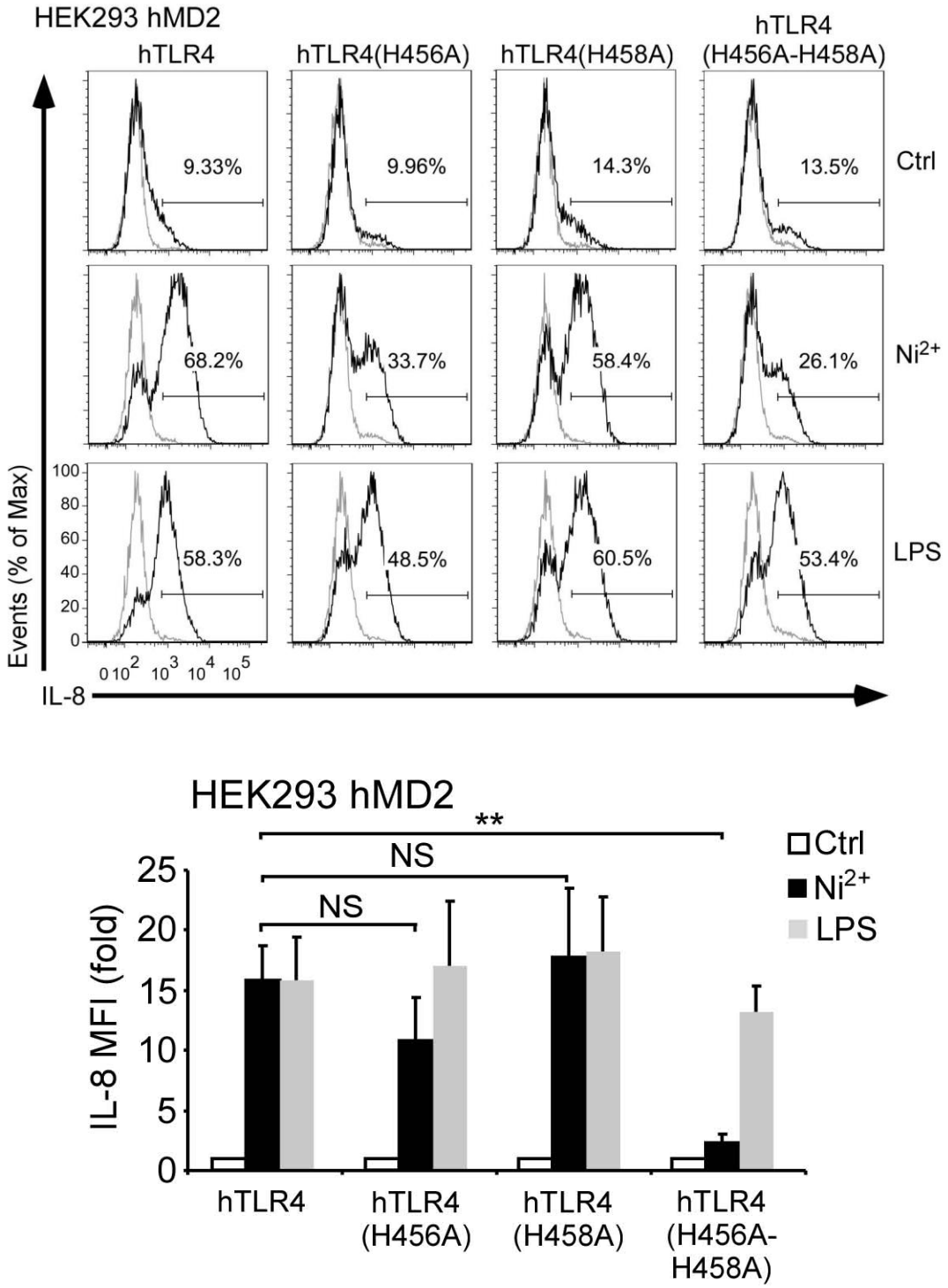

Fig. 28: Flow cytometry of intracellular IL-8 staining for the indicated HA-positive cell population as identified by HA-co-immunostaining and appropriate gating (*upper panel*). HEK293 cells stably expressing hMD2 were transfected with HA-TLR4 constructs containing the indicated point mutations or empty expression vector as control. Cells were exposed to medium (Ctrl), Ni^{2+} (1.5 mM) or LPS (*S. minnesota* R595; 1 µg ml^{-1}) for 8 h and subsequently processed for intracellular flow cytometry to detect IL-8. Black profiles represent IL-8 expression and grey profiles denote isotype controls. Flow cytometric quantification of averaged isotype-corrected median fluorescence intensities, MFI (*lower panel*) from three independent experiments ± s.d. Cells have been gated for positive transfection by anti-HA co-staining.

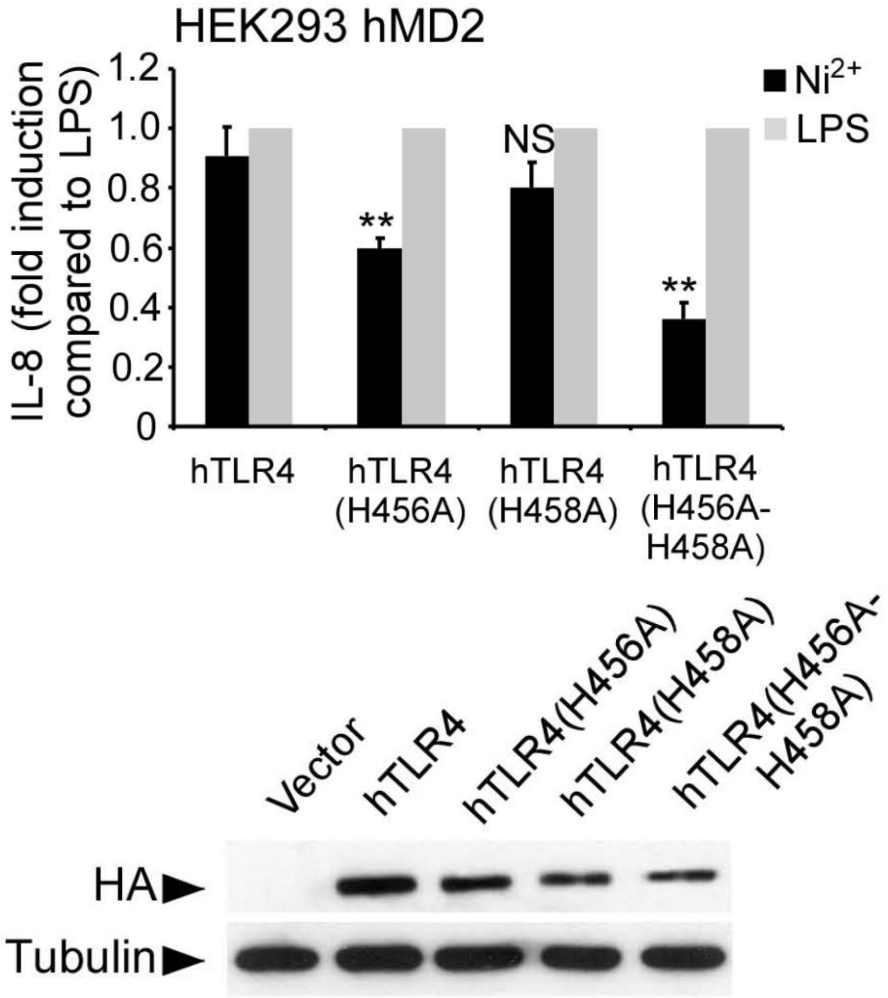

Fig. 29: ELISA analysis of IL-8 release in response to stimulation with Ni^{2+} (*upper panel*). Successful expression of the hTLR4 transgenes was confirmed by western blot for the HA-tag (*lower panel*). HEK293 stably expressing hMD2 were transfected with HA-tagged TLR4 constructs containing the indicated point mutations or empty expression vector as control. Cells were exposed to medium (Ctrl), Ni^{2+} (1.5 mM) or LPS (*S. minnesota* R595; 1 µg ml^{-1}) for 8 h and subsequently processed for ELISA to detect IL-8. Data are shown in relation to induction by LPS (arbitrarily set to 1) and represent averages ± s.d of three independent experiments.

Double insertion of histidines in mTLR4 at 454 and 456 positions was sufficient to mimic the human situation. Indeed, expression of mTLR4 (Y454H-N456H) double mutant in HEK cells imparted a significant Ni^{2+} responsiveness (**Fig. 30**). From these experiments, it is very clear that distinctive amino acids in hTLR4 impose the observed species difference for Ni^{2+} recognition by cells of human and murine origin.

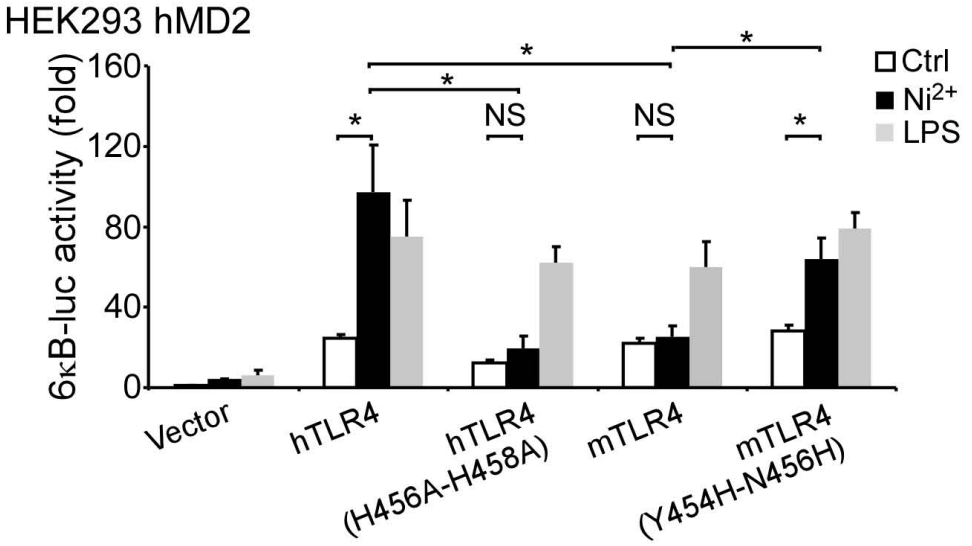

Fig. 30: Luciferase activity of a transfected 6κB-luc reporter in HEK293-hMD2 cells transfected with hTLR4, hTLR4 bearing inactivating alanine replacements at the putative metal-binding histidines (hTLR4-H456A-H458A), murine TLR4 (mTLR4), or a "humanized" mTLR4 mutant containing histidine substitutions at the corresponding positions in the mouse sequence (mTLR4-Y454H-N456H), respectively. Cells were stimulated with medium (Ctrl), Ni^{2+} (1.5 mM) or LPS (*S. minnesota* R595; 1 µg ml^{-1}) for 8 h. Data represent mean fold values of three independent experiments ± s.d. * $p < 0.01$, NS, not significant (unpaired *t*-test).

4.10 Co^{2+} activates hTLR4/MD2 in a similar fashion to that of Ni^{2+}

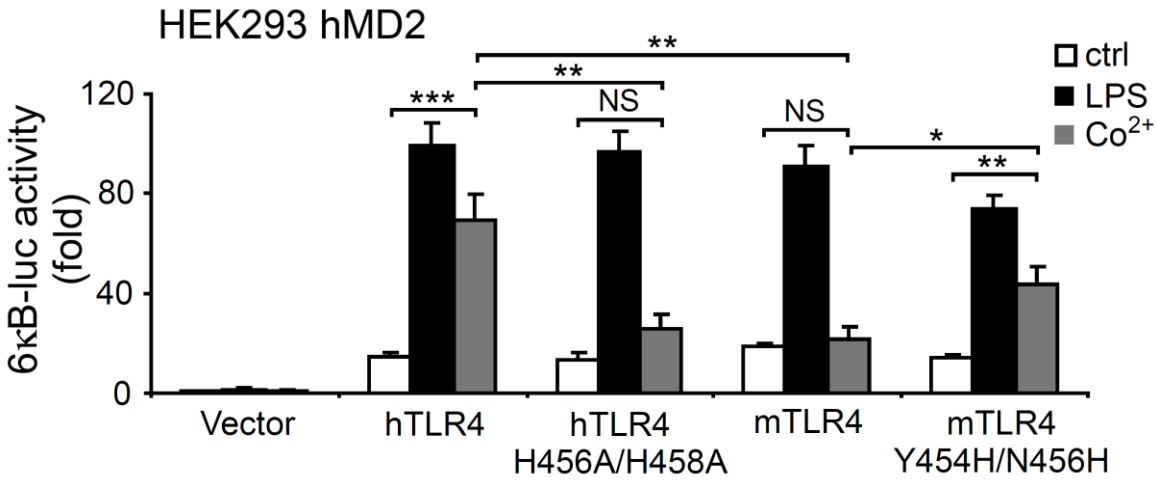

Fig. 31: Co^{2+}-induced luciferase activity of a 6κB-luc reporter upon transfection of HEK293 hMD2 cells with indicated constructs. Cells were stimulated with medium (Ctrl), Co^{2+} (1.5 mM) or LPS (*S. minnesota* R595; 1 µg ml^{-1}) for 8 h. Bar diagrams represent mean fold values of three independent experiments ± S.D. * $p < 0.05$, ** $p < 0.01$, *** $p < 0.001$, NS - not significant (unpaired *t*-test).

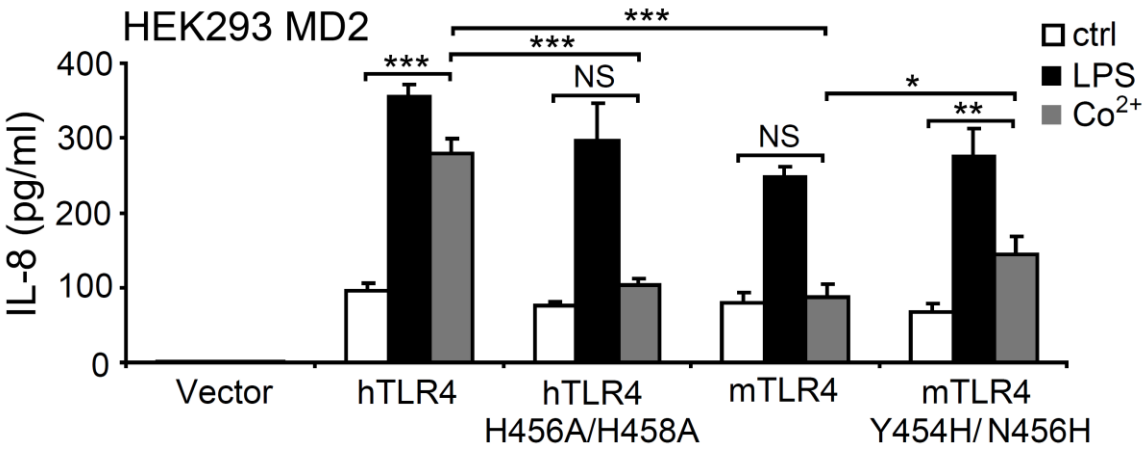

Fig. 32: IL-8 release measured by ELISA of supernatants from HEK293 hMD2 cells transfected with indicated constructs. Cells were stimulated with medium (Ctrl), Co^{2+} (1.5 mM) or LPS (*S. minnesota* R595; 1 µg ml^{-1}) for 8 h. Data represent averages of three independent experiments ± S.D. * $p < 0.05$, ** $p < 0.01$, *** $p < 0.001$, NS, not significant (unpaired *t*-test).

To evaluate if the Co^{2+}-induced proinflammatory gene expression is also dependent on non-conserved histidines H456 and H458 of hTLR4, we used the previously generated alanine double mutants. Replacement of histidines with alanine at both 456 and 458 positions delivered a striking reduction of Co^{2+} responsiveness in all the experiments including 6κB-dependent promoter-reporter gene assay (**Fig. 31**), IL-8 ELISA (**Fig. 32**) or flow cytometry for IL-8 (**Fig. 33**).

Contrarily, "humanized" mTLR4 (Y454H-N456H) expression in HEK293 hMD2 cells rendered responsiveness to Co^{2+} (**Fig. 31, 32**). From these experiments, it is very clear that Ni^{2+} and Co^{2+} activate the proinflammatory cascades in a similar fashion through TLR4 activation followed by NF-κB stimulation. Remarkably, all the mutants were able to render responsiveness to LPS (**Fig. 31-33**), demonstrating that both the ligands require different sequences for TLR4 binding and activation.

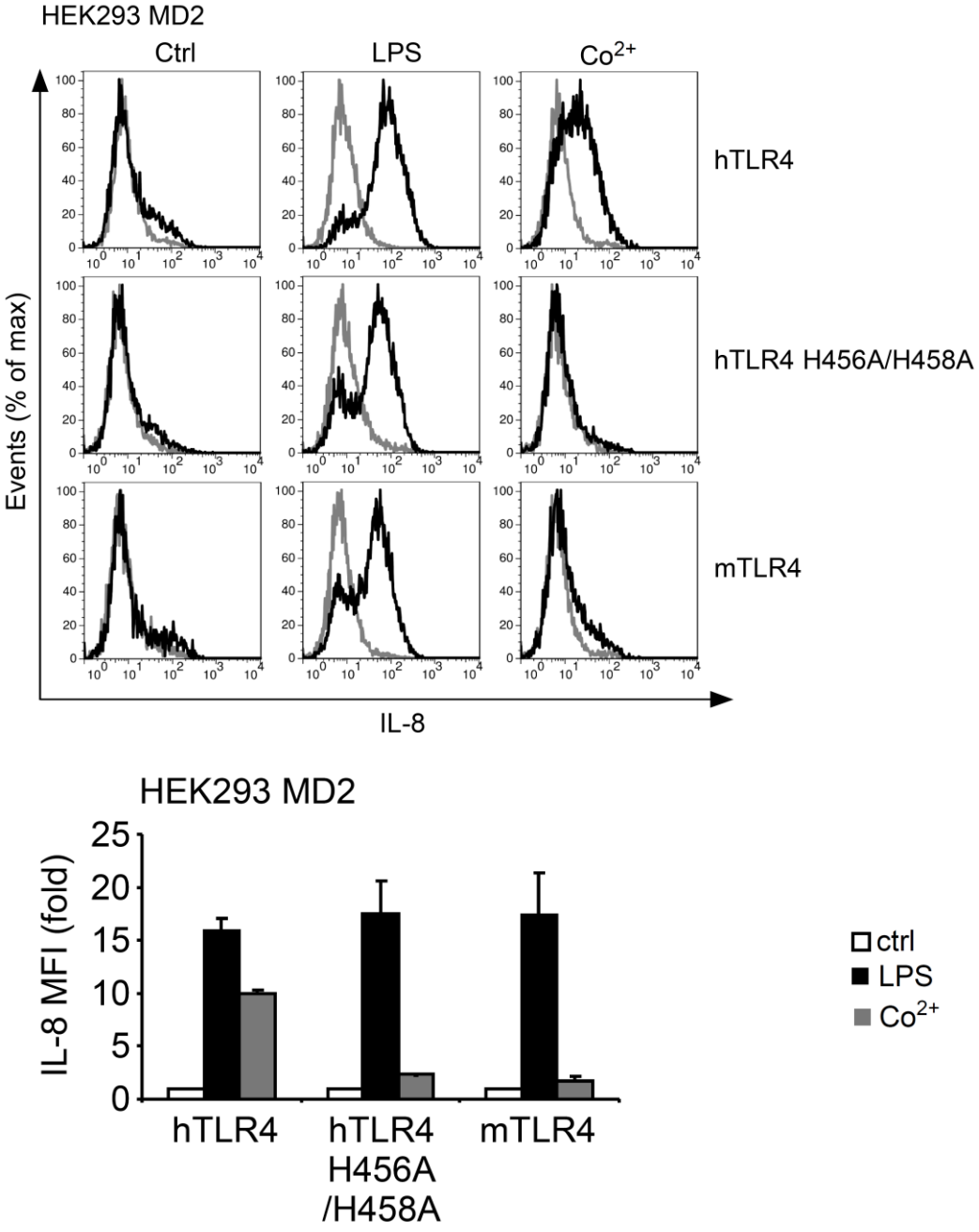

Fig. 33: Flow cytometric staining of intracellular IL-8 protein expressed by the positively transfected cell population (*upper panel*). Transfection of the indicated constructs was monitored by HA-immunostaining and gating on the HA-positive population. Representative overlays of IL-8 staining (*black lines*) and isotype-staining (*grey lines*) of three independent experiments are shown. Flow cytometric quantification (*lower panel*) of the staining (*upper panel*). Data represent means of isotype-corrected median fluorescence intensities (MFIs) of IL-8-staining calculated for the HA-gated population ± S.D.

4.11 Metal allergens Ni^{2+}/Co^{2+} facilitate hTLR4 homodimerisation independent of hMD2

It is clearly understood that some TLRs can be activated as homodimers whereas some can function only as heterodimers [104]. The first step in TLR4 activation is its homodimerisation [115]. By using co-immunoprecipitation analysis, we evaluated the

capabilities of Ni^{2+} and Co^{2+}, similar to LPS, to induce hTLR4 dimerisation. To this end, HEK293 WT or HEK293 MD2 cells were transfected with unique hTLR4 constructs coupled with either HA tag or FLAG tag or a combination of both. Subsequently, these cells were stimulated with Ni^{2+}, Co^{2+} or LPS as control. A feeble band representing the basal interaction complex of HA-hTLR4 and FLAG-hTLR4 is seen in the α-FLAG-immunoprecipitations (IPs) of HEK293 MD2 cells co-transfected with HA-hTLR4/FLAG -hTLR4 (**Fig. 34**) but not in the IPs of single constructs.

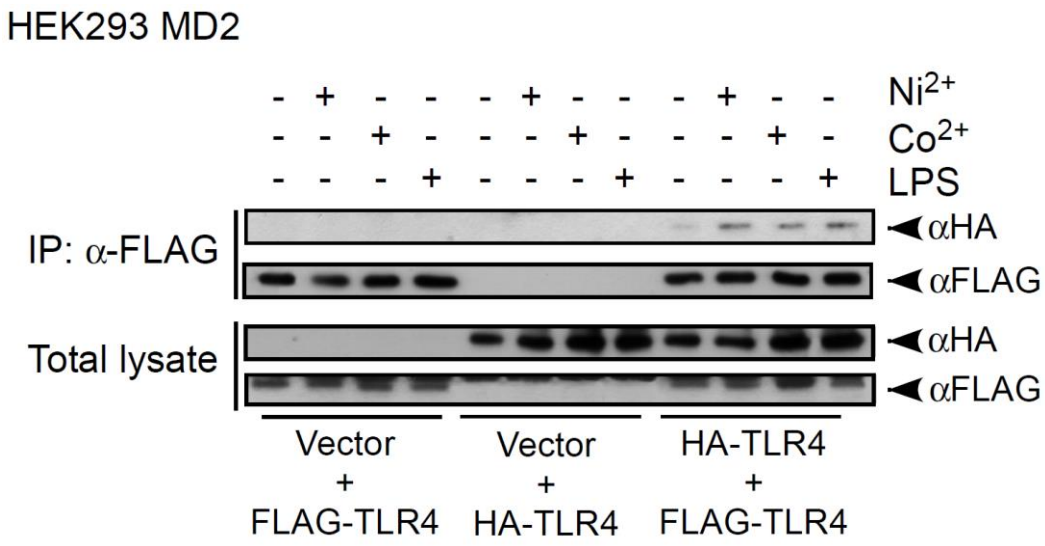

Fig. 34: HEK293 MD2 cells were co-transfected with the indicated combinations of HA- or FLAG-tagged TLR4 constructs and stimulated with medium (Ctrl), Ni^{2+} (1.5 mM), Co^{2+} (1.5 mM) or LPS (*S. minnesota* R595; 1 µg ml^{-1}) for 30 min. Cell lysates were immunoprecipitated with α-FLAG antibody and formed complexes visualized by immunoblot with an α-HA antibody. Membranes were reprobed with α-FLAG antibody to confirm equal immunoprecipitation. α-HA and α-FLAG western blots with total lysate are shown to illustrate similar transfection efficiencies. Immunoblots are representative of three to four independent experiments.

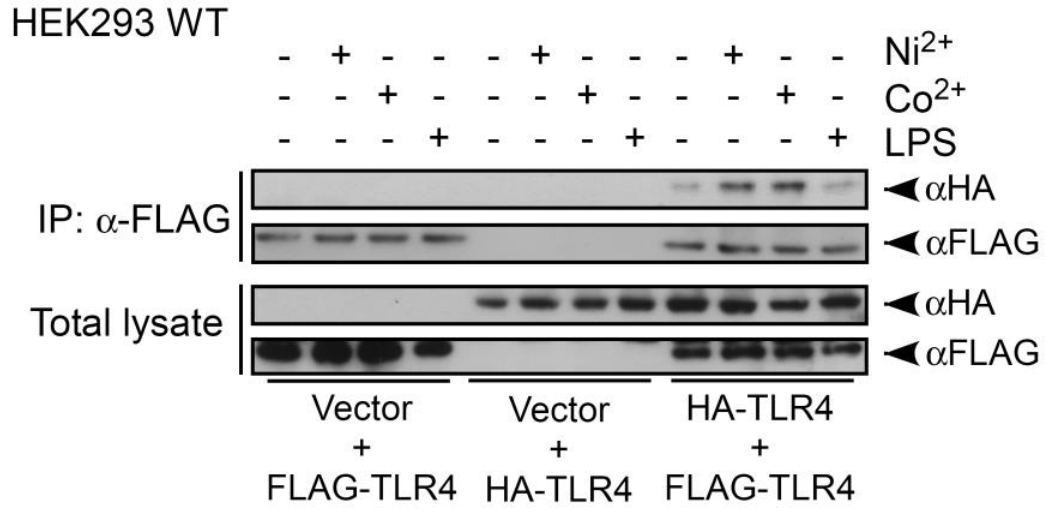

Fig. 35: HEK293 WT cells were co-transfected with the indicated combinations of HA- or FLAG-tagged TLR4 constructs and stimulated with medium (Ctrl), Ni^{2+} (1.5 mM), Co^{2+} (1.5 mM) or LPS (*S. minnesota*

R595; 1 µg ml^{-1}) for 30 min. Cell lysates were immunoprecipitated with α-FLAG antibody and formed complexes visualized by immunoblot with an α-HA antibody. Membranes were reprobed with α-FLAG antibody to confirm equal immunoprecipitation. α-HA and α-FLAG western blots with total lysate are shown to illustrate similar transfection efficiencies. Immunoblots are representative of three to four independent experiments.

Nevertheless, the hTLR4-MD2 heterodimer complex formation was significantly upregulated upon stimulation of Ni^{2+} or Co^{2+} or LPS. Strikingly, both the metal allergens aided the heterodimer alignment of FLAG-hTLR4 and HA-hTLR4 in the absence of MD2, whereas LPS was inept to do so (**Fig. 35**).

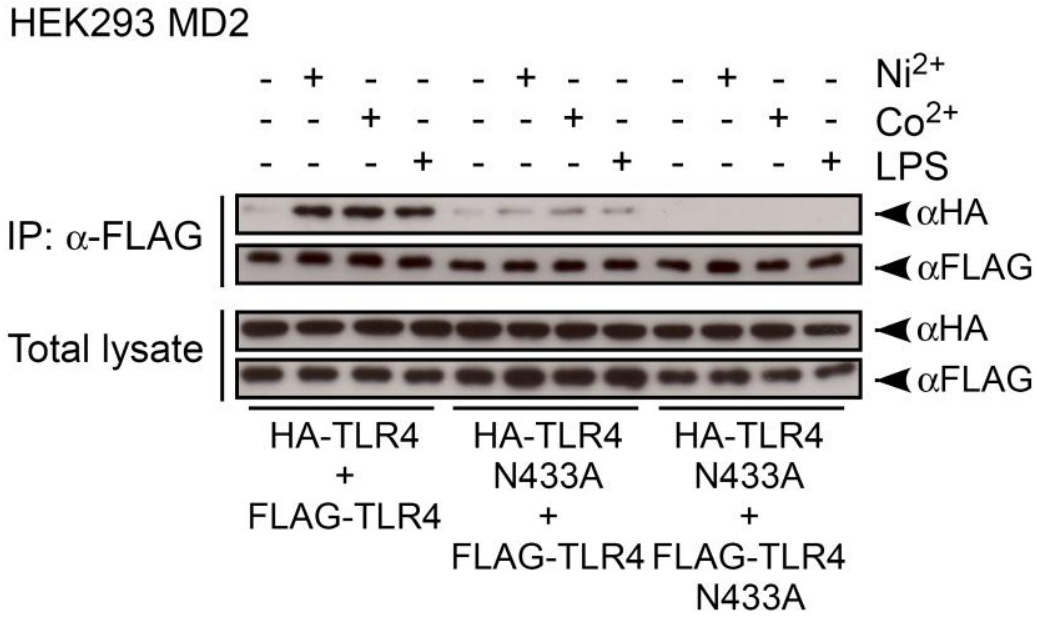

Fig. 36: HEK293 MD2 cells were co-transfected with the indicated combinations of HA- or FLAG-tagged TLR4 constructs or TLR4 N433A constructs and stimulated with medium (Ctrl), Ni^{2+} (1.5 mM), Co^{2+} (1.5 mM) or LPS (*S. minnesota* R595; 1 µg ml^{-1}) for 30 min. Cell lysates were immunoprecipitated with α-FLAG antibody and formed complexes visualized by immunoblot with an α-HA antibody. Membranes were reprobed with α-FLAG antibody to confirm equal immunoprecipitation. α-HA and α-FLAG western blots with total lysate are shown to illustrate similar transfection efficiencies. Immunoblots are representative of three to four independent experiments.

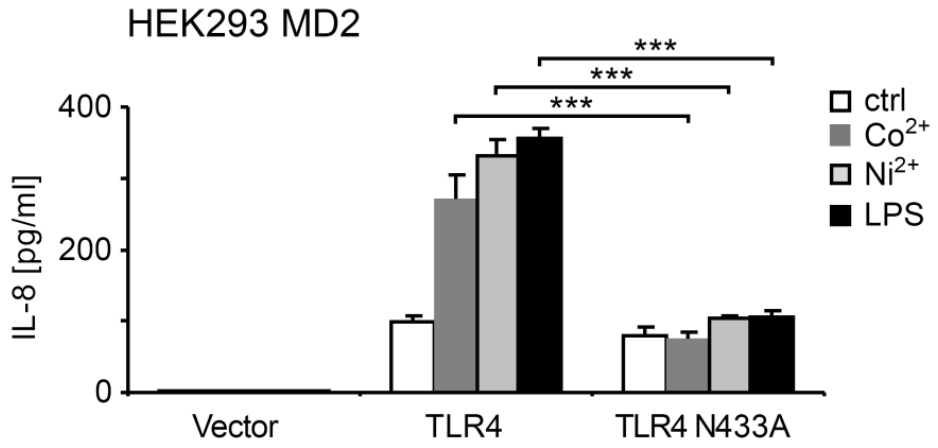

Fig. 37: Analysis of metal allergen- or LPS-induced IL-8 production in supernatants from HEK293 MD2 cells transfected with HA-hTLR4 or HA-hTLR4 N433A, respectively. The cells were stimulated with

medium (Ctrl), Ni^{2+} (1.5 mM), Co^{2+} (1.5 mM) or LPS (*S. minnesota* R595; 1 µg ml^{-1}) for 8 h. Data represents mean ± S.D. of three independent experiments. *** $p < 0.001$ (unpaired *t*-test).

The dimerisation domain of the hTLR4 has been vividly described by Park and colleagues in their crystal structure analysis [92]. To prove that receptor dimerisation is indeed critical for the TLR4 activation and downstream signaling, we replaced asparagine at 433 position with an alanine. This asparagine residue at 433 position in the dimerisation interface of hTLR4 is necessary during dimerisation for direct contact with the second TLR4 molecule [92]. HEK293 cells expressing hMD2 were transfected with combinations of HA-hTLR4/FLAG-hTLR4, HA-hTLR4-N433A/FLAG-hTLR4 or HA-hTLR4-N433A/ FLAG-hTLR4-N433A and stimulated with medium, Ni^{2+}, Co^{2+} or LPS, respectively. Cells were then harvested and lysates were utilised for co-immunoprecipitation experiments using α-FLAG-IPs followed by an immunoblot with an α-HA antibody.

A steady decline in hTLR4 dimerisation is visible (**Fig. 36**) due to the mutation of a single or double N433 residue upon all the stimulants. In the end hTLR4 complex was untraceable not even a basal or stimulus-dependent complex when HA-hTLR4-N433A and FLAG-hTLR4-N433A were co-transfected. This shows that deficiency of both the N433 residues from the opposing TLR4 monomers is antagonistic for interaction or dimerisation. In concordance, HEK293-hMD2 cells transfected with HA-hTLR4-N433A could not trigger the release of more than basal level IL-8 upon Ni^{2+}, Co^{2+} or LPS stimulations indicating that hTLR4 dimerisation is the first and foremost step essential for receptor activation by both metal allergens and LPS (**Fig. 37**).

4.12 sTLR4 can inhibit Ni^{2+}/Co^{2+}-induced NF-κB activation

The presumed metal-binding histidines at 456 and 458 are in close proximity to the asparagine at 433 in dimerisation domain of hTLR4 [92]. Blocking off H456 and H458 by using a peptide or small molecule inhibitor may hinder the LPS-induced dimerisation leading to sepsis in spite of the dispensability of both the histidines on LPS triggered hTLR4 activation [78]. The next alternative was to take advantage of the difference in MD2 requirement for hTLR4 dimerisation, which was the second distinguishing quality of both the stimuli. Therefore, we synthesized a soluble form of hTLR4 (sTLR4) comprising its ectodomain (aa 27-627) fused N-terminally to the signal peptide of the Igk-chain to direct it to the secretory pathway [116]. This mutant was then transfected into

HEK293 cells resulting in an MD2-independent secretion of sTLR4 into the culture medium (**Fig. 38**). This conditioned supernatant medium was then collected and transferred onto the recipient cells, which were positive for hTLR4/MD2, to analyse the ability of the accumulated sTLR4 to block off the metal allergens- or LPS-induced proinflammatory responses. To our surprise, the addition of MD2-free sTLR4 conditioned medium hindered only the Ni^{2+} or Co^{2+} mediated IL-8 release when transferred to HEK293-TLR4/MD2 cells (**Fig. 39**) or HUVECs (**Fig. 40**) while the LPS triggered IL-8 release was unaltered.

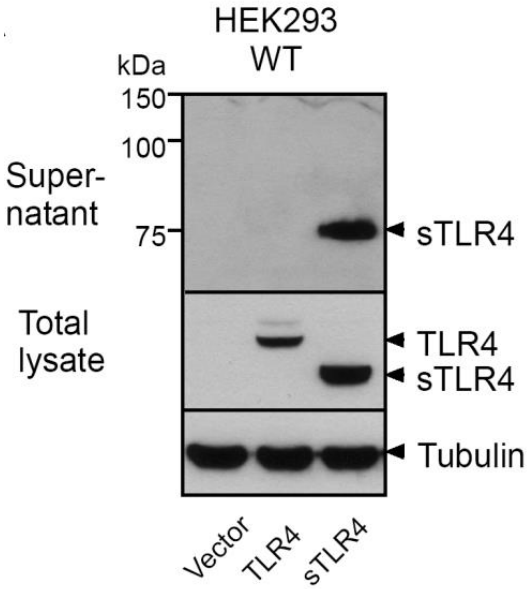

Fig. 38: Western blot analysis of the indicated HA-tagged TLR4 proteins in supernatants and total lysates from transfected HEK293 WT cells. Data demonstrate MD2-independent release of truncated sTLR4 into the culture supernatant. Immunoblots are representative of three independent experiments.

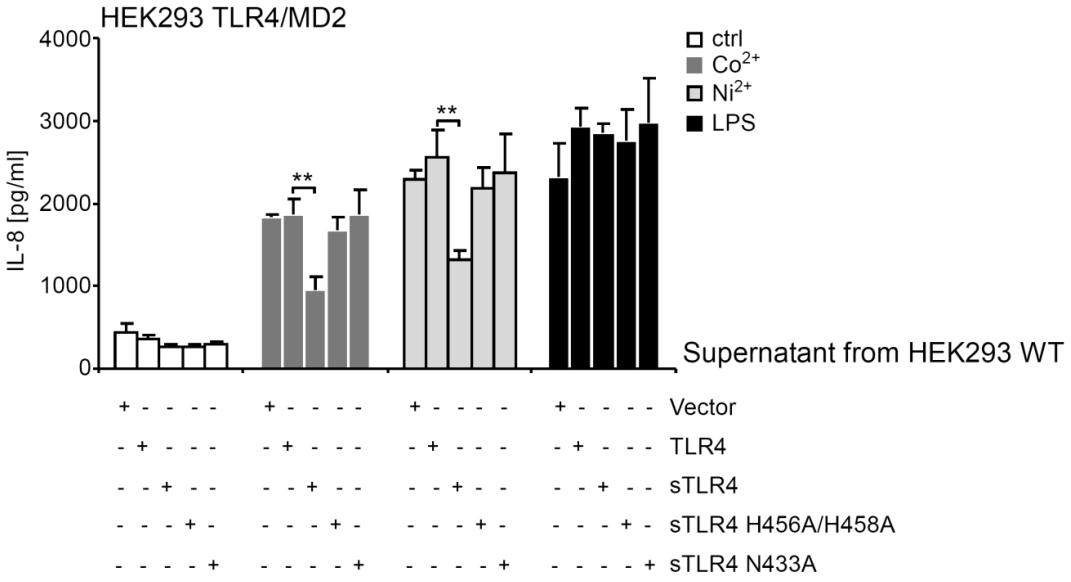

Fig. 39: IL-8 ELISA of HEK293 hTLR4/hMD2 cells incubated with undiluted supernatants produced by HEK293 WT cells transfected with the indicated constructs. Supernatants were taken 48 h after transfection

of the producer lines and freshly supplemented with medium (Ctrl), Ni^{2+} (1.5 mM), Co^{2+} (1.5 mM) or LPS (*S. minnesota* R595; 1 µg ml^{-1}) for 30 min prior to addition to the HEK293 hTLR4/hMD2 cells and incubated for 8 h. Data represents mean ± S.D. of three independent experiments. ** $p < 0.01$ (unpaired t-test).

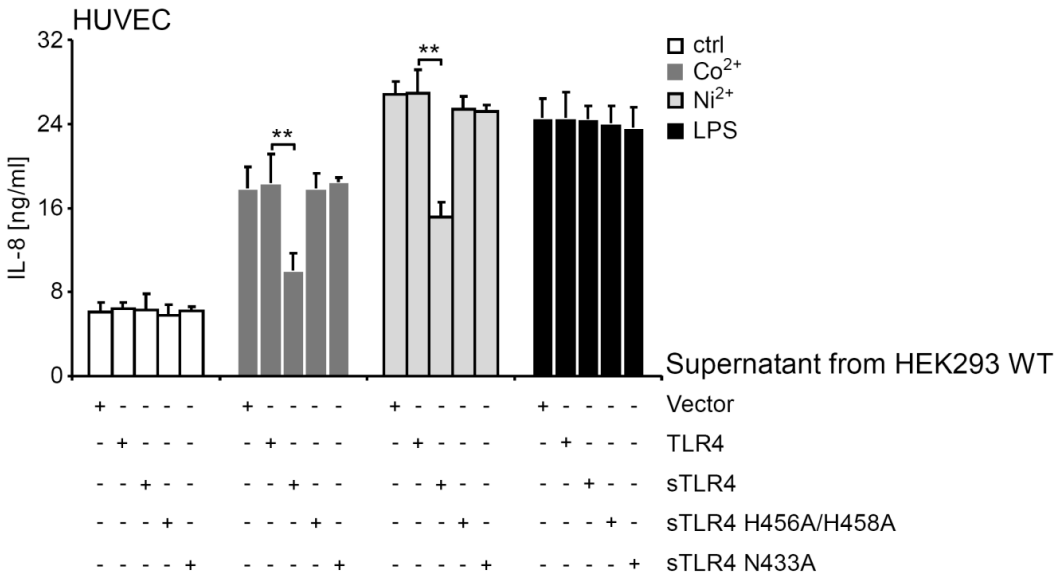

Fig. 40: IL-8 ELISA of HUVECs incubated with undiluted supernatants produced by HEK wild-type cells transfected with the indicated constructs. Supernatants were taken 48 h after transfection of the producer lines and freshly supplemented with medium (Ctrl), Ni^{2+} (1.5 mM), Co^{2+} (1.5 mM) or LPS (*S. minnesota* R595; 1 µg ml^{-1}) for 30 min prior to addition to the HUVECs and incubated for 8 h. Data represent mean ± S.D. of three independent experiments. ** $p < 0.01$ (unpaired *t*-test).

In parallel experiments, neither sTLR4 H456/458A nor sTLR4-N433A mutant were able to block the metal allergen mediated IL-8 production indicating that the above-mentioned inhibition apparently required both metal-binding capacity as well as dimerisation ability (**Fig. 39, 40**). Therefore, the observed inhibition may depend on bonding of free metal ions to sTLR4 homodimers in the absence of free MD2.

From the published crystal structure of hTLR4-MD2 heterodimer [92] and our own mutagenesis data, we hypothesize a structural model in which Co^{2+} or Ni^{2+} cross-links the two receptor monomers via specific histidine side chains triggering formation of a dimer that structurally resembles the one induced by LPS (**Fig. 25, 41**).

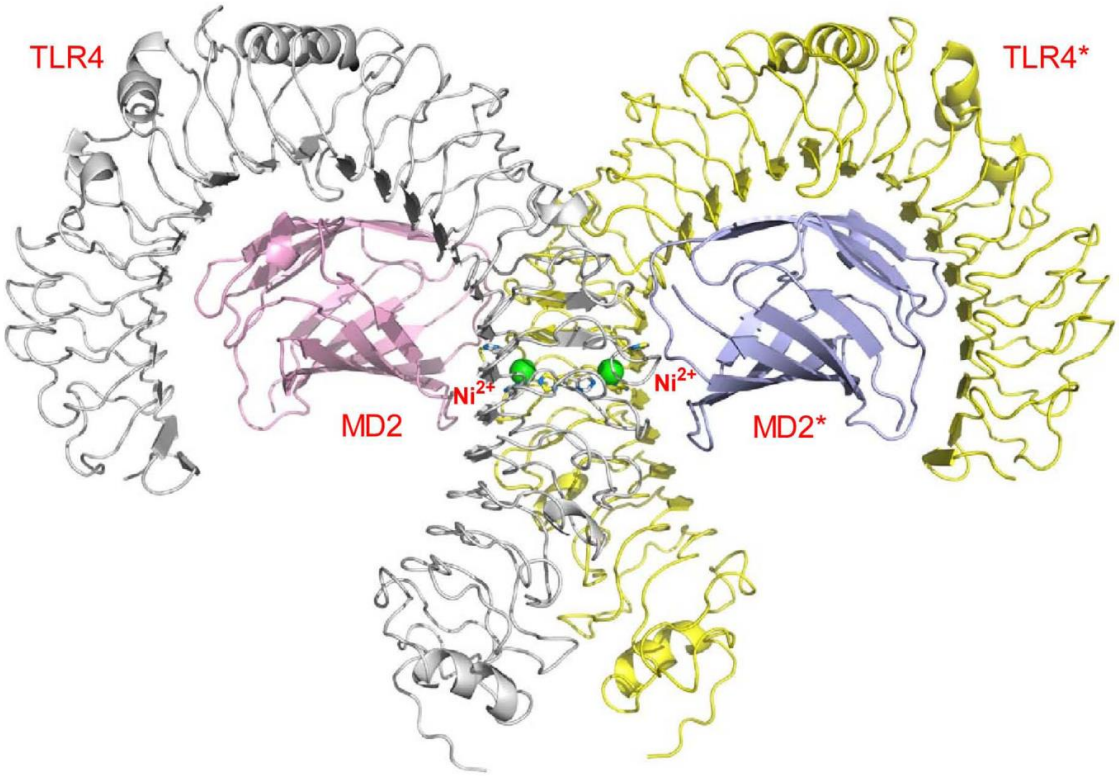

Fig. 41: Structural modeling of Ni^{2+} interaction with hTLR4. Modeling of the 2(Ni^{2+})-2(hTLR4)-2(MD2) complex in ribbon representation (side view) with the putative positions of the bound Ni^{2+} molecules indicated. The model is based on the crystal structure of the hTLR4-hMD2 complex (PDB entry 3FXI) with LPS omitted. Molecular modeling and graphics preparation was performed using PyMOL software. Interaction of Co^{2+} with hTLR4 resembles to that of Ni^{2+}.

5 Discussion

Skin diseases have a menacing socio-economic impact on the quality of life for millions of people worldwide. Particularly allergic responses to the metal allergens are the most common form of contact allergy in the developed countries. Moreover, metal allergy frequency is steadily increasing due to their wide distribution in a variety of products encountered in daily life ranging from metal coins, costume jewelry and body piercing to medical devices such as cardiovascular stents, orthopaedic and dental implants.

For the development of contact allergies two signals are required, namely the T cell-mediated signal and an adjuvant proinflammatory signal. However, it is currently unclear how allergy-relevant cells sense the presence of a contact allergen to trigger this co-stimulatory response. Thus, in the present study we aimed at elucidating the cellular sensing mechanisms of the contact allergens Ni^{2+} and Co^{2+}.

In the periodic table of elements, Ni^{2+} and Co^{2+} reside in adjacent places and they share many similar chemical properties including the affinity to bind histidine [117]. Their atomic masses also are very much comparable namely 58.6934 and 58.9332 u, respectively. Both these transition metals are unique as they prefer to form a octahedral coordination geometry over tetrahedral or other geometries favored by other transition metal ions [118]. They also reside in neighboring places in the natural order of stability for divalent metals (Irving-Williams series). These two properties of Ni^{2+} and Co^{2+} are the two major contributing factors for selectivity of metal binding to proteins [119]. Convincingly, other divalent metal ions lacking allergic potential like manganese failed to activate NF-κB in ECs *in vitro* [66]. Binding of Ni^{2+}/Co^{2+} to hTLR4, in contrast to other divalent metal ions, is not simply a matter of balancing the charge but is mainly regulated by other physicochemical properties of the metal ion. The similarity in the mode of action between Ni^{2+} and Co^{2+} however fosters the possibility that contact with either of the two haptens may provide cross sensitization to the other, which may have critical consequences for preventing therapeutic approaches. In this context, it was recently established that Ni^{2+} acts as a strong adjuvant in Co^{2+} sensitization [120].

Sensitization to contact allergens involves a thorough assessment by resident skin cells [110]. We provide here the first evidence that major cell types of the skin like DCs, ECs and cells of the macrophage lineage possess the ability to react to metal allergens Ni^{2+} and

Co^{2+} by initiating an array of proinflammatory responses. The aforementioned cell types possess fully functional hTLR4 and MD2 as evidenced by their LPS responsiveness.

A remarkable finding observed in this study was that keratinocytes, the predominant cell type of the epidermis, failed to respond to Ni^{2+} and Co^{2+}. Furthermore, the expression of hTLR4 in keratinocytes is debatable as there is ample contradictory data [16, 17, 19, 121, 122]. However, most of the studies are in concordance to our inference that primary human keratinocytes lack functional expression of hTLR4. Interestingly, the researchers who claim that keratinocytes express TLR4 were unable to show an LPS mediated proinflammatory activation except when employing unusually high concentrations of LPS like more than 100 μg ml^{-1} [19]. These concentrations are around 100-1000 times more than the concentrations needed to activate HUVEC or THP-1 cells in our studies. Nonetheless, if keratinocytes under some specific conditions express very little amounts of hTLR4, the level of expression is doubtful to be adequate to initiate the essential innate immune signal for sensitization to metal induced contact allergy. This situation opposes the established theory that keratinocytes play a vital role in the initial perception at least to these contact allergens [110].

In the presence of a priming signal like TNF, keratinocytes may be yet able to initiate proinflammatory responses to extrinsic agents by the activation of inflammasome [123], a multi-protein complex linking innate immune receptors of the NACHT, leucine rich repeat, and PYD containing family (NLRP), which trigger the release of cytokines like interleukin-1 beta (IL-1β) and IL-18 via a caspase-1-dependent mechanism [124]. Besides, keratinocytes are known to synthesise a large array of cytokines upon proinflammatory activation [125]. Therefore, keratinocytes may play vital role in the sensing of other contact allergens. Additionally, they may even exert regulatory functions or may have a role to play in the later phases of metal induced ACD.

Gene silencing studies using RNA interference (RNAi) clearly showed the requirement of both TLR4 and MD2 for Ni^{2+}/Co^{2+}-induced proinflammatory gene expression. This is in accordance to the requirement of LPS, the natural ligand for TLR4. Potential contamination of Ni^{2+}/Co^{2+} by LPS was excluded by the addition of polymyxin B sulphate, an LPS inactivating drug.

The presently known more than 4000 contact allergens are able to initiate contact allergy though they depict a vast structural diversity among themselves. However, it is extremely

unlikely that they all have a common mechanism (e.g. direct proinflammatory activation of hTLR4) to induce ACD. Nevertheless, in a few instances a secondary mode of innate immune activation through TLR4 provocation has been proposed. It has been published that DNCB initiates CHS in mice by activating TLR2 and TLR4 by releasing a low molecular weight hyaluronan [83]. It is a very well recognized intrinsic activator of TLR2 and TLR4 [126] generated by oxidative degradation of high molecular weight hyaluronan from the extracellular matrix (ECM). Another recently found mode of innate immune activation is via inflammasome pathway, which was mentioned in one of the earlier paragraphs. A recent study showed that Ni^{2+} can trigger IL-1β secretion by activating NLRP3-ASC-caspase-1 inflammasome complex [127]. To trigger inflammasome activation, a priming signal is required that not only elevates IL-1β expression but also induces expression of key inflammasome components. Only when this prerequisite is met, stimulus-induced NLR- and caspase-1 activation resulting in cleavage and release of IL-1β can ensue. In most cases, the priming signal is experimentally provided by LPS stimulation, suggesting a crosstalk of TLR4 signaling and inflammasome activation.

Our critical outcome that both Ni^{2+} and Co^{2+} utilize a similar mode of action via hTLR4 activation underlines the similarity of these two metal allergens seen in clinical studies [36]. Interestingly, we realized that Ni^{2+}/Co^{2+}-induced proinflammatory signaling cascades are species-specific and principally involve the non-conserved histidines at 456 and 458 in hTLR4 but not in mTLR4. This newly identified species dependency of metal-induced activation of hTLR4 resolves the obscurity why currently available murine models indispensably involve additional co-stimulatory agents or adjuvants for metal-induced CHS [75, 128]. Supporting our findings, a recent study has shown that Co^{2+} released from metal-on-metal hip joint replacements can generate an endotoxin-like response by activating hTLR4 in neighboring immune cells [94]. Using a commercially available human reporter cell line stimulated with either LPS or Co^{2+} or Ni^{2+}, they measured alkaline phosphatase secretion resulting from the activation of TLR4. In accordance with our results, their murine reporter cell line could only be activated by LPS but not by Co^{2+} or Ni^{2+}. In conjunction to our hypothesis, palladium was also indicated recently to initiate innate immune responses via a direct activation of TLR4 signaling [37].

Furthermore, using our mutagenesis data and the published crystal structure of the hTLR4-hMD2 complex we propose a model of activation by Ni^{2+}/Co^{2+}. While neither the hTLR4 H431-H456-H458 triplet nor the histidine doublet formed by the closely spaced H458

residues at the interface of two TLR4 monomers have the proper distances and side chain geometry to form a high affinity binding site, minor local conformational adjustments allow an interdigitated arrangement of the histidine side chains from both hTLR4 monomers and, due to the increased structural flexibility in this mode of interaction, lead to two putative chelating sites for the metal ions at the interface. This model can nicely explain the complex role of the individual histidine residues that became apparent from the mutagenesis studies: elimination of a single histidine at any of the positions 431, 456 or 458 alone had no or only minor effects on Ni^{2+}/Co^{2+} responsiveness while substitution of any pair of histidine residues by alanine led to a loss of receptor activation.

In support of our data, a recent study has proven that Ni^{2+} binds to H431, H456 and H458 of the hTLR4 [129]. Using a 32 amino acid fragment of hTLR4 starting from 429 to 460, they provide a substantial mass spectrophotometric and NMR based evidences of Ni^{2+} binding to histidines.

The hypothesized $(Ni^{2+}/Co^{2+})_2$-$(hTLR4)_2$ complex can be designed without hindering the gross quaternary structure of the heterodimeric hTLR4 complex initiated by LPS. The published x-ray crystal structure of the LPS-hTLR4-MD2 complex has revealed that numerous already known hydrophobic and hydrophilic interactions promote dimerisation of the individual monomers. Even though strong chemical bonding is involved in the docking of Ni^{2+}/Co^{2+} to the imidazole moieties of the histidines in hTLR4, the type of cross-linking between two TLR4 monomers induced by Ni^{2+}/Co^{2+} leads to a structurally very identical stereo-dimer that is easily accessible for downstream signaling. As a result, proinflammatory gene cascades are triggered that finally leads to the co-stimulatory signal needed for effective sensitization and elicitation of ACD [130] (see **Fig. 42**).

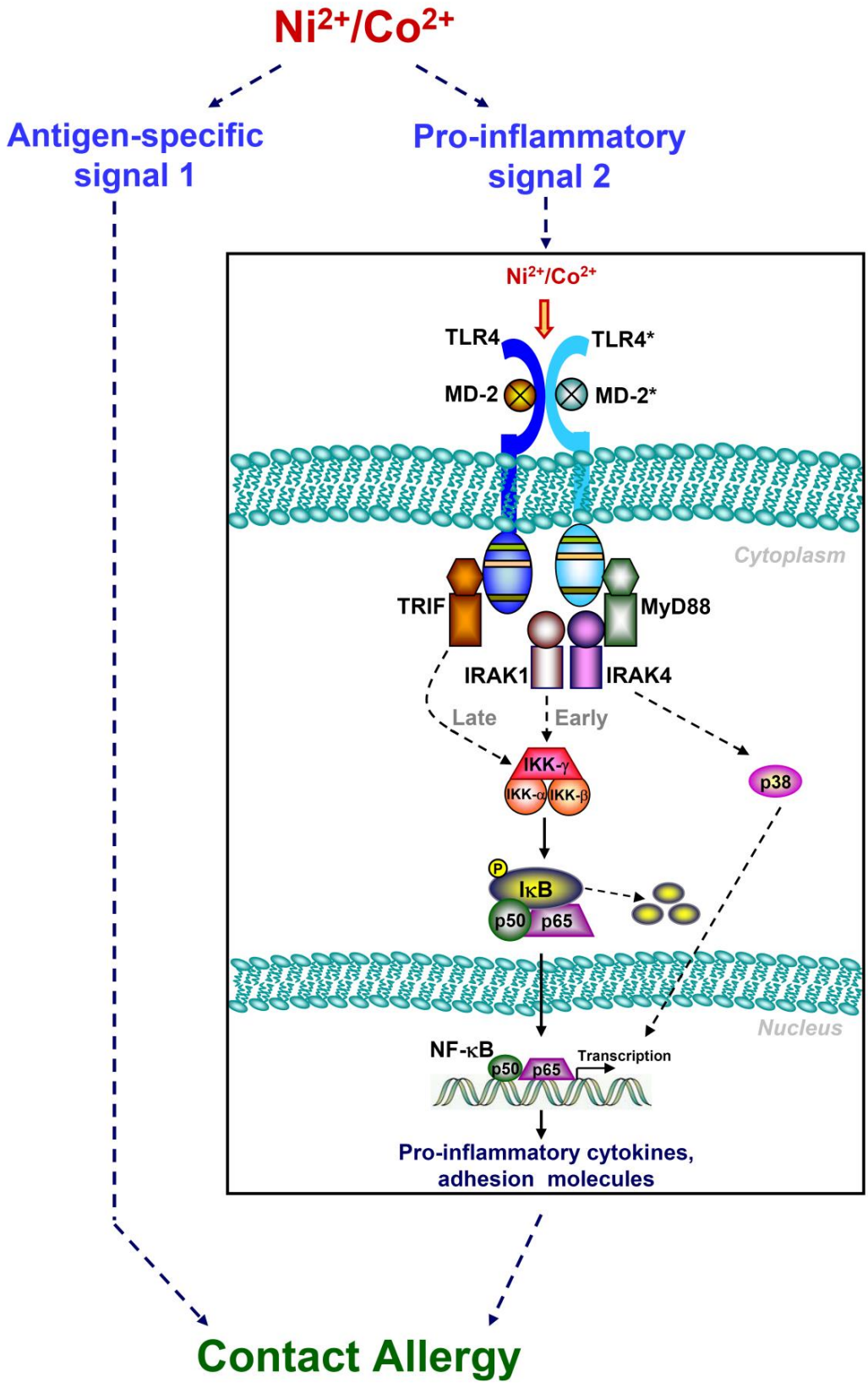

Fig. 42: Proinflammatory signaling pathways activated by Ni^{2+}/Co^{2+}. For induction of contact allergy to Ni^{2+}/Co^{2+} two signals are required: an antigen-specific, T cell-activating signal and a proinflammatory signal. The latter signal is sensed by hTLR4/hMD2 resulting in the activation of NF-κB and p38 and subsequent expression of cytokines, adhesion molecules and type I interferons.

Notably, the mode of action of these two metal allergens observed in this study differs from that of the one described for the major house dust mite allergen, Derp2 which activates TLR4 only in the presence of LPS [131], while Ni^{2+}/Co^{2+}-induced TLR4 activation is independent of LPS. In addition, Derp2, which functionally mimics MD2, acts as a sensitizer for LPS rather than a direct activator of TLR4 signaling unlike Ni^{2+}/Co^{2+}. A very recent study has also provided evidences for binding of a cationic lipid nanocarrier molecule, diC14-amidine to hTLR4 dependent of MD2 [132].

Remarkably, our data demonstrate that the important residues responsible for metal binding located in the ectodomain of TLR4 are unique and different from those reported for LPS. This may provide a novel lead in fostering exclusive compounds that specifically target these cross-linking in TLR4 with no interference to the other functionalities of the receptor. Thus, our study has a potential to contribute to innovative strategies for prophylaxis and improved therapeutic efficacy of ACD to Ni^{2+}/Co^{2+} that are not anymore dependent on application of topical immunosupressants. Taking benefit of the unusual species preferences of TLR4 responses, our data strongly emphasizes that evaluation of allergenicity, toxicity of potent chemicals/allergens in rodent models might not correspond to the phenomenon in humans, and care should be taken to interpret those results.

Our data from the dimerisation defective hTLR4 mutant clearly demonstrates that TLR4 cross-linking is indeed essential for the metal-induced proinflammatory activation. Of note, the mutated asparagine residue at 433 position is in close proximity to the anticipated metal binding histidines namely H456 and H458 [92].

Largely, our findings prove dimerisation of TLR4 as a conventional method of Ni^{2+}/Co^{2+}-induced innate immune activation. Importantly, differing from LPS, cross-linking of TLR4 happened without the involvement of MD2 (**Fig. 43**). This remarkable finding may open new therapeutic frontiers as deduced from our sTLR4 blocking studies, while it also raises questions concerning the function of MD2 in the metal-induced activation of TLR4. However, a recent study by Oblak and colleagues established that MD2 aids the anchoring of TLR4 monomers by imparting supportive hydrophobic bonding that stabilizes the heterohexameric complex of TLR4-MD2-Ni^{2+}/Co^{2+} in an appropriate confirmation leading to downstream signaling [133].

From the clinical perspective, our experiments not only promise new treatment opportunities using sTLR4 variants or sTLR4-derived peptides but also warrant caution

about strategies directly targeting metal-binding to inhibit metal-induced hypersensitivity responses as such efforts are prone to affect LPS-induced TLR4 dimerisation and bacterial responses as well.

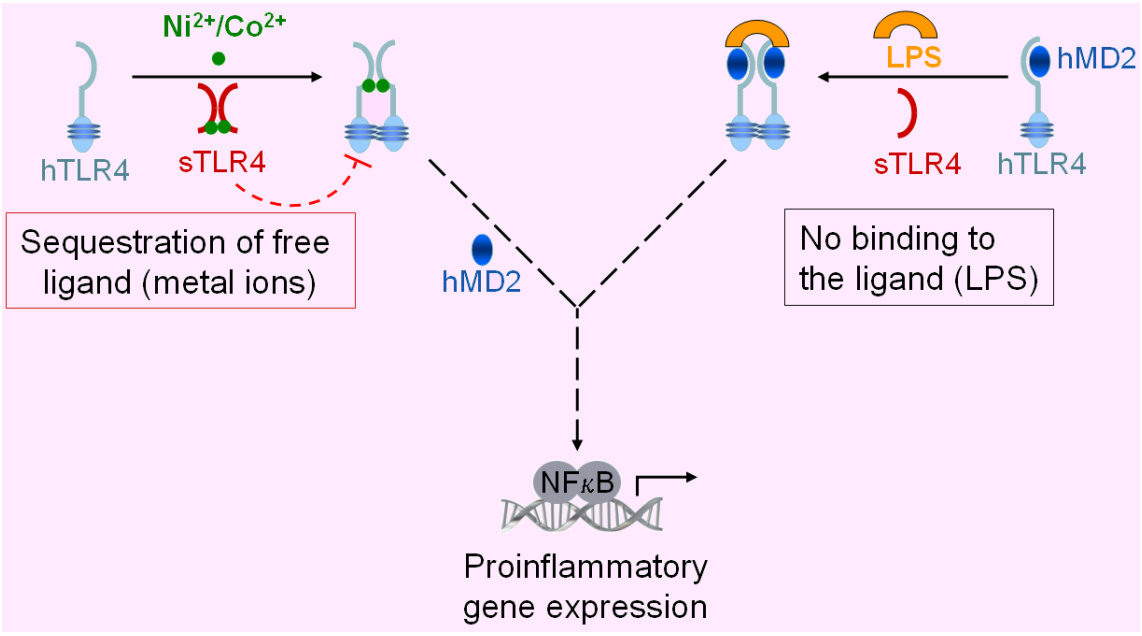

Fig 43: Model for sTLR4-dependent inhibition of metal-induced proinflammatory gene expression. sTLR4 sequesters the free metal ions independent of MD2, thereby blocking the membrane bound TLR4 mediated proinflammatory response. Conversely, LPS cannot mimic the situation, as its binding to TLR4 is MD2 driven.

6 Summary

Allergic contact dermatitis (ACD) caused by the metal ions Ni^{2+} and Co^{2+} affect almost one in five people in the western world. Sources for these metals include numerous day-to-day products like metal coins, costume jewelry, body piercing, medical implants, hair dyes and ceramics. Moreover, both metals are widely used in the building, metallurgical and electronic industries classifying metal-induced ACD as major work-related disease with considerable impact on professional careers and working ability of affected individuals. Despite the undisputed need for specific and well-tolerated therapies, current treatment options are limited to the use of topical corticosteroids, which are prone to major side effects, particularly upon the long-term administration obligatory with those patients.

Here, we dissected the molecular mechanism required for Ni^{2+}-induced hTLR4 activation and extended our analysis to Co^{2+}-induced proinflammatory responses. Using supplementation experiments in naturally hTLR4-deficent primary human keratinocytes and HEK293 cells we show that Co^{2+} resembles Ni^{2+} by activating hTLR4/MD2 in a species-dependent manner requiring presence of the non-conserved histidines H456 and H458 within the proposed metal-binding domain of hTLR4 that flanks its dimerisation interface. Using a novel dimerisation-mutant of hTLR4 we provide first direct evidence that metal allergens, similar to LPS, strictly require hTLR4 dimerisation to trigger proinflammatory gene expression. This confirms our structural model, which predicts hTLR4 activation to occur by bridging of two hTLR4 molecules simultaneously bound by two metal ions to the non-conserved histidines H456 and H458. Most importantly, however, we show here that Ni^{2+} and Co^{2+}, in contrast to LPS, do not require MD2 to induce hTLR4 dimerisation since both metals readily induced complex formation of differently tagged hTLR4 proteins in co-immunoprecipitation studies with MD2-free HEK293 cells. We believe that this observation holds great potential for therapeutic exploitation since administration of a soluble form of hTLR4 (sTLR4) produced in the absence of MD2 was capable to significantly reduce Ni^{2+} and Co^{2+}-induced cytokine production in metal-sensitive cells while LPS responsiveness remained unchanged.

In summary, our data show that metal allergens differ in at least two aspects from LPS: For one, they strictly require presence of the non-conserved histidines H456 and H458 to activate hTLR4 and, secondly, they induce hTLR4 dimerisation independently of MD2.

Thus, our results may provide the basis for novel therapies that aim at specifically inhibiting metal-induced ACD in a clinically manageable way.

7 Zusammenfassung

Allergische Kontaktdermatitis (ACD) verursacht durch die Metallionen Nickel und Kobalt stellt ein häufiges Gesundheitsproblem in den Industrieländern dar und betrifft fast ein Fünftel der Bevölkerung der westlichen Welt. Quellen für diese Metalle umfassen zahlreiche alltäglich Produkte wie Metallmünzen, Modeschmuck, Piercingschmuck, medizinische Implantate, Haarfärbemittel und Keramiken. Darüber hinaus sind beide Metalle in der Gebäude-, Metall- und Elektronikindustrie weit verbreitet, was die durch Metallionen verursachte allergische Kontaktdermatitis zu einer bedeutenden Berufskrankheit macht. Der Einfluss auf die Arbeitsfähigkeit und damit den beruflichen Werdegang der betroffenen Personen ist erheblich. Trotz des unbestrittenen Bedarfs an spezifischen und gut verträglichen Therapien sind die derzeitigen Behandlungsmöglichkeiten auf die Verwendung von topischen Kortikosteroiden beschränkt, welche vor allem bei der notwendigen längerfristigen Behandlung starke Nebenwirkungen verursachen.

In dieser Studie haben wir den molekularen Mechanismus, welcher der nickelinduzierten hTLR4-Aktivierung zugrunde liegt untersucht und unsere Analyse auf die kobaltinduzierte proinflammatorische Immunantwort ausgedehnt. Mit Hilfe von Supplementationsexperimenten an natürlich hTLR4-defizienten primären humanen Keratinozyten und HEK293-Zellen konnten wir zeigen, dass Kobalt – analog zu Nickel – hTLR4/MD2 speziesabhängig aktiviert. Dabei ist die Anwesenheit der konservierten Histidine H456 und H458, welche die hTLR4 Dimerisierungsschnittstellen flankieren, innerhalb der vorher experimentell ermittelten Metallbindungsdomäne von hTLR4 notwendig. Unter Verwendung einer neuartigen Dimerisierungsmutante von hTLR4 liefern wir einen ersten direkten Hinweis darauf, dass Metallallergene - ähnlich wie LPS - eine hTLR4-Dimerisierung unbedingt benötigen, um die Expression von proinflammatorischen Genen auszulösen. Dies konnte mit unserem Strukturmodell bestätigt werden, welches prognostiziert, dass die hTLR4-Aktivierung auf Kreuzvernetzung zweier hTLR4-Moleküle beruht, wobei zwei Metallionen gleichzeitig an die konservierten Histidine H456 und H458 von zwei unterschiedlichen hTLR4-Molekülen gebunden werden. Zustätzlich konnten wir zeigen dass Nickel und Kobalt - im Gegensatz zu LPS - zur hTLR4-Dimerisierung kein MD2 benötigen, da beide Metalle die

Komplexbildung unterschiedlich markierter hTLR4-Proteine auch in Co-Immunpräzipitationsstudien mit MD2-freien HEK293-Zellen induzieren konnten. Wir glauben, dass diese Beobachtung ein großes Potential zur Entwicklung spezifischer Therapien besitzt, da die Verabreichung einer löslichen Form von hTLR4 (sTLR4), die in Abwesenheit von MD2 produziert wurde, sowohl die Nickel- als auch Kobalt-induzierte Zytokinproduktion in metallsensibilisierten Zellen signifikant zu reduzieren vermochte, während die zelluläre Antwort auf LPS unbeeinträchtigt blieb.

Zusammenfassend zeigen unsere Daten, dass sich Metallallergene in mindestens zwei Eigenschaften von LPS unterscheiden: Zum einen benötigen sie unbedingt die Anwesenheit der nichtkonservierten Histidine H456 und H458, um hTLR4 zu aktivieren und zum anderen induzieren sie die hTLR4-Dimerisierung unabhängig von MD2. Daher können unsere Ergebnisse die Grundlage für neuartige Therapien liefern, die auf eine spezifische Hemmung von metallinduziertem ACD in einer klinisch leicht zu handhabenden Weise abzielen.

8 Bibliography

1. Mahler, V., J. Geier, and A. Schnuch, *Current trends in patch testing - new data from the German Contact Dermatitis Research Group (DKG) and the Information Network of Departments of Dermatology (IVDK).* J Dtsch Dermatol Ges, 2014. **12**(7): p. 583-92.
2. Thyssen, J.P. and T. Menne, *Metal allergy--a review on exposures, penetration, genetics, prevalence, and clinical implications.* Chem Res Toxicol, 2010. **23**(2): p. 309-18.
3. Medzhitov, R., *Recognition of microorganisms and activation of the immune response.* Nature, 2007. **449**(7164): p. 819-26.
4. Kumar, H., T. Kawai, and S. Akira, *Pathogen recognition by the innate immune system.* Int Rev Immunol, 2011. **30**(1): p. 16-34.
5. Botos, I., D.M. Segal, and D.R. Davies, *The structural biology of Toll-like receptors.* Structure, 2011. **19**(4): p. 447-59.
6. Ermertcan, A.T., F. Ozturk, and K. Gunduz, *Toll-like receptors and skin.* J Eur Acad Dermatol Venereol, 2011. **25**(9): p. 997-1006.
7. Cook, D.N., D.S. Pisetsky, and D.A. Schwartz, *Toll-like receptors in the pathogenesis of human disease.* Nat Immunol, 2004. **5**(10): p. 975-9.
8. Chen, K., et al., *Toll-like receptors in inflammation, infection and cancer.* Int Immunopharmacol, 2007. **7**(10): p. 1271-85.
9. Ospelt, C. and S. Gay, *TLRs and chronic inflammation.* Int J Biochem Cell Biol, 2010. **42**(4): p. 495-505.
10. Valins, W., S. Amini, and B. Berman, *The Expression of Toll-like Receptors in Dermatological Diseases and the Therapeutic Effect of Current and Newer Topical Toll-like Receptor Modulators.* J Clin Aesthet Dermatol, 2010. **3**(9): p. 20-9.
11. Hari, A., et al., *Toll-like receptors: role in dermatological disease.* Mediators Inflamm, 2010. **2010**: p. 437246.
12. Reichrath, J., *The skin is a fascinating endocrine organ.* Dermatoendocrinol, 2009. **1**(4): p. 195-6.
13. English, J.S., R.S. Dawe, and J. Ferguson, *Environmental effects and skin disease.* Br Med Bull, 2003. **68**: p. 129-42.

14. Di Meglio, P., G.K. Perera, and F.O. Nestle, *The multitasking organ: recent insights into skin immune function.* Immunity, 2011. **35**(6): p. 857-69.
15. Kobayashi, M., et al., *Expression of toll-like receptor 2, NOD2 and dectin-1 and stimulatory effects of their ligands and histamine in normal human keratinocytes.* Br J Dermatol, 2009. **160**(2): p. 297-304.
16. Song, P.I., et al., *Human keratinocytes express functional CD14 and toll-like receptor 4.* J Invest Dermatol, 2002. **119**(2): p. 424-32.
17. Baker, B.S., et al., *Normal keratinocytes express Toll-like receptors (TLRs) 1, 2 and 5: modulation of TLR expression in chronic plaque psoriasis.* Br J Dermatol, 2003. **148**(4): p. 670-9.
18. Miller, L.S., et al., *TGF-alpha regulates TLR expression and function on epidermal keratinocytes.* J Immunol, 2005. **174**(10): p. 6137-43.
19. Lebre, M.C., et al., *Human keratinocytes express functional Toll-like receptor 3, 4, 5, and 9.* J Invest Dermatol, 2007. **127**(2): p. 331-41.
20. Martin, S.F., et al., *Mechanisms of chemical-induced innate immunity in allergic contact dermatitis.* Allergy, 2011.
21. Peiser, M., et al., *Allergic contact dermatitis: epidemiology, molecular mechanisms, in vitro methods and regulatory aspects. Current knowledge assembled at an international workshop at BfR, Germany.* Cell Mol Life Sci, 2012. **69**(5): p. 763-81.
22. Belsito, D.V., *Occupational contact dermatitis: etiology, prevalence, and resultant impairment/disability.* J Am Acad Dermatol, 2005. **53**(2): p. 303-13.
23. Martin, S.F., *New concepts in cutaneous allergy.* Contact Dermatitis, 2015. **72**(1): p. 2-10.
24. de Groot, A.C., *Patch testing: test concentrations and vehicles for 4350 chemicals*. 2008: Acdegroot Publ.
25. Hultmann, P., in *Handbook on the Toxicology of Metals*, F.B. Nordberg GF, Nordberg M, Friberg LT, Editor. 2007, Academic Press: San Diego. p. 197-211.
26. Kimber, I., et al., *Allergic contact dermatitis: a commentary on the relationship between T lymphocytes and skin sensitising potency.* Toxicology, 2012. **291**(1-3): p. 18-24.
27. Karlberg, A.T., et al., *Allergic contact dermatitis--formation, structural requirements, and reactivity of skin sensitizers.* Chem Res Toxicol, 2008. **21**(1): p. 53-69.

28. Weber, F.C., et al., *Neutrophils are required for both the sensitization and elicitation phase of contact hypersensitivity.* J Exp Med, 2015. **212**(1): p. 15-22.
29. Amin, K., *The role of mast cells in allergic inflammation.* Respir Med, 2012. **106**(1): p. 9-14.
30. Sharpe, A.H. and A.K. Abbas, *T-cell costimulation--biology, therapeutic potential, and challenges.* N Engl J Med, 2006. **355**(10): p. 973-5.
31. Fyhrquist-Vanni, N., H. Alenius, and A. Lauerma, *Contact dermatitis.* Dermatol Clin, 2007. **25**(4): p. 613-23, x.
32. Fischer, T., *Prevention of irritant dermatitis.* Occup Med, 1986. **1**(2): p. 335-42.
33. White, J.M., *Patch testing: what allergists should know.* Clin Exp Allergy, 2012. **42**(2): p. 180-5.
34. Pacheco, K.A., *Allergy to Surgical Implants.* J Allergy Clin Immunol Pract, 2015. **3**(5): p. 683-95.
35. Fowler, J., Jr., et al., *Gold allergy in North America.* Am J Contact Dermat, 2001. **12**(1): p. 3-5.
36. Minang, J.T., et al., *Nickel, cobalt, chromium, palladium and gold induce a mixed Th1- and Th2-type cytokine response in vitro in subjects with contact allergy to the respective metals.* Clin Exp Immunol, 2006. **146**(3): p. 417-26.
37. Rachmawati, D., et al., *Transition metal sensing by Toll-like receptor-4: next to nickel, cobalt and palladium are potent human dendritic cell stimulators.* Contact Dermatitis, 2013. **68**(6): p. 331-8.
38. Saito, M., et al., *Molecular Mechanisms of Nickel Allergy.* Int J Mol Sci, 2016. **17**(2).
39. Wohrl, S., et al., *A cream containing the chelator DTPA (diethylenetriaminepenta-acetic acid) can prevent contact allergic reactions to metals.* Contact Dermatitis, 2001. **44**(4): p. 224-8.
40. Thierse, H.J., et al., *T cell receptor (TCR) interaction with haptens: metal ions as non-classical haptens.* Toxicology, 2005. **209**(2): p. 101-7.
41. Garner, L.A., *Contact dermatitis to metals.* Dermatol Ther, 2004. **17**(4): p. 321-7.
42. Salnikow, K., et al., *The involvement of hypoxia-inducible transcription factor-1-dependent pathway in nickel carcinogenesis.* Cancer Res, 2003. **63**(13): p. 3524-30.
43. Mattila, L., et al., *Prevalence of nickel allergy among Finnish university students in 1995.* Contact Dermatitis, 2001. **44**(4): p. 218-23.

44. Nestle, F.O., H. Speidel, and M.O. Speidel, *Metallurgy: high nickel release from 1- and 2-euro coins.* Nature, 2002. **419**(6903): p. 132.
45. Liden, C., L. Skare, and M. Vahter, *Release of nickel from coins and deposition onto skin from coin handling--comparing euro coins and SEK.* Contact Dermatitis, 2008. **59**(1): p. 31-7.
46. Saint-Mezard, P., et al., *Allergic contact dermatitis.* Eur J Dermatol, 2004. **14**(5): p. 284-95.
47. Forte, G., F. Petrucci, and B. Bocca, *Metal allergens of growing significance: epidemiology, immunotoxicology, strategies for testing and prevention.* Inflamm Allergy Drug Targets, 2008. **7**(3): p. 145-62.
48. Goldberg, M.A., S.P. Dunning, and H.F. Bunn, *Regulation of the erythropoietin gene: evidence that the oxygen sensor is a heme protein.* Science, 1988. **242**(4884): p. 1412-5.
49. Black, J., *Systemic effects of biomaterials.* Biomaterials, 1984. **5**(1): p. 11-8.
50. Koster, R., et al., *Nickel and molybdenum contact allergies in patients with coronary in-stent restenosis.* Lancet, 2000. **356**(9245): p. 1895-7.
51. Wataha, J.C., S.K. Nelson, and P.E. Lockwood, *Elemental release from dental casting alloys into biological media with and without protein.* Dent Mater, 2001. **17**(5): p. 409-14.
52. Diepgen, T.L., *Occupational skin-disease data in Europe.* Int Arch Occup Environ Health, 2003. **76**(5): p. 331-8.
53. Diepgen, T.L. and P.J. Coenraads, *The epidemiology of occupational contact dermatitis.* Int Arch Occup Environ Health, 1999. **72**(8): p. 496-506.
54. Dickel, H., et al., *[Incidence of occupation-related skin diseases in skin-exposure occupational groups]*. Hautarzt, 2001. **52**(7): p. 615-23.
55. Kadyk, D.L., et al., *Quality of life in patients with allergic contact dermatitis.* J Am Acad Dermatol, 2003. **49**(6): p. 1037-48.
56. Schmidt, M. and M. Goebeler, *Immunology of metal allergies.* J Dtsch Dermatol Ges, 2015. **13**(7): p. 653-60.
57. Goebeler, M., et al., *Differential and sequential expression of multiple chemokines during elicitation of allergic contact hypersensitivity.* Am J Pathol, 2001. **158**(2): p. 431-40.
58. Busse, R., I. Fleming, and M. Hecker, *Signal transduction in endothelium-dependent vasodilatation.* Eur Heart J, 1993. **14 Suppl I**: p. 2-9.

59. Viemann, D., et al., *The contact allergen nickel triggers a unique inflammatory and proangiogenic gene expression pattern via activation of NF-kappaB and hypoxia-inducible factor-1alpha.* J Immunol, 2007. **178**(5): p. 3198-207.
60. Nourshargh, S. and R. Alon, *Leukocyte migration into inflamed tissues.* Immunity, 2014. **41**(5): p. 694-707.
61. Osborn, L., *Leukocyte adhesion to endothelium in inflammation.* Cell, 1990. **62**(1): p. 3-6.
62. Beekhuizen, H. and R. van Furth, *Monocyte adherence to human vascular endothelium.* J Leukoc Biol, 1993. **54**(4): p. 363-78.
63. Denk, A., et al., *Activation of NF-kappa B via the Ikappa B kinase complex is both essential and sufficient for proinflammatory gene expression in primary endothelial cells.* J Biol Chem, 2001. **276**(30): p. 28451-8.
64. Michiels, C., *Endothelial cell functions.* J Cell Physiol, 2003. **196**(3): p. 430-43.
65. Pober, J.S. and R.S. Cotran, *Cytokines and endothelial cell biology.* Physiol Rev, 1990. **70**(2): p. 427-51.
66. Goebeler, M., et al., *Activation of nuclear factor-kappa B and gene expression in human endothelial cells by the common haptens nickel and cobalt.* J Immunol, 1995. **155**(5): p. 2459-67.
67. Sen, R. and D. Baltimore, *Inducibility of kappa immunoglobulin enhancer-binding protein Nf-kappa B by a posttranslational mechanism.* Cell, 1986. **47**(6): p. 921-8.
68. Baldwin, A.S., Jr., *The NF-kappa B and I kappa B proteins: new discoveries and insights.* Annu Rev Immunol, 1996. **14**: p. 649-83.
69. Baldwin, A.S., Jr., *Series introduction: the transcription factor NF-kappaB and human disease.* J Clin Invest, 2001. **107**(1): p. 3-6.
70. Yamaoka, S., et al., *Complementation cloning of NEMO, a component of the IkappaB kinase complex essential for NF-kappaB activation.* Cell, 1998. **93**(7): p. 1231-40.
71. Israel, A., *The IKK complex: an integrator of all signals that activate NF-kappaB?* Trends Cell Biol, 2000. **10**(4): p. 129-33.
72. Karin, M. and M. Delhase, *The I kappa B kinase (IKK) and NF-kappa B: key elements of proinflammatory signalling.* Semin Immunol, 2000. **12**(1): p. 85-98.
73. Janssens, S. and R. Beyaert, *Functional diversity and regulation of different interleukin-1 receptor-associated kinase (IRAK) family members.* Mol Cell, 2003. **11**(2): p. 293-302.

74. Pahl, H.L., *Activators and target genes of Rel/NF-kappaB transcription factors.* Oncogene, 1999. **18**(49): p. 6853-66.
75. Artik, S., et al., *Nickel allergy in mice: enhanced sensitization capacity of nickel at higher oxidation states.* J Immunol, 1999. **163**(3): p. 1143-52.
76. Frantzen, E., et al., *Changes in phenotypically distinct phagocyte subpopulations during nonspecific modulation of contact sensitization.* Int Arch Allergy Immunol, 1993. **101**(2): p. 182-9.
77. Grabbe, S., et al., *Dissection of antigenic and irritative effects of epicutaneously applied haptens in mice. Evidence that not the antigenic component but nonspecific proinflammatory effects of haptens determine the concentration-dependent elicitation of allergic contact dermatitis.* J Clin Invest, 1996. **98**(5): p. 1158-64.
78. Schmidt, M. and M. Goebeler, *Nickel allergies: paying the Toll for innate immunity.* J Mol Med (Berl), 2011. **89**(10): p. 961-70.
79. Vocanson, M., et al., *Effector and regulatory mechanisms in allergic contact dermatitis.* Allergy, 2009. **64**(12): p. 1699-714.
80. McFadden, J.P., et al., *Why does allergic contact dermatitis exist?* Br J Dermatol, 2013. **168**(4): p. 692-9.
81. Grabbe, S. and T. Schwarz, *Immunoregulatory mechanisms involved in elicitation of allergic contact hypersensitivity.* Am J Contact Dermat, 1996. **7**(4): p. 238-46.
82. Ross, R. and A.B. Reske-Kunz, *The role of NO in contact hypersensitivity.* Int Immunopharmacol, 2001. **1**(8): p. 1469-78.
83. Martin, S.F., et al., *Toll-like receptor and IL-12 signaling control susceptibility to contact hypersensitivity.* J Exp Med, 2008. **205**(9): p. 2151-62.
84. Jain, A., S. Kaczanowska, and E. Davila, *IL-1 Receptor-Associated Kinase Signaling and Its Role in Inflammation, Cancer Progression, and Therapy Resistance.* Front Immunol, 2014. **5**: p. 553.
85. Kang, J.Y. and J.O. Lee, *Structural biology of the Toll-like receptor family.* Annu Rev Biochem, 2011. **80**: p. 917-41.
86. Jin, M.S. and J.O. Lee, *Structures of the toll-like receptor family and its ligand complexes.* Immunity, 2008. **29**(2): p. 182-91.
87. Takeda, K., T. Kaisho, and S. Akira, *Toll-like receptors.* Annu Rev Immunol, 2003. **21**: p. 335-76.
88. Medzhitov, R., *Toll-like receptors and innate immunity.* Nat Rev Immunol, 2001. **1**(2): p. 135-45.

89. Akira, S., S. Uematsu, and O. Takeuchi, *Pathogen recognition and innate immunity.* Cell, 2006. **124**(4): p. 783-801.
90. Akashi-Takamura, S. and K. Miyake, *TLR accessory molecules.* Curr Opin Immunol, 2008. **20**(4): p. 420-5.
91. Kim, H.M., et al., *Crystal structure of the TLR4-MD-2 complex with bound endotoxin antagonist Eritoran.* Cell, 2007. **130**(5): p. 906-17.
92. Park, B.S., et al., *The structural basis of lipopolysaccharide recognition by the TLR4-MD-2 complex.* Nature, 2009. **458**(7242): p. 1191-5.
93. Kawai, T. and S. Akira, *Antiviral signaling through pattern recognition receptors.* J Biochem, 2007. **141**(2): p. 137-45.
94. Tyson-Capper, A.J., et al., *Metal-on-metal hips: cobalt can induce an endotoxin-like response.* Ann Rheum Dis, 2013. **72**(3): p. 460-1.
95. Sambrook J, F.E., Maniatis T, *Molecular Cloning*, in *Molecular Cloning*. 1989, Cold Spring Harbor Laboratory Press: Cold Spring Harbor, NY.
96. Muroi, M., T. Ohnishi, and K. Tanamoto, *MD-2, a novel accessory molecule, is involved in species-specific actions of Salmonella lipid A.* Infect Immun, 2002. **70**(7): p. 3546-50.
97. Hajjar, A.M., et al., *Human Toll-like receptor 4 recognizes host-specific LPS modifications.* Nat Immunol, 2002. **3**(4): p. 354-9.
98. Renkl, A.C., et al., *Osteopontin functionally activates dendritic cells and induces their differentiation toward a Th1-polarizing phenotype.* Blood, 2005. **106**(3): p. 946-55.
99. Graham, F.L. and A.J. van der Eb, *A new technique for the assay of infectivity of human adenovirus 5 DNA.* Virology, 1973. **52**(2): p. 456-67.
100. Czymai, T., et al., *FOXO3 modulates endothelial gene expression and function by classical and alternative mechanisms.* J Biol Chem, 2010. **285**(14): p. 10163-78.
101. Sanger, F., S. Nicklen, and A.R. Coulson, *DNA sequencing with chain-terminating inhibitors.* Proc Natl Acad Sci U S A, 1977. **74**(12): p. 5463-7.
102. Goebeler, M., et al., *Multiple signaling pathways regulate NF-kappaB-dependent transcription of the monocyte chemoattractant protein-1 gene in primary endothelial cells.* Blood, 2001. **97**(1): p. 46-55.
103. Eisenbarth, S.C., et al., *Crucial role for the Nalp3 inflammasome in the immunostimulatory properties of aluminium adjuvants.* Nature, 2008. **453**(7198): p. 1122-6.

104. Kawai, T. and S. Akira, *The role of pattern-recognition receptors in innate immunity: update on Toll-like receptors.* Nat Immunol, 2010. **11**(5): p. 373-84.
105. Muller, V., et al., *Candida albicans triggers activation of distinct signaling pathways to establish a proinflammatory gene expression program in primary human endothelial cells.* J Immunol, 2007. **179**(12): p. 8435-45.
106. Wesche, H., et al., *MyD88: an adapter that recruits IRAK to the IL-1 receptor complex.* Immunity, 1997. **7**(6): p. 837-47.
107. Divanovic, S., et al., *Negative regulation of Toll-like receptor 4 signaling by the Toll-like receptor homolog RP105.* Nat Immunol, 2005. **6**(6): p. 571-8.
108. Viemann, D., et al., *Transcriptional profiling of IKK2/NF-kappa B- and p38 MAP kinase-dependent gene expression in TNF-alpha-stimulated primary human endothelial cells.* Blood, 2004. **103**(9): p. 3365-73.
109. Padovan, E., et al., *IFN-alpha2a induces IP-10/CXCL10 and MIG/CXCL9 production in monocyte-derived dendritic cells and enhances their capacity to attract and stimulate CD8+ effector T cells.* J Leukoc Biol, 2002. **71**(4): p. 669-76.
110. Kaplan, D.H., B.Z. Igyarto, and A.A. Gaspari, *Early immune events in the induction of allergic contact dermatitis.* Nat Rev Immunol, 2012. **12**(2): p. 114-24.
111. Grabbe, S. and T. Schwarz, *Immunoregulatory mechanisms involved in elicitation of allergic contact hypersensitivity.* Immunol Today, 1998. **19**(1): p. 37-44.
112. Poltorak, A., et al., *Defective LPS signaling in C3H/HeJ and C57BL/10ScCr mice: mutations in Tlr4 gene.* Science, 1998. **282**(5396): p. 2085-8.
113. Schmidt, M., et al., *Ras-independent activation of the Raf/MEK/ERK pathway upon calcium-induced differentiation of keratinocytes.* J Biol Chem, 2000. **275**(52): p. 41011-7.
114. Brinen, L.S., et al., *X-ray structures of a designed binding site in trypsin show metal-dependent geometry.* Biochemistry, 1996. **35**(19): p. 5999-6009.
115. Wong, S.W., et al., *Fatty acids modulate Toll-like receptor 4 activation through regulation of receptor dimerization and recruitment into lipid rafts in a reactive oxygen species-dependent manner.* J Biol Chem, 2009. **284**(40): p. 27384-92.
116. Coloma, M.J., et al., *Novel vectors for the expression of antibody molecules using variable regions generated by polymerase chain reaction.* J Immunol Methods, 1992. **152**(1): p. 89-104.

117. McDonald, C.C. and W.D. Phillips, *A Nuclear Magnetic Resonance Study of Structures of Cobalt(II)-Histidine Complexes.* Journal of the American Chemical Society, 1963. **85**(23): p. 3736-3742.
118. Rulisek, L. and J. Vondrasek, *Coordination geometries of selected transition metal ions (Co2+, Ni2+, Cu2+, Zn2+, Cd2+, and Hg2+) in metalloproteins.* J Inorg Biochem, 1998. **71**(3-4): p. 115-27.
119. Waldron, K.J., et al., *Metalloproteins and metal sensing.* Nature, 2009. **460**(7257): p. 823-30.
120. Bonefeld, C.M., et al., *Nickel acts as an adjuvant during cobalt sensitization.* Exp Dermatol, 2015. **24**(3): p. 229-31.
121. Kawai, K., et al., *Expression of functional Toll-like receptor 2 on human epidermal keratinocytes.* J Dermatol Sci, 2002. **30**(3): p. 185-94.
122. Kollisch, G., et al., *Various members of the Toll-like receptor family contribute to the innate immune response of human epidermal keratinocytes.* Immunology, 2005. **114**(4): p. 531-41.
123. Watanabe, H., et al., *Activation of the IL-1beta-processing inflammasome is involved in contact hypersensitivity.* J Invest Dermatol, 2007. **127**(8): p. 1956-63.
124. Schroder, K. and J. Tschopp, *The inflammasomes.* Cell, 2010. **140**(6): p. 821-32.
125. Nestle, F.O., et al., *Skin immune sentinels in health and disease.* Nat Rev Immunol, 2009. **9**(10): p. 679-91.
126. Jiang, D., et al., *Regulation of lung injury and repair by Toll-like receptors and hyaluronan.* Nat Med, 2005. **11**(11): p. 1173-9.
127. Li, X. and F. Zhong, *Nickel induces interleukin-1beta secretion via the NLRP3-ASC-caspase-1 pathway.* Inflammation, 2014. **37**(2): p. 457-66.
128. Sato, N., et al., *Lipopolysaccharide promotes and augments metal allergies in mice, dependent on innate immunity and histidine decarboxylase.* Clin Exp Allergy, 2007. **37**(5): p. 743-51.
129. Zoroddu, M.A., et al., *Ni(II) binding to the 429-460 peptide fragment from human Toll like receptor (hTLR4): a crucial role for nickel-induced contact allergy?* Dalton Trans, 2014. **43**(7): p. 2764-71.
130. Freudenberg, M.A., et al., *Innate and adaptive immune responses in contact dermatitis: analogy with infections.* G Ital Dermatol Venereol, 2009. **144**(2): p. 173-85.

131. Trompette, A., et al., *Allergenicity resulting from functional mimicry of a Toll-like receptor complex protein.* Nature, 2009. **457**(7229): p. 585-8.
132. Lonez, C., et al., *Critical residues involved in Toll-like receptor 4 activation by cationic lipid nanocarriers are not located at the lipopolysaccharide-binding interface.* Cell Mol Life Sci, 2015. **72**(20): p. 3971-82.
133. Oblak, A., J. Pohar, and R. Jerala, *MD-2 determinants of nickel and cobalt-mediated activation of human TLR4.* PLoS One, 2015. **10**(3): p. e0120583.

9 Abbreviations

ACD	Allergic contact dermatitis
BSA	Bovine serum albumin
C	Celsius
CHS	Contact hypersensitivity
Co^{2+}	Cobalt
dd H_2O	Double distilled water
DMEM	Dulbecco's Modified Eagle's Medium
DMSO	Dimethyl sulfoxide
DNA	Deoxyribonucleic acid
ds	Double strand
DTT	Dithiothreithol
dn	Dominant negative
ECs	Endothelial cells
E. coli	*Escherichia coli*
ECL	Enhanced chemiluminescence
EDTA	Ethylenediamine-tetra acetic acid
ELISA	Enzyme-linked immunosorbent assay
FBS	Fetal bovine serum
FITC	Fluorescein isothiocyanate - coupled
h	Hour
HRP	Horse radish peroxidase
IKK	I-κB kinase
IL	Interleukin
kDa	Kilodalton
LPS	Lipopolysaccharide
M	Molar
mA	Milli ampere
mg	Milli gram
min	Minutes
ml	Milli litre
MyD88	Myeloid differential factor 88
NF-κB	Nuclear factor kappa-light-chain-enhancer of activated B cells
Ni^{2+}	Nickel
OD	Optical density
PAGE	Polyacrylamide Gel Electrophoresis
PBS	Phosphate buffered saline
PCR	Polymerase Chain Reaction
PFA	Paraformaldehyde
PMB	Polymyxin B sulfate
pmol	Pico mol
PRRs	Pattern-recognition receptors
PVDF	Polyvinylidene difluoride
RNA	Ribonucleic acid
SDS	Sodium dodecylsulfate
SEM	Standard error of the mean
ss	Single stranded
TBS	Tris buffered saline
TBST	Tris buffered saline with tween 20
TLB	Triton lysis buffer
TLR	Toll-like receptor
V	Volt
μg	Micro gram
μl	Micro litre
μm	Micro metre

10 Acknowledgements

I sincerely thank my mentor, Prof. Dr. Matthias Goebeler, for giving me an opportunity to work in this exciting project and providing me excellent research facilities in his laboratory. His profound insight and passion for Science were not only an immense source of motivation but also tremendously nurtured my research skills. I owe him a lot for his constant support throughout my Ph.D. work as well as during the hard times in my personal life.

This study was purely not possible without the whole-hearted guidance of Prof. Dr. Marc Schmidt. He helped me understand the basics of allergology, immunology and the nuances of scientific writing. His fervor and commitment for research was highly inspirational, particularly during the tricky situations. I am grateful to him for always insisting me to achieve bigger targets. His friendly attitude made my initial days of living in a foreign country as easy as possible.

Words are not enough to thank Prof. Dr. Thilo Jakob for accepting me as his Ph.D. student without any hesitation. I am also grateful to Prof. Dr. Uwe Gieler and PD Dr. Eva Peters for their constant encouragement and helping me to register for my Ph.D. degree program in JLU Giessen.

I also thank Prof. Dr. Stefan F. Martin (Freiburg), Prof. Dr. Marina Freudenberg (Freiburg), Prof. Dr. Arne Skerra (Munich) and Prof. Dr. Thomas Vogl (Muenster) for their wonderful collaboration in our project.

I thank my former colleagues of our laboratory, Dr. Verena Müller, Dr. Nils Ohnesorge, Dr. Tobias Czymai and Dr. Ravikumar Komaravolu for their valuable suggestions, encouragement and enlightening discussions. Technical assistance of Ms. Nicole Schmidt, Ms. Annika Huss, Ms. Ruth Alt and Ms. Silke Garkisch is deeply appreciated.

I am indebted to my co-brother, Dr. Yuvaraj Srinivasan for lending his help in a number of ways. I am thankful to my friends, Dr. Vasudharani Devanathan, Dr. Manju Rajender, Dr. Rajender Nandigama, Dr. Ranjithkumar Rajendran, Dr. Mahalakshmi Subramanian, Ms. Kokilavani Sivaraman, Dr. Balaji Samikannu, Mr. Kishore Nallapati, Ms. Naga Deepa Kandula, Dr. Suhail Ahmed Kabeer, Dr. Venkata Satagopam Pardhasaradhi,

Dr. Sowjanya Kallakuri, Dr. Kiran Kumar Bali, Dr. Harish Srinivasan and Dr. Meeta Kulkarni for always being there through my good and bad times.

I would also like to thank my family members and all my friends. My wife, my parents and my parents-in-law have always been encouraging and supportive, and they all gave a warm and cozy environment for my daughter so that I could perform my experiments in the lab and write my thesis. Without their help, this thesis could not have been completed.

Finally, I would like to thank the Lord Almighty for being with me in all circumstances and for His eternal love.

Der Lebenslauf wurde aus der elektronischen Version der Arbeit entfernt.

The curriculum vitae was removed from the electronic version of the paper.

12 Publications list

12.1 Publications and Patent

1. Kavitha TS, Parthasarathy C, Sivakumar R, Badrinarayanan R and Balasubramanian K (2006). Effects of excess corticosterone on NADPH generating enzymes and glucose oxidation in Leydig cells of adult rats. *Human and Experimental Toxicology*, 25(3): 119-125.
2. Badrinarayanan R, Rengarajan S, Nithya P and Balasubramanian K (2006). Corticosterone directly impairs the mRNA expression of 3β- and 17β-HSD in adult rat Leydig cells. *Biochemistry and Cell Biology*, 84(5): 745-754.
3. Marc Schmidt, Mike Hupe, Nicole Endres, Badrinarayanan Raghavan, Shyam Kavuri, Peter Geserick, Matthias Goebeler and Martin Leverkus (2010). The contact allergen nickel sensitizes primary human endothelial cells and keratinocytes to TRAIL-mediated apoptosis. *Journal of Cellular and Molecular Medicine,* 14(6B): 1760-76.
4. Marc Schmidt, Badrinarayanan Raghavan, Verena Müller, Thomas Vogl, György Fejer, Sandrine Tchaptchet, Simone Keck, Christoph Kalis, Peter J Nielsen, Chris Galanos, Johannes Roth, Arne Skerra, Stefan F Martin, Marina Freudenberg and Matthias Goebeler (2010). Crucial role for human Toll-like receptor 4 in the development of contact allergy to nickel. *Nature Immunology*, 11(9): 814-9.
5. Badrinarayanan Raghavan, Stefan F Martin, Philipp R Esser, Matthias Goebeler and Marc Schmidt (2012). Metal allergens nickel and cobalt facilitate TLR4 homodimerization independently of MD2. *EMBO reports*, 13(12): 1109-15.
6. Frank R Rommel*, Badrinarayanan Raghavan*, Renate Paddenberg, Wolfgang Kummer, Susanne Tumala, Gunter Lochnit, Uwe Gieler, Eva MJ Peters (2015). Suitability of nicotinic acetylcholine receptor α7 and muscarinic acetylcholine receptor 3 antibodies for immune detection: evaluation in murine skin. *Journal of Histochemistry and Cytochemistry*, 63(5): 329-39. * Equal contribution

PATENT

- **Invention related to contact allergens.** WIPO Patent Application WO/2012/016973 (PCT/EP2011/063271), Inventors: Badrinarayanan Raghavan, Marc Schmidt and Matthias Goebeler.

12.2 Published abstracts

1. Marc Schmidt, Badrinarayanan Raghavan, Verena Müller, Thomas Vogl, György Fejer, Sandrine Tchaptchet, Simone Keck, Christoph Kalis, Peter J Nielsen, Chris Galanos, Johannes Roth, Arne Skerra, Stefan F Martin, Marina Freudenberg and Matthias Goebeler (2011). Human Toll-like receptor 4: A crucial receptor for the development of contact eczema to metal haptens. *Journal of Investigative Dermatology*, **131**(2s): s94.

2. Marc Schmidt, Badrinarayanan Raghavan, Verena Müller, Thomas Vogl, György Fejer, Sandrine Tchaptchet, Simone Keck, Christoph Kalis, Peter J Nielsen, Chris Galanos, Johannes Roth, Arne Skerra, Stefan F Martin, Marina Freudenberg and Matthias Goebeler (2011). Crucial role for human Toll-like receptor 4 in the development of contact allergy to nickel. *Experimental Dermatology*, **20** (2): 164.

3. Badrinarayanan Raghavan, Stefan F Martin, Philipp R Esser, Matthias Goebeler and Marc Schmidt (2012). Metal allergens nickel and cobalt facilitate human Toll-like receptor 4 homodimerisation independently of MD2. *Journal of Investigative Dermatology*, **132** (2s): s112.

4. Badrinarayanan Raghavan, Matthias Goebeler and Marc Schmidt (2012). Contact allergens cobalt and nickel induce proinflammatory gene expression by facilitating TLR4 receptor dimerisation. *Experimental Dermatology*, **21**(3): e4.

5. Badrinarayanan Raghavan, Stefan F Martin, Philipp R Esser, Matthias Goebeler and Marc Schmidt (2013). Metal allergens nickel and cobalt facilitate human Toll-like receptor 4 homodimerisation independently of MD2. *Experimental Dermatology*, **22** (3): e4.

13 Declaration

I hereby declare that this dissertation is based on my original work and that it has not been previously presented in this or any other university for any degree. I have also abided by the principles of good scientific and laboratory practices laid down in the charter of the Justus Liebig University of Giessen in carrying out the experiments described in the dissertation.

By

……..

Badrinarayanan Raghavan
Giessen, Germany